

A COMBINED MOLECULAR AND ISOTOPIC STUDY OF SULFUR BACTERIA IN
MEROMICTIC LAKES OF THE PACIFIC NORTHWEST

James Howard Harris IV

Submitted to the faculty of the University Graduate School
in partial fulfillment of the requirements
for the degree
Master of Science
in the School of Earth Sciences,
Indiana University

December 2023

Accepted by the Graduate Faculty of Indiana University, in partial fulfillment of the requirements for the degree of Master of Science.

Master's Thesis Committee

William P. Gilhooly III, PhD, Chair

Gregory K. Druschel, PhD

Broxton W. Bird, PhD

© 2023

James Howard Harris IV

DEDICATION

This thesis is dedicated to my grandpas – Jim Harris and Leland Poling – my foremost examples of how earnest curiosity can enrich a life. You’ve long since charmed me into taking it to heart.

ACKNOWLEDGEMENTS

I want to thank Todd Benson for giving me the encouragement that I initially needed to pursue completing this project, and for providing the employment accommodations that have granted me the freedom and firm footing to achieve it. This was directly made possible by your support, and you have my immeasurable gratitude.

And my advisor – Bill Gilhooly. Bill, you held a door open for me that you could have long since let shut. You gave me time, energy, and trust that you had no obligation to give. You've been my advocate as well as my mentor. Thank you, for your frank, unflinching dedication to see me through this endeavor and for your steady confidence in me that you've always done so well to convey. This thesis has been a decade in the making. Thank you for sticking with me.

I also would like to thank Byron Steinman, Greg Druschel, Broxton Bird Christine Picard, and EJ Crane for letting me use their labs, their equipment, and their time. You've each helped me tremendously in honing this project into something I'm extremely proud of.

More, I've been given an abundance of help from several generous undergrads over the years, both in the lab and in the field, who each have my gratitude – Kat Holper, Daniel Orazi, Joe Robert, Jake Walker, Ellie Wind, Eric Alt, and notably, Shan Khan. In addition to spending months of his valuable free time tinkering in the lab with me as an undergraduate, he provided me with a roof and good company when I returned to Indy to finish this project years later. Thank you, Shan. I count myself lucky to have you in my life.

James Howard Harris IV

A COMBINED MOLECULAR AND ISOTOPIC STUDY OF SULFUR
BACTERIA IN MEROMICTIC LAKES OF THE PACIFIC NORTHWEST

The isotope effects that result from the activity of modern sulfur metabolizing bacteria serve as analogs to interpreting the sulfur isotope values preserved in the geologic record. This biogenic signal is vital to reconstructing the history of Earth's ancient oceans and atmosphere. However, the isotope compositions imprinted by these bacteria were influenced by multiple factors that must be considered when using these values to make interpretations about environmental change. These factors include: (1) sulfate availability, (2) the rapid and quantitative reoxidation of sulfide (i.e., cryptic sulfur cycling), (3) the initial oxygen isotope compositions of sulfate and water, and (4) the taxonomic structure of sulfur-metabolizing bacterial communities. To address these questions, this project studied four permanently stratified, anoxic and sulfidic (euxinic), lakes in southern British Columbia, Canada, and northern Washington, USA, that have a wide range of sulfate concentrations, from 0.15 – 120 mM.

This project resulted in six key findings – (1) the measurement of large $\Delta^{34}\text{S}_{\text{SO}_4\text{-H}_2\text{S}}$ values at micromolar sulfate concentrations, (2) the consistent occurrence of $\delta^{18}\text{O}_{\text{SO}_4}$ minima at the chemocline that may be imparted during cryptic sulfur cycling, (3) that subsequent $\delta^{18}\text{O}_{\text{SO}_4}$ enrichments consistently preceded sulfide accumulation and $\delta^{34}\text{S}_{\text{SO}_4}$ enrichment in the suboxic zone of the water column, (4) that initial epilimnion $\Delta^{18}\text{O}_{\text{SO}_4\text{-H}_2\text{O}}$ values placed constraints on the maximum extent of $\delta^{18}\text{O}_{\text{SO}_4}$ evolution that occurred beneath the chemocline, (5) that observable changes in the metabolic composition of sulfur bacterial communities accompanied key inflections in the sulfur

and oxygen isotope profiles of sulfate and sulfide within the water column, and (6) that, despite large overall differences in community structure, $\Delta^{34}\text{S}_{\text{SO}_4\text{-H}_2\text{S}}$ and $\Delta^{18}\text{O}_{\text{SO}_4\text{-H}_2\text{O}}$ values ultimately reached similar magnitudes in each lake.

William P. Gilhooly III, PhD, Chair

Gregory K. Druschel, PhD

Broxton W. Bird, PhD

TABLE OF CONTENTS

LIST OF TABLES	ix
LIST OF FIGURES	x
LIST OF ABBREVIATIONS.....	xi
I. INTRODUCTION	1
1.1. Isotopes as Evidence of Modern and Ancient Microbial Activity	1
1.2. Statement of Problem and Hypotheses	2
1.2.1. Hypothesis #1.....	3
1.2.2. Hypotheses #2A and #2B.....	4
1.2.2.1 Hypothesis #2A.....	5
1.2.2.1 Hypothesis #2B.....	6
1.2.3. Hypothesis #3.....	7
1.3. Background.....	9
1.3.1. The utility of sulfur and oxygen isotopes	9
1.3.2. Stable isotope reporting	15
1.4. Project significance.....	18
II. MATERIALS AND METHODS.....	20
2.1. Study sites	20
2.2. Water column sampling	22
2.3. Water sample preparation.....	24
2.4. Stable isotope measurements	25
2.5. Ion and sulfur concentration measurements	26
2.6. Genetic Sequencing	27
2.7. Operational Taxonomic Units	27
2.8. Functional analysis.....	31
2.9. A note on abundances.....	34
III. RESULTS.....	36
3.1. O ₂ , conductivity, pH, and temperature.....	37
3.2. Sulfur concentrations	39
3.3. Stable Isotopes	40
3.4. Community structure of sulfur bacteria	43
3.4.1. Conservative representation of sulfur community structure.....	48
3.4.2. Broadest possible sulfur community structure.....	50
IV. DISCUSSION	53
4.1. Sulfate concentration and $\Delta^{34}\text{S}_{\text{SO}_4\text{-H}_2\text{S}}$	53
4.2. Water column $\delta^{18}\text{O}_{\text{SO}_4}$ during cryptic sulfur cycling	57
4.3. Relative rates and magnitudes of $\delta^{18}\text{O}_{\text{SO}_4}$ evolution.....	70
4.4 Microbial community structures	78
V. CONCLUSIONS	89
5.1 Recommendations for future work	89
APPENDICES	91
Appendix A $\delta^{34}\text{S}$ vs $\delta^{18}\text{O}$ distillation models.....	91
Appendix B: Categorized operational taxonomic unit abundances.....	94
REFERENCES	118
CURRICULUM VITAE	

LIST OF TABLES

Table 1: Green sulfur bacteria.....	94
Table 2: Purple sulfur bacteria.....	95
Table 3: Sulfate reducers	96
Table 4: Potential sulfate reducers.....	98
Table 5: Sulfate reducers that can potentially disproportionate.....	98
Table 6: Sulfur oxidizers.....	101
Table 7: Potential sulfur oxidizers	101
Table 8: Potential sulfur reducers	106
Table 9: Potential oxidizers and/or reducers.....	111
Table 10: Lime Blue Lake 11 m OTU counts for all sulfur-metabolizing taxa.....	112

LIST OF FIGURES

Figure 1: Idealized euxinic lake water column profiles of dissolved oxygen and the isotopic compositions of sulfate and sulfide.....	13
Figure 2: Example of paired sulfur and oxygen model demonstrating the array of solutions for rapid (linear) and slow (curvilinear) rates of sulfate reduction	18
Figure 3: Areal imagery of the study lakes – Cleland Lake, British Columbia, Canada (A), and Lime Blue Lake (B), Castor Lake (C), and Scanlon (D), Washington, USA	21
Figure 4: Example of several lines within a fasta file.....	29
Figure 5: Water column profiles of dissolved oxygen (LDO), specific conductivity (SpC), pH, sulfate concentrations (SO ₄), elemental sulfur concentrations (S ⁰), sulfide concentrations (H ₂ S), the sulfur isotope compositions of sulfide and sulfate, and the oxygen isotope compositions of sulfate and water for all four study lakes	36
Figure 6: Visualization of how functional categories were assigned based on the metabolic composition of three hypothetical taxa.	47
Figure 7: Relative (%) abundances of water column bacteria that were members of predominantly sulfur-metabolizing taxa	48
Figure 8: Abundances of all water column bacteria that share membership with any number of sulfur-metabolizers at their assigned taxonomic level or below	50
Figure 9: Water column sulfur isotope profiles	54
Figure 10: Weathering pyritic shale and marble along the shoreline of Castor Lake.....	57
Figure 11: Comparison of $\delta^{18}\text{O}_{\text{SO}_4}$ and $\delta^{18}\text{O}_{\text{H}_2\text{O}}$ for surface waters (open symbols) and water column values at depth of oxygen isotope excursion (filled symbols) in each lake.....	59
Figure 12: Water column profiles of dissolved oxygen (LDO) and oxidative redox potential (ORP) in Cleland, Lime Blue, Castor, and Scanlon Lakes	62
Figure 13: Distribution of $\delta^{18}\text{O}_{\text{SO}_4}$ in all four study lakes	65
Figure 14: Water column $\delta^{34}\text{S}_{\text{SO}_4}$ and $\delta^{18}\text{O}_{\text{SO}_4}$ in each study lake	69
Figure 15: Oxygen isotope compositions of water ($\delta^{18}\text{O}_{\text{H}_2\text{O}}$) and sulfate ($\delta^{18}\text{O}_{\text{SO}_4}$).....	71
Figure 16: Depth-normalized $\delta^{18}\text{O}_{\text{SO}_4}$ and $\delta^{34}\text{S}_{\text{SO}_4}$ values from each lake	72
Figure 17: Model demonstration of how differences between $\delta^{18}\text{O}_{\text{H}_2\text{O}}$ and initial $\delta^{18}\text{O}_{\text{SO}_4}$ values influence the magnitude of $\delta^{18}\text{O}_{\text{SO}_4}$ evolution that can occur during sulfate reduction.....	73
Figure 18: Plot showing hypolimnion $\delta^{34}\text{S}_{\text{SO}_4}$ and $\delta^{18}\text{O}_{\text{SO}_4}$ evolution with depth in each study lake	74
Figure 19: Taxonomically inclusive upper-bound estimations of sulfur bacterial abundances	81
Figure 20: Cleland Lake $\delta^{34}\text{S}_{\text{SO}_4}$ and $\delta^{18}\text{O}_{\text{SO}_4}$ data plotted over distillation model results	91
Figure 21: Lime Blue Lake, Castor Lake, and Scanlon Lake $\delta^{34}\text{S}_{\text{SO}_4}$ and $\delta^{18}\text{O}_{\text{SO}_4}$ data plotted over distillation model results	93

LIST OF ABBREVIATIONS

CAS - Carbonate-associated sulfate
CL - Castor Lake
CLBC - Cleland Lake
DSP - Metabolic sulfur disproportionation; also used here as shorthand for bacteria that can perform sulfur disproportionation
DSR - Dissimilatory sulfate reduction
GSB - Green sulfur bacteria
LB - Lime Blue Lake
LDO - Luminescent dissolved oxygen
ORP - Oxidative/reductive potential
OTU - Operational taxonomic unit
PCR - Polymerase chain reaction
PSB - Purple sulfur bacteria
SL - Scanlon Lake
Sox - Metabolic sulfur oxidation pathway; also used as an adjective or shorthand for bacteria that carry out the Sox pathway, e.g., "Sox bacteria"
SpC - Specific conductivity
SRB - Sulfate reducing bacteria
WC - Water column
BP – before present; in standard practice, “present day” refers to January 1, 1950

I. INTRODUCTION

1.1. Isotopes as Evidence of Modern and Ancient Microbial Activity

The isotope effects that result from the activity of extant microorganisms are modern analogs to the biosignatures imparted by past microbial processes operative in the Precambrian oceans and, thus, are vital in reconstructing the history of the oceans and atmosphere (Meyer and Kump, 2008; Donald E. Canfield et al., 2010; Gomes and Hurtgen, 2013; Leavitt et al., 2013). Fractionation of sulfur and oxygen isotopes of sulfate mediated by sulfur-metabolizing bacteria in modern lakes provides insight into the isotope signals that are recorded in ancient marine sediments. Prior to the Neoproterozoic Oxygenation Event (800-580 million years ago; Ma) atmospheric oxygen levels in the ocean and atmosphere were orders of magnitude lower than modern concentrations (Canfield and Teske, 1996; Canfield, 1998; Pavlov and Kasting, 2002; Canfield et al., 2007; Sessions et al., 2009; Och and Shields-Zhou, 2012). During this period of oxygen free (anoxic) conditions in Earth's history, microbial communities of anaerobic bacteria are hypothesized to have been the predominant living organisms in the oceans (Brocks et al., 2005; Johnston et al., 2009; Ozaki et al., 2019).

Taking advantage of the wide range of oxidation states for sulfur (-2 to +6), many genera of anaerobic bacteria gain energy from the oxidation, reduction, and disproportionation of the varied molecular forms of inorganic sulfur in the natural environment. Lineages of bacteria involved in the cycling of the varied forms of sulfur are ancient and diverse, with sulfate reducing bacteria likely emerging before 3.47 Ga (Shen et al., 2001; Shen and Buick, 2004). Sulfur bacteria living today possess metabolisms that have persisted since the Archean and have measurable effects on the

distribution of sulfur and oxygen isotopes. Importantly, many of the isotopic analyses that can be performed on samples taken from modern environments can also be made on samples from the geologic record during time periods when sulfur-bearing minerals were preserved in ancient marine sediments.

The secular variation in the sulfur isotope composition of pyrite (Canfield, 2005; Fike et al., 2015; Havig et al., 2017) and the less complete record of sulfate preserved in barite, gypsum and carbonate associated sulfate (Paytan et al., 1996, 2002; Paytan and Griffith, 2007) have provided important information about the evolving redox state of the marine biosphere. However, recent revaluations of these records (Fike et al., 2015; Havig et al., 2017) indicate there are several biotic (e.g., sulfate reduction rate) and physical factors (e.g., sedimentation rate) that complicate the interpretation of these geologic records (Leavitt et al., 2013; Wing and Halevy, 2014; Pasquier et al., 2017). The value of studying the modern euxinic (anoxic and sulfidic) lakes that harbor these bacteria is that, by improving the models that describe the sulfur cycle in these lakes, we can address these complications and thereby improve models describing the cycles of the past.

1.2. Statement of Problem and Hypotheses

The isotope compositions imprinted by sulfur metabolizing bacteria are influenced by multiple factors that must be considered when using these values to make interpretations about environmental change. Four of these factors were the focus of this work: (1) how the concentration of sulfate impacts the isotope effects of sulfate reducing bacteria, (2) how rapid and quantitative reoxidation of sulfide (i.e., cryptic sulfur cycling) influences the oxygen isotope composition of sulfate at the chemocline, (3) how the

initial oxygen isotope compositions of sulfate and water in the epilimnion can influence the compositional shifts in oxygen isotopes of sulfate imparted by sulfate reducing bacteria in the hypolimnion and confound estimates of reduction rates, and (4) how the taxonomic structure of sulfur-metabolizing bacterial communities can influence the isotope compositions of sulfide and sulfate. These factors can be characterized as environmental (sulfate concentration, epilimnion sulfate and water isotope compositions), metabolic (relative sulfate reduction and sulfide oxidation rates), and ecological (community structure). The degree to which these factors influenced the isotope composition of pyrite and other sulfur bearing minerals in ancient marine sediments is important to assess in order to accurately reconstruct the chemical history of the atmosphere and oceans. The following hypotheses are tested in four lakes located in the same bedrock geology and climatic zone, yet with differing concentrations of water column sulfate.

1.2.1. Hypothesis #1

The net sulfur isotopic offset between sulfate and sulfide ($\Delta^{34}S_{SO_4-H_2S}$) does not scale with the water column concentration of sulfate, such that lower concentrations of sulfate do not necessarily result in smaller offsets between sulfate and sulfide. Sulfate concentration has been regarded as a significant factor controlling the isotopic difference between sulfate and sulfide produced during the process of sulfate reduction (Harrison and Thode, 1958; Kaplan and Rittenberg, 1964; Chambers and Trudinger, 1979; Cameron, 1982; Canfield and Teske, 1996; Habicht et al., 2002; Crowe et al., 2014). High concentrations of sulfate potentially result in sulfate reducing bacteria taking up

sulfate that is, overall, isotopically depleted in ^{34}S . This is because molecules that are isotopically lighter tend to be more reactive, making ^{32}S -bearing sulfate more reactive than ^{34}S -bearing sulfate. When sulfate concentrations are low, there is less competition between sulfate molecules for reaction sites, which results in more ^{34}S entering the cell. Conversely, a larger sulfate pool could theoretically result in sulfate reducers consuming a greater percentage of ^{32}S -sulfate molecules than they would with a smaller sulfate pool (Habicht et al., 2002). When sulfate is below what has been considered a limiting concentration (200 μM), the isotopic fractionation is expected to decrease (Habicht et al., 2002). However, there have been cases where large isotope offsets between sulfate and sulfide (60 – 70‰) have been observed in low-sulfate lakes, such as Lake Cadagno in Switzerland (1.1 – 2 mM sulfate) (Donald E. Canfield et al., 2010), and this value might vary between taxa (Sim, 2019). To test this hypothesis, I analyzed the sulfur and oxygen isotope compositions of sulfate from four lakes with differing sulfate concentrations, ranging between 2 and 15 mM.

1.2.2. Hypotheses #2A and #2B

Two factors that can influence the oxygen isotope composition of sulfate include: (1) cryptic sulfur cycling, and (2) the initial $\Delta^{18}\text{O}_{\text{SO}_4\text{-H}_2\text{O}}$ value at the topmost depth where sulfate reduction is occurring. Each will be addressed by one of the following hypotheses.

1.2.2.1 Hypothesis #2A

The lowest $\delta^{18}O_{SO_4}$ value in the water column will occur in the chemocline, followed by monotonic $\delta^{18}O_{SO_4}$ enrichment within the remainder of the hypolimnion.

$\delta^{18}O_{SO_4}$ values of residual sulfate increase during net sulfate reduction due to metabolic back reaction, reaching a maximum value equal to the fractionation factor of the sulfite-water oxygen equilibrium exchange reaction (Brunner and Bernasconi, 2005; Brunner et al., 2005a; Antler et al., 2013). This maximum $\delta^{18}O_{SO_4}$ value is reached when sulfate reduction is slow enough to allow intracellular sulfite-bound oxygen to fully equilibrate with the oxygen bound to ambient water (Betts and Voss, 1970; Booth, 1985; Antler et al., 2013).

Intracellular sulfite is an intermediate valent phase of sulfur that resides in a transient pool within the metabolic framework of sulfate reducing microorganisms during the reduction of sulfate to sulfide. At near neutral pH, intracellular sulfite rapidly exchanges oxygen with water on the timescale of minutes or shorter (Betts and Voss, 1970; Booth, 1985; Antler et al., 2013), which can result in sulfite with theoretical $\delta^{18}O$ values up to 29‰ higher than that of the ambient water (Markovic et al., 2016), though lower values between 9.5 and 15.2‰ are typical for sulfate-water fractionations measured in modern euxinic systems (Gomes and Johnston, 2017). At slow reduction rates, back-reactions along the metabolic pathway that result in sulfite being re-oxidized back to sulfate occur more frequently. Sulfate is only known to exchange oxygen with water when exposed to high temperatures and low pH, so this back-reacted sulfate will retain the new oxygen isotope composition. Once exported from the cell, it will mix with ambient sulfate and locally increase the $\delta^{18}O_{SO_4}$ value of the pool.

This process of $\delta^{18}\text{O}_{\text{SO}_4}$ enrichment would be tempered by reoxidation of sulfide by chemotrophic and phototrophic Sox bacteria. When sulfide reoxidation occurs at a rate equal to that of sulfate reduction (a condition called cryptic sulfur cycling, which will be discussed at length in following sections), sulfate with relatively ^{18}O -depleted oxygen – sourced from ambient water by the Sox pathway – will be continually reintroduced to the sulfate pool. This low- $\delta^{18}\text{O}$ sulfate will offset any $\delta^{18}\text{O}_{\text{SO}_4}$ enrichment that might otherwise accumulate due to back reactions during sulfate reduction and will ultimately result in a lower $\delta^{18}\text{O}_{\text{SO}_4}$ value than at any other point in the water column. This negative $\delta^{18}\text{O}_{\text{SO}_4}$ excursion will give way to $\delta^{18}\text{O}_{\text{SO}_4}$ enrichment in the depths below as the capacity for Sox subsides and the ^{18}O effects of sulfate reduction become predominant.

As with hypothesis #1, four lakes with different sulfate concentrations were studied and stable isotope mass spectrometry was carried out on water samples collected from these sites, analyzing $\delta^{18}\text{O}_{\text{SO}_4}$ and $\delta^{18}\text{O}_{\text{H}_2\text{O}}$.

1.2.2.1 Hypothesis #2B

$\Delta^{18}\text{O}_{\text{SO}_4\text{-H}_2\text{O}}$ values at the base of the epilimnion will control the extent to which $\delta^{18}\text{O}_{\text{SO}_4}$ values can increase within the hypolimnion. There are upper limits to the oxygen isotope fractionation that dissimilatory sulfate reduction can impart on sulfate by virtue of the energetics of the equilibrium oxygen exchange reaction between sulfite and water. If initial top-hypolimnion $\Delta^{18}\text{O}_{\text{SO}_4\text{-H}_2\text{O}}$ values are already near the maximum fractionation that sulfite-water equilibrium exchange can produce, then there will be little headroom for $\delta^{18}\text{O}_{\text{SO}_4}$ values to further increase over $\delta^{18}\text{O}_{\text{H}_2\text{O}}$ values in the depths below, which will limit $\delta^{18}\text{O}_{\text{SO}_4}$ evolution. The more negative that the $\delta^{18}\text{O}_{\text{SO}_4}$ value is relative to $\delta^{18}\text{O}_{\text{H}_2\text{O}}$ at

the onset of dissimilatory sulfate reduction, the larger the degree of possible change in $\delta^{18}\text{O}_{\text{SO}_4}$ values will be. The amount of $\Delta^{18}\text{O}_{\text{SO}_4\text{-H}_2\text{O}}$ headroom that is available constrains the range of possible $\delta^{18}\text{O}_{\text{SO}_4}$ values in which the oxygen isotope effect of dissimilatory sulfate reduction can be expressed. The variance in epilimnion $\Delta^{18}\text{O}_{\text{SO}_4\text{-H}_2\text{O}}$ values between the study lakes provided a basis to test this hypothesis by comparing these initial epilimnion $\Delta^{18}\text{O}_{\text{SO}_4\text{-H}_2\text{O}}$ values with respective magnitudes of hypolimnion $\delta^{18}\text{O}_{\text{SO}_4}$ evolution.

1.2.3. Hypothesis #3

Microbial community structure will influence the isotopic composition of sulfur and oxygen in sulfate. Sulfur-metabolizing bacteria that belong to divergent taxa often produce sulfur isotope fractionations between sulfide and sulfate, and oxygen isotope fractionations between sulfate and water, that are distinct and characteristic of the metabolic pathways found among members of each respective taxa. It follows that the specific taxonomic composition of a sulfur bacterial community can affect the specific isotopic compositions of reduced and oxidized sulfur.

Four major categories of sulfur-metabolizing bacteria – sulfate reducers, phototrophic sulfide oxidizers, chemotrophic sulfide oxidizers, and sulfur disproportionators – are all major contributors to the sulfur cycle in euxinic environments (Canfield and Raiswell, 1999). These bacteria alter the sulfur isotope composition of sulfate and sulfide to different degrees. The fractionation imparted during microbial sulfate reduction is relatively large (with $\Delta^{34}\text{S}_{\text{SO}_4\text{-H}_2\text{S}}$ values up to +66‰) (Sim et al., 2011; Leavitt et al., 2013). The production of ^{34}S -depleted sulfide renders the residual

sulfate pool ^{34}S -enriched. Phototrophic sulfide-oxidizing purple and green sulfur bacteria produce relatively small sulfur isotope fractionations, between 0 and +6‰ (Zerkle et al., 2009; Brabec et al., 2012). Many lithotrophic sulfur oxidizers have been shown to produce similarly small, but typically negative fractionations in the range of -4 to 0‰ (Kaplan and Rafter, 1958; Poser et al., 2014). A known exception is the sulfide oxidizing cable bacterium *Desulfurivibrio alkaliphilus* that produces fractionations of up to +12‰ (Pellerin et al., 2019). By returning ^{34}S -depleted sulfide back to the sulfate pool, sulfide oxidation acts in reverse to the ^{34}S -enrichment imparted by sulfate reduction on the sulfate pool while altering the ^{34}S composition of sulfide pool by some degree (Findlay et al., 2019; Guo et al., 2020). Disproportionating bacteria metabolize sulfur intermediates such as elemental sulfur, polysulfides, and thiosulfate to produce both sulfide and sulfate as end products, and they impart relatively larger fractionations – several studies have shown that disproportionation of elemental sulfur can yield sulfide depleted in ^{34}S by -0.9 to -15.5‰ and sulfate enriched in ^{34}S by -0.6 to +35‰ (Canfield and Thamdrup, 1994; Canfield et al., 1998; Böttcher et al., 2001, 2005; Böttcher, M.E. Thamdrup and Vennemann, 2001; Poser et al., 2016). Sulfate produced by disproportionation can also be ^{18}O -enriched relative to water, which serves as the oxygen source. For example, elemental sulfur disproportionation can yield sulfate that is ^{18}O -enriched by +8 to +12‰ in the presence of manganese oxides and by 16.1 to 17.5‰ if iron oxides are available (Gomes and Johnston, 2017).

The habitats of each of these microbial varieties overlap, and aggregations comprising virtually any combination growing together can be found in natural samples of euxinic water. The specific isotopic compositions of water column sulfate and sulfide

are directly influenced by the taxonomic compositions of these microbial aggregations. Consequently, the patterns in sulfate and sulfide isotope data from natural water samples should necessarily be limited to that which is possible given the community compositions of sulfur bacteria in those samples, and substantial changes in community structure within the water column should correspond with observable changes in isotopic behavior.

To test this hypothesis, I sequenced and analyzed 16S gene DNA present in water samples collected from four study lakes. These sequence data were then compared to the sulfur isotope data acquired from samples from the same depths. Comparing these two sets of data, it is possible to assess the relatedness between community structure and the isotope composition of sulfate and sulfide.

1.3. Background

1.3.1. The utility of sulfur and oxygen isotopes

Based on the geochemical, mineralogical, and paleontological record (Farquhar et al., 2000; Canfield et al., 2007; Johnson et al., 2014; Lyons et al., 2014) oxygen levels in the biosphere prior to the Phanerozoic were lower than they are at present, ranging from $<10^{-5}$ present atmospheric levels prior to ~2.5 Ga to between 1 and 40% until the late Proterozoic (Lyons et al., 2014). One of the outstanding questions in biological evolution is why it took nearly two billion years after the Great Oxidation Event for metazoans to evolve. The history of oxygen on Earth has been heavily informed by sulfur and oxygen isotopes in sediments, which is mediated by the activity of microbial life, principally sulfur metabolizing bacteria. Studying these bacteria in modern natural settings, as was done in this project, brings the sulfur cycle in these systems into sharper focus, which

allows us to build more robust models of ancient systems with the nuances of modern systems as our guide.

Stable isotopes of sulfur and oxygen are useful because they, like other stable isotopes, do not undergo spontaneous radioactive decay and both elements are ubiquitous in the biosphere and are heavily involved in biogeochemical cycles. Both have known abundances (Coplen et al., 2002), and these abundances can be measured and compared. Sulfur has four stable isotopes: ^{32}S (95.03957% of total sulfur on earth), ^{33}S (0.75865%), ^{34}S (4.59719%), and ^{36}S (0.01459%). Oxygen has three stable isotopes: ^{16}O (99.76206%), ^{17}O (0.03790%) and ^{18}O (0.20004%). Because isotopes of the same element differ slightly in chemical reactivity, the abundances of these isotopes naturally vary between different compounds due to differences in reaction kinetics and equilibrium processes. This partitioning of different isotopes of the same element between different compounds is called isotope fractionation. The degree of isotope fractionation that occurs between two compounds is indicative of the processes, abiotic or biotic, that formed the compound. Therefore, biological processes that give rise to certain ratios of these isotopes in sulfate and sulfide in modern anoxic lakes likely resemble the processes that gave rise to the same ratios during the Proterozoic, which is why these isotopes have found use in this study and others.

Sulfate delivered from the continents to the ocean by rivers is ultimately derived from oxidative weathering of sulfur-bearing minerals under present atmospheric levels of oxygen (21%). Global riverine inputs maintain the concentration of sulfate in the oceans at approximately 28 mM (Burke et al., 2018). Under reducing conditions, or when subject to reducing bacterial metabolisms, sulfate can be converted ultimately to hydrogen

sulfide. At the interfaces of oxic and anoxic water columns and sediments, a wide variety of intermediate sulfur compounds (elemental sulfur, sulfite, thiosulfate, and polysulfides) are produced by biological and chemical reactions (Jørgensen, 1990; Overmann et al., 1996; Zopfi et al., 2004). Many bacterial metabolisms have evolved to use each of these forms of sulfur as electron donors and acceptors, oxidizing reduced forms of sulfur, reducing oxidized forms, or doing both using the process of disproportionation (Thamdrup et al., 1993; Canfield and Thamdrup, 1994). Because these forms of sulfur are both substrates and products of a range of bacteria, each can accumulate in appreciable concentrations in the natural environment and are important components in the carbon-sulfur cycle. These compounds can be measured, yielding data that is informative of the sulfur cycle in these systems (Habicht et al., 1998; Zerkle et al., 2010; Hamilton et al., 2014; Kurek et al., 2018).

The wide range in oxidation state (-2 to +6) of sulfur makes this element energetically favorable to a variety of microbially mediated reactions. Oxidized sulfur compounds and organic carbon are produced by sulfur oxidizers, both of which in turn are consumed by sulfur reducing bacteria, which then re-reduce the sulfur into substrates that are consumed by sulfur oxidizers (Overmann et al., 1996; Hamilton et al., 2014; Wilbanks et al., 2014). For example, sulfate reducing *Desulfovibrio* species oxidize organic substrates by using sulfate as the terminal-electron acceptor, reducing sulfate to sulfide as a result. Some autotrophic bacteria derive energy by the oxidation of reduced sulfur compounds. Bacterial sulfide oxidation occurs at rates three orders of magnitude faster than abiotic oxidation (Luther et al., 2011) and can reoxidize 50-90% of reduced

sulfur back to sulfate in modern sediments (Jørgensen, 1977; Zopfi et al., 2001; Pellerin et al., 2015; Jørgensen et al., 2019).

Much of bacterial sulfur oxidation is mediated by a specific set of enzymes that, in concert, comprise what has been termed the Sox pathway. The pathway is a mechanism by which electrons are liberated from reduced sulfur compounds, which are needed to replenish electrons that have been shunted from the electron transport chain to produce NADPH, the reductant in CO₂ fixation. Genes encoding these Sox proteins are ubiquitous among even distantly related autotrophic taxa in varying degrees of completeness, which suggests that the capacity for Sox has been spread via horizontal gene transfer. These disparate taxa include the phototrophic green sulfur bacteria (GSB) and purple sulfur bacteria (PSB), as well as a variety of obligate and facultative chemolithotrophs, the latter of which includes some species of phototrophs. GSB and PSB are examples of taxa which do not have the full complement of Sox genes. Both, instead, carry out sulfide oxidation by combining truncated forms of the Sox pathway with sulfate reduction pathways that are run in reverse (Ghosh and Dam, 2009).

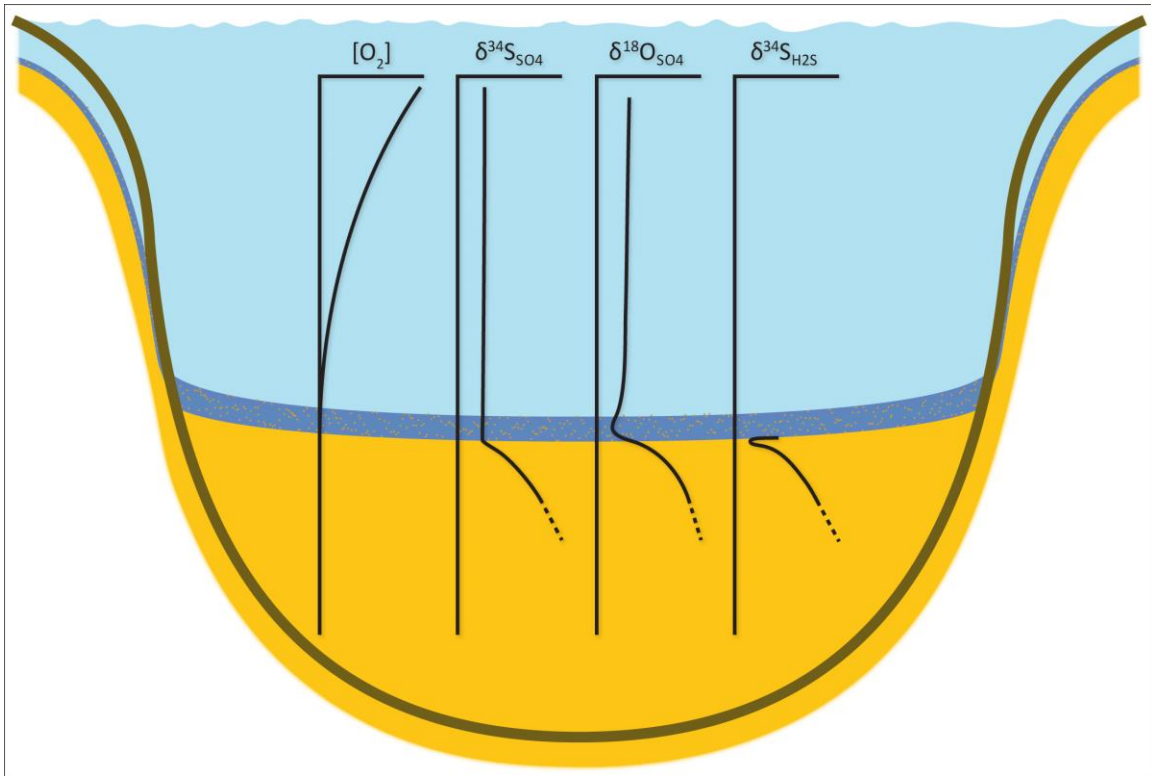


Figure 1: Idealized euxinic lake water column profiles of dissolved oxygen and the isotopic compositions of sulfate and sulfide.

When performing these redox transformations of sulfur compounds, sulfur metabolizing bacteria impart signatures in sulfur isotopes of their metabolic end-products, wherein sulfate becomes enriched in ^{34}S and sulfide becomes depleted in ^{34}S . The magnitudes of these fractionations depend on sulfate reduction rates, sulfate concentration, and the composition of the microbial community (Johnston et al., 2007; Bradley et al., 2011; Sim et al., 2011; Leavitt et al., 2013). The oxygen isotope composition of sulfate is also altered in characteristic ways when involved in these microbial pathways, where $\delta^{18}O$ has been found to increase in residual sulfate during microbial sulfate reduction (Mizutani and Rafter, 1969; Böttcher et al., 1998; Brunner et

al., 2005b, 2012; Turchyn et al., 2010; Antler et al., 2013). These rules of thumb can be complicated by situations where the sulfur cycle is tightly coupled between sulfur reducers and oxidizers and results in no measurable consumption of sulfate or sulfide. Aptly named, “cryptic sulfur cycling” occurs in settings where the rates of sulfate reduction and sulfide oxidation are equal. This is most likely to occur near the top of the euxinic zone, where sulfate reduction is occurring but at a rate that is readily matched by rapid microbial sulfide oxidation that immediately and quantitatively returns the produced sulfide back to the sulfate pool. Though the throughput of sulfur could be large, cryptic sulfur cycling does not produce any measurable net flux of sulfur between oxidized and reduced pools or any of the associated sulfur isotope effects. It does, however, result in distinct alterations to the oxygen isotope composition of sulfate (Aller et al., 2010).

These end-products of microbial sulfur cycling can react to form minerals, such as pyrite (FeS_2), barite (BaSO_4), or carbonate that has incorporated sulfate (carbonate associated sulfate, or CAS) into the mineral lattice. These minerals are then deposited and preserved in marine sediments, the isotopic compositions of which can be analyzed as proxies for past microbial activity. If modern water column dynamics are fully calibrated, then changes in these isotope signatures observed in the sedimentary record can be used to reconstruct the redox state and the predominant sulfur metabolisms that were operative in ancient aquatic environments and to follow how these environments changed over time (Canfield and Teske, 1996; Farquhar et al., 2000; Johnston, 2011; Leavitt et al., 2013).

1.3.2. Stable isotope reporting

Isotope compositions are reported in standard δ notation as follows:

$$\delta = \left(\frac{R_{sample}}{R_{standard}} - 1 \right)$$

where $R = {}^{34}\text{S}/{}^{32}\text{S}$ or ${}^{18}\text{O}/{}^{16}\text{O}$ and δ is a number expressed as a fraction of 1000 in permil (‰). Samples with positive δ values ($> 0\text{‰}$) are enriched in the heavier isotope relative to the standard, and negative δ values are depleted in the heavier isotope.

Differences in δ values between samples of the same substance can indicate a difference in the processes that were involved in the formation of the substance or that have acted on the substance following its formation.

The isotopic offset between two molecules is calculated as $\Delta_{AB} = \delta_A - \delta_B$. Herein, the sulfur isotopic difference between water column sulfate and sulfide is $\Delta^{34}\text{S}_{\text{SO}_4\text{-H}_2\text{S}} = \delta^{34}\text{S}_{\text{SO}_4} - \delta^{34}\text{S}_{\text{H}_2\text{S}}$, and the oxygen isotope offsets between sulfate and water is $\Delta^{18}\text{O}_{\text{SO}_4\text{-H}_2\text{O}} = \delta^{18}\text{O}_{\text{SO}_4} - \delta^{18}\text{O}_{\text{H}_2\text{O}}$. These differences can be used to assess the extent of sulfate reduction in the water column and/or the mechanisms of sulfide oxidation. This approach allows one to characterize the extent of fractionation; however, a more accurate calculation is used for the modelling presented below. For these numerical treatments, the fractionation between two compounds and their respective isotope ratios (R_A and R_B) is represented as the enrichment factor (ϵ) where $\epsilon = (R_A/R_B - 1)$ is expressed in ‰.

A modeling approach using paired sulfur and oxygen isotopes of sulfate was used to assess relative rates and internal reaction pathways occurring during dissimilatory sulfate reduction (Antler et al., 2013; Gilhooly et al., 2016). These models are functions which produce arrays along which $\delta^{34}\text{S}_{\text{SO}_4}$ and $\delta^{18}\text{O}_{\text{SO}_4}$ measurements taken from each respective sample might fall when plotted against one another in a $\delta^{34}\text{S}_{\text{SO}_4}$ - $\delta^{18}\text{O}_{\text{SO}_4}$

isotope plot. The model inputs include the ratios of forward and backward fluxes of sulfur at three steps along the dissimilatory sulfate reduction pathway. These input ratios determine the shape of the modelled array, where no reverse flux will produce a straight line, and increasingly larger reverse fluxes will generally produce solutions that are increasingly curvilinear. The best fit solution to the measured $\delta^{34}\text{S}_{\text{SO}_4}$ - $\delta^{18}\text{O}_{\text{SO}_4}$ data provides insight into the movement of sulfur through the sulfate reduction pathway (Figure 2).

The forward and backward sulfur flux ratios ($X = b/f$) and associated isotope fractionations serving as inputs to the model are those that occur during (1) the uptake of sulfate into the cell (X_1 ; $\epsilon^{34}\text{S} = -3\text{‰}$; $\epsilon^{18}\text{O} = -0.75\text{‰}$), (2) the reduction of adenosine 5'-phosphosulfate (APS) to sulfite (X_2 ; $\epsilon^{34}\text{S} = 25\text{‰}$; $\epsilon^{18}\text{O} = 6.25\text{‰}$), and (3) the reduction of sulfite to sulfide (X_3 ; $\epsilon^{34}\text{S} = 25\text{‰}$; $\epsilon^{18}\text{O} = 6.25\text{‰}$). When sulfate reduction rates are rapid, all sulfate taken in by the cell is ultimately reduced to sulfide and no back-reaction occurs. In this case, the product $X_1 \cdot X_3$ will equal 0 so the model output will be a solution to the linear function,

$$\delta^{18}\text{O}_{\text{SO}_4(t)} = \frac{\epsilon^{18}\text{O}_{total}}{\epsilon^{34}\text{S}_{total}} \cdot \left(\delta^{34}\text{S}_{\text{SO}_4(t)} - \delta^{34}\text{S}_{\text{SO}_4(o)} \right) + \delta^{18}\text{O}_{\text{SO}_4(o)}$$

where the sulfur isotope composition of the residual sulfate pool ($\delta^{34}\text{S}_{\text{SO}_4(t)}$) is dependent only on the total isotope fractionation factors for oxygen and sulfur along the entire reduction pathway ($\epsilon^{34}\text{S}_{total}$ and $\epsilon^{18}\text{O}_{total}$), and the initial sulfur and oxygen isotope compositions of the sulfate pool ($\delta^{34}\text{S}_{\text{SO}_4(o)}$ and $\delta^{18}\text{O}_{\text{SO}_4(o)}$).

When sulfate reduction rates are relatively slow, back-reactions result in a non-linear response that can be modelled according to,

$$\delta^{18}\text{O}_{\text{SO}_4(t)} = \delta^{18}\text{O}_{\text{SO}_4(\text{A.E.})} - \exp\left(-\theta_0 \cdot \frac{\delta^{34}\text{S}_{\text{SO}_4(t)} - \delta^{34}\text{S}_{\text{SO}_4(o)}}{\varepsilon^{34}\text{S}_{\text{total}}}\right) \cdot \left(\delta^{18}\text{O}_{\text{SO}_4(\text{A.E.})} - \delta^{18}\text{O}_{\text{SO}_4(o)}\right)$$

which is additionally dependent on the apparent equilibrium oxygen isotope composition of sulfate ($\delta^{18}\text{O}_{\text{SO}_4(\text{A.E.})}$) and a term (θ_0) that describes the relationship between oxygen

isotope exchange and the rate of sulfate reduction, where $\theta_0 = \frac{X_1 \cdot X_2 \cdot X_3}{1 - X_1 \cdot X_2 \cdot X_3}$. In summary,

these models replicate either the linear trend observed during relatively rapid rates of sulfate reduction or the curvilinear trajectories during relatively slow rates of sulfate reduction (Figure 2). Note that $\delta^{18}\text{O}_{\text{SO}_4}$ values asymptotically approach an upper bound in the curvilinear trend. Sulfate that has been reoxidized back along the DSR pathway and reintroduced to the sulfate pool will have an equilibrated $\delta^{18}\text{O}$ value ($\delta^{18}\text{O}_{\text{SO}_4(\text{A.E.})}$) that is equal to the value of $\delta^{18}\text{O}_{\text{H}_2\text{O}}$ plus the value of $\varepsilon^{18}\text{O}_{\text{total}}$. These values are fixed in this model, so $\delta^{18}\text{O}_{\text{SO}_4(t)}$ will approach the value of $\delta^{18}\text{O}_{\text{SO}_4(\text{A.E.})}$ over the course of sulfate reduction.

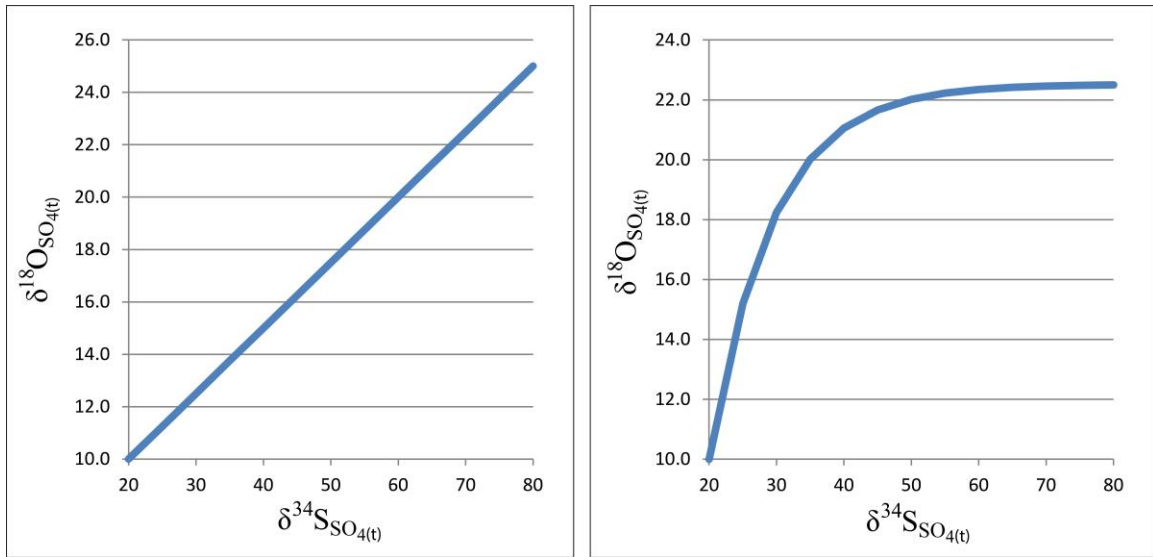


Figure 2: Example of paired sulfur and oxygen model demonstrating the array of solutions for rapid (linear) and slow (curvilinear) rates of sulfate reduction.

1.4. Project significance

Presented here is a combined genetic and isotopic study of four meromictic lakes in the Pacific Northwest that harbor diverse and varied communities of sulfur-metabolizing bacteria. This work was conducted to investigate the relationships between sulfate concentration, sulfur bacterial community structure, and the isotope composition of sulfate and sulfide in natural euxinic environments. Water column profiles for each lake were constructed that detail the abundance of key sulfur metabolisms, sulfur and oxygen isotope variability, and various chemical and physical parameters. The range of environmental and ecological conditions in the lakes helps elucidate how the interplay between biology and environment results in the isotopic variability recorded in sedimentary sulfates and sulfides. The relationships between these lake profiles provide a valuable vantage point in exploring the ways in which bacterial community structure and environmental differences can contribute to the sulfur isotope composition in modern

euxinic environments. Water column isotope chemistry and paired genetic analyses were conducted to better interpret the sulfate and sulfide isotope variability in the context of the community structure of the sulfur metabolizing bacteria that produced these isotopic fingerprints.

II. MATERIALS AND METHODS

2.1. Study sites

Cleland Lake is in southeast British Columbia, Canada ($50^{\circ}49'N$, $116^{\circ}23'W$), and Lime Blue Lake, Castor Lake, and Scanlon Lake ($48^{\circ}32'N$, $119^{\circ}35'W$) are in northern Washington, USA (Figure 3). The lithology of the Cleland catchment is composed of siliciclastic carbonate metasedimentary rock of the Mesoproterozoic Purcell Supergroup (Cui et al., 2017). Lime Blue, Castor, and Scanlon Lakes are in the same lithology composed of metasedimentary and metavolcanic rocks of the Triassic Cave Mountain Formation (Washington State Department of Natural Resources Division of Geology and Earth Resources, 2016).

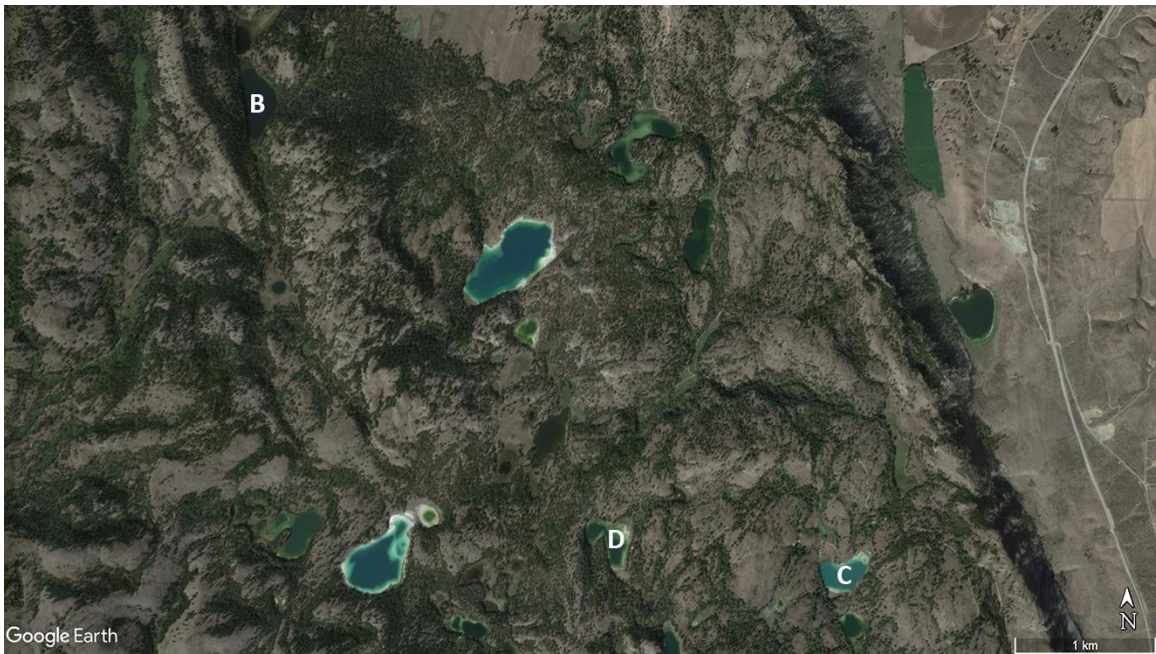


Figure 3: Areal imagery of the study lakes – Cleland Lake, British Columbia, Canada (A), and Lime Blue Lake (B), Castor Lake (C), and Scanlon (D), Washington, USA.

The lakes were stratified at the time of our sampling, and sediment cores from Lime Blue, Castor, and Scanlon lakes are each laminated. The laminae in the cores have been undisturbed since the deposition of a 5 cm tephra layer present in each core, which is a strong indication that the bottom waters in each lake have been devoid of oxygen since at least the deposition of this tephra layer. The tephra layer was deposited during the 470 yr BP Mount St. Helens eruption, and this layer is present in many cores collected from lakes in the Pacific Northwest (Mullineaux, 1996).

The lakes ranged in depth, with Scanlon Lake (6 m) being the shallowest, Castor and Lime Blue (11.5 m and 16 m respectively) being of intermediate depth, and Cleland Lake (30 m) being the deepest. All lakes had euxinic bottom waters. Sulfur in these lakes is derived from weathering bedrock in their catchments. For example, fragments of pyritic shale and slate were found along the shores of Castor Lake and Lime Blue Lake, and heavily fractured bedrock of the same lithology was exposed on the hillsides.

2.2. Water column sampling

Water column profiles for dissolved oxygen, temperature, pH, salinity, turbidity, conductivity, and oxidation-reduction potential (ORP) were taken with a Hydrolab (OTT HydroMet). Water samples were collected at discrete depths using a peristaltic pump and a custom sampling intake designed not to disturb the vertical structure of the water column (Gilhooly, unpublished). The sampling head consisted of two 13 cm square acrylic plates affixed by plastic bolts in the corners with a 0.5 cm gap. This design draws water horizontally over a large area, which reduces the fraction of water pulled from

depths above and below the intended sampling depth. This design is particularly useful when large gradations in redox occur over small depth intervals.

1 L of unfiltered water was collected from each sampling depth in plastic bottles for stable isotope analysis. For samples collected from anoxic waters, 5 g of zinc acetate dihydrate was added to the collection bottles before sampling to convert free sulfide to zinc sulfide, which is much more resistant to oxidation. These bottles were also purged with argon shortly before collection to prevent oxygen exposure while filling. Two 5 ml volumes of water were collected for ion chromatography and water isotope analysis. 25 mg zinc acetate was added to anoxic ion chromatography sample vials. Elemental sulfur samples were collected in 15 ml volumes and injected into sealed glass vials containing 15 g chloroform, which is miscible with elemental sulfur and highly toxic, preventing microbial oxidation of the sample. Samples were kept chilled on the boat and stored in coolers kept cold with ice until transferred to a laboratory refrigerator.

Sulfide concentrations were measured in the field at the time of sample collection, with the exception of Cleland Lake samples, which were analyzed in the lab at IUPUI using high pressure liquid chromatography (HPLC). Total dissolved sulfide was determined using a modified Cline method (Cline, 1969) and a field spectrophotometer (Hach DR 2800). Lake water was mixed with 0.5 ml of sulfuric acid solution and 0.5 ml of methylene blue solution (Hach) and left to react for 5 minutes. Solutions turned shades of blue in proportion to the amount of sulfide in the sample. The intensity of this color change was measured by absorbance at 665 nm of solutions with a target concentration of $520 \mu\text{g/L S}^{2-}$ (95% confidence interval within $\pm 16 \mu\text{g/L S}^{2-}$).

DNA samples were collected by anaerobically filling sterile syringes with 50ml of sample water and expressing the water through a sterile 0.22 μm Sterivex filter cartridge. Filters were sealed in sterile centrifuge tubes and kept chilled on the boat until they were stored in dry ice on shore.

2.3. Water sample preparation

Zinc sulfide precipitate was filtered from 1 L lake water samples onto 0.22 μm cellulose acetate membrane filters. Acid volatile sulfide (AVS) was liberated from the filtered solids by cold 6 N hydrochloric acid extraction for 45 minutes. In this process, sulfide volatilized by the acid was carried by nitrogen carrier gas into a 10% ammonium hydroxide trap, containing 5% zinc acetate, where the sulfide gas was reprecipitated back into zinc sulfide. AVS extraction was necessary because lake water samples were not filtered upon collection, so the zinc acetate precipitates in sample bottles also contained material that was suspended in the sampled lake water. Volatilizing out only the sulfide during these extractions separated sulfide from other, solid forms of sulfur (organic, elemental, etc.) that may have been present in the sample and may have had sulfur isotope compositions different than the sulfide. The bubble traps containing zinc sulfide were converted to silver sulfide by addition of 10% silver nitrate solution and allowed to react for 24 hours. Silver sulfide suspensions were filtered onto 0.22 μm filters, dried at 60 $^{\circ}\text{C}$, and homogenized into a fine powder for sulfur isotope analysis.

Filtrate from the 1 L samples was reacted with 200 ml of barium chloride solution (250 g/L) to form barium sulfate and allowed to react for 24 hours. Barium sulfate solids were then filtered onto 0.22 μm cellulose acetate filters, briefly acidified with 3N HCl to

remove barium carbonate co-precipitates, rinsed to neutral pH, dried at 60 °C, and homogenized into a fine powder for sulfur isotope analysis.

2.4. Stable isotope measurements

Approximately 400 µg (\pm 20 µg) of silver sulfide or barium sulfate precipitate was weighed into 3x5 mm tin cups and mixed with 3 mg vanadium pentoxide to ensure complete combustion. The isotope composition of sulfides and sulfates were measured on a Delta V Plus (Thermo) isotope ratio mass spectrometer (IRMS) connected under continuous helium flow to an elemental analyzer (Costech Analytical). Sulfur samples were combusted to sulfur dioxide at 980 °C and separated from other combustion gases on a 2 m GC column at 90 °C then transferred by helium carrier gas into the IRMS. Sample data were normalized to Vienna Canyon Diablo Troilite (VCDT) using references IAEA-S-1 ($\delta^{34}\text{S} = -0.30\text{‰}$), IAEA-S-2 ($\delta^{34}\text{S} = +22.62\text{‰}$), and IAEA-S-3 ($\delta^{34}\text{S} = -32.49\text{‰}$) for sulfides and NBS 127 ($\delta^{34}\text{S} = 21.1\text{‰}$), IAEA-SO-5 ($\delta^{34}\text{S} = 0.49\text{‰}$), and IAEA-SO-6 ($\delta^{34}\text{S} = -34.05\text{‰}$) for sulfates. Analytical precision based on replicate analyses of reference materials was within 0.2‰.

Oxygen isotopes of sulfate were measured by weighing 150 µg (\pm 10 µg) of barium sulfate into 3x5 mm silver cups and mixed with 3 mg graphite powder to ensure complete reaction. Sulfate-oxygen was converted into carbon monoxide by pyrolysis at 1400 °C in a TC/EA (Thermo) coupled to the IRMS under continuous helium flow. Raw sample data were corrected to Vienna Standard Mean Ocean Water (VSMOW) using reference materials NBS 127 ($\delta^{18}\text{O} = +8.59\text{‰}$), IAEA-SO-5 ($\delta^{18}\text{O} = +12.13\text{‰}$), and IAEA-SO-6 ($\delta^{18}\text{O} = -11.35\text{‰}$). Analytical precision was within 0.3‰.

Water isotope samples were filtered (0.22 μm) and analyzed for $\delta^{18}\text{O}$ using a Picarro L2130-I Analyzer. Coupled to the Picarro was an autosampler and high precision water vaporizer unit. Drift and memory were corrected for using the methods presented in Van Geldern and Barth (2012). These corrected values were further corrected to the Vienna Standard Mean Ocean Water (VSMOW) using standards from Los Gatos. Precision for $\delta^{18}\text{O}$ was 0.1‰.

2.5. Ion and sulfur concentration measurements

Dried weights of silver sulfide and barium sulfate recovered for stable isotope measurement were used to gravimetrically verify sulfide and sulfate concentrations at each sample depth. These gravimetric calculations were corrected using the percent sulfur value measured during isotopic analysis. Concentrations of sulfate and chloride were also measured by ion chromatography (Thermo, Dionex ICS-1100).

Elemental sulfur concentrations were measured from the whole water samples by HPLC (Thermo, Ultimate 3000). A glass syringe was used to extract chloroform with dissolved elemental sulfur from the field collection vials. The chloroform was allowed to evaporate in glass vials. HPLC grade methanol was then added to the vials, resolubilizing the sample. Aliquots of the samples were then run through the HPLC. Those samples with elemental sulfur concentrations outside of the detection range of the instrument were rerun after being serially diluted with HPLC grade methanol until a measurable concentration was obtained.

2.6. Genetic Sequencing

The Sterivex filter cartridges were shipped on dry ice to Dr. EJ Crane's laboratory at the Department of Biology of Pomona College in Claremont, California. Here, samples were prepared using the DNeasy PowerWater Sterivex kit (Qiagen) and sent to MR DNA in Shallowater, TX for Illumina sequencing of the 16s rRNA Gene.

Sample DNA was amplified at MR DNA using primers targeting the V4 variable region of the 16s rRNA gene. The forward primers contained barcodes (explained in section 2.7). DNA was processed through 30 cycles of PCR using the HotStarTaq Plus Master Mix Kit (Qiagen, USA). The first cycle was run at 94 °C for 3 minutes. The following 28 cycles were each run at 94 °C for 30 seconds, 53 °C for 40 seconds and 72 °C for 60 seconds. The final elongation step was run at 72 °C for 5 minutes.

The success of the amplification was checked by electrophoresis of the PCR products in 2% agarose gel. This was also used to group the PCR products into pools according to molecular weight and DNA concentration. Calibrated Ampure XP beads were then used to purify the pooled samples. DNA libraries (collections of DNA strands of similar length with known barcodes) were then prepared from the purified pools using the Illumina TruSeq DNA library preparation protocol. The DNA libraries were sequenced on a MiSeq using manufacturer guidelines.

2.7. Operational Taxonomic Units

The returned sequence data was used to generate a table of operational taxonomic units (OTUs). OTUs are clusters of sequence reads that are sufficiently similar to each other such that they can be considered representative of a single taxon. A standard

threshold of 97% sequence similarity was used to differentiate OTUs. Once OTU clustering was performed on all reads in the sample set, the relative abundance of each OTU was calculated and compared across samples to reveal differences in community structure between samples.

OTU clustering was performed using an open-reference method. This method clusters similar sample sequences around sequences with known taxonomies in a reference database. In addition to this, all reads that do not have sufficiently close matches in the database are then clustered de novo. Open-reference clustering was used here so that OTUs comprised of reads that did not have close database matches could still be included in subsequent analyses. This method was chosen over two others: (1) Closed-reference clustering, which, like open reference clustering, compares each read in a sample set to a reference database, but produces OTU tables constructed only from reads that are sufficiently similar to sequences in the reference database and discards all reads that are not. (2) De novo OTU clustering generates OTUs by clustering reads against each other without referring to an external sequence database - only sequence similarity between reads in a sample set are used to establish OTU clusters. This was not preferred because, without the use of a reference database, no taxonomies are assigned to OTUs, which would preclude functional analyses.

Fastq is the preferred file format for CLC Workbench, the software in Dr. Christine Picard's laboratory that was used for most of the genetic analyses in this work. The sequence data received from MR DNA came in the form of fasta files, which are files that contain a set of reads (sequences of base pairs) in plain text (Figure 4). Fasta files consist of discrete, alternating lines – one line containing a read label and metadata,

followed by a line containing the base pairs in that read. Quality scores for each nucleotide in the read were also recorded during sequencing. A higher quality score for a nucleotide indicates higher confidence that that nucleotide was read correctly. These quality scores are stored in a separate qual file. Fasta and qual files can be combined into a single fastq file, which contains combined sequence and quality data for each read.

```
>15L::M02542:55:000000000-ACR4C:1:2110:12409:4033 1:N:0:5
AACGAACGCTGACGGCGTGCTTAACACACGCAAGTCGCACGAGAATTTCCGCCTTCGGGTGGAATAGTAAAGTGGC
>28::M02542:55:000000000-ACR4C:1:2111:21983:16196 1:N:0:5
ATTGAACGCTGGCGGCATGCCTAACACATGCAAGTCGAACGCGAAAGGGCTTTGGCCTGAGTAGAGTGGCGGACGG
>15L::M02542:55:000000000-ACR4C:1:1106:25157:19549 1:N:0:5
AACGAACGCTGGCGGCATGCCTAACACATGCAAGTCGGACGCGAAAGGGAATTCGGTCCTGAGAAGAGTGGCGCAC
>15L::M02542:55:000000000-ACR4C:1:2107:25641:7400 1:N:0:5
GACGAACGCTGGCGGCATGCCTAACACATGCAAGTCGAACGATGAAGCTGGAGCTTGCTCCAGTGGATTAGTGGCG
>14L::M02542:55:000000000-ACR4C:1:2107:26419:12864 1:N:0:5
GACGAACGCTGGCGGCATGCCTAACACATGCAAGTCGAACGGGGTATATTTAGCAATAAATGTATCTAGTGGCGGA
```

Figure 4: Example of several lines within a fasta file.

MR DNA sent two sets of fasta and qual files, one set with reads that still contained barcode and primer sequences and one set with reads that were trimmed of primers and barcodes. Barcodes are short nucleotide sequences (those used by MR DNA were 8 bases in length) added to the beginning of each amplicon. Because all samples were processed together in a single Illumina sequencing run, all sequence reads were included in a single output fasta file and barcodes were used to sort amplicon sequences back into groups according to the samples that they originated from. Each barcode was unique to one sample, so 7 different barcodes were used in the run containing the 7 samples collected in this study. The untrimmed reads in this fasta file also contained the primer sequence that was used when amplifying the sample DNA. The trimmed fasta file

contained reads that were trimmed of their barcodes and primer sequences and, instead, the label metadata of each read contained the name of the sample the read originated from. This trimmed fasta file was used to avoid unnecessary trimming and demultiplexing (sorting reads into their respective samples).

The trimmed fasta file was combined with its corresponding qual file, converted to fastq format using the FastqFastaQualConverter software available on the MRDNA website. After conversion, the fastq file was imported into CLC Genomics Workbench using the Illumina import method. The reads in the fastq file were not paired, so the “paired reads” option was not selected. “Remove failed Reads” was the only radio button selected. After importing, the reads were sorted into their respective samples based on the read names using the “Sort Sequences by Name” feature in CLC Workbench to separate fastq files created for each sample.

The creation of OTU tables in CLC requires a “trim adapter list”, which is a list of sequences that are designated to be trimmed in the workflow. Because the fastq file was already trimmed, a new “blank” trim adapter list was created that contained no sequences. Creation of OTUs also required a reference database, which was downloaded within the software using the “Download Amplicon-Based Reference Database” feature. Greengenes, UNITE, and SILVA were available, but only SILVA was used in this study because Greengenes, at the time of writing this, has not been updated since 2013, and UNITE contains only fungal sequences. SILVA contains both prokaryote and eukaryote sequences and is still actively updated. SILVA v132 was the version available for download in CLC Workbench, so this is the version that was used to generate the OTU table.

The “Data QC and OTU Clustering” workflow was used to create the OTU table, and default values were used unless otherwise specified. The SILVA 16S v132 97% reference database was used, and the similarity percentage threshold for OTU clustering was set to be determined by the database (97%). The “Allow creation of new OTUs” option was selected. This option enables open-reference clustering, which clusters sequences that are below the specified sequence similarity of 97% to any sequence in the reference database into de novo OTUs. The taxonomy similarity percentage sub-option at this step was left at the default value of 80%. The output of this operation is a single OTU table, containing taxonomic assignments for most OTUs, abundances of each OTU in each sample, and the representative centroid sequence for each OTU. OTUs with a combined abundance across all samples lower than 10 were discarded.

Centroid sequences of de novo OTUs were searched on BLAST using both the Microbial Nucleotide and Standard Nucleotide queries (blast.ncbi.nlm.nih.gov/Blast.cgi), on the 16S-based ID tool on EZBioCloud (ezbiocloud.net) (Yoon et al., 2017), and on SILVA’s ACT web tool (arb-silva.de/aligner) to check relatedness to sulfur taxa.

2.8. Functional analysis

OTUs were then annotated with the functional roles each might play in the sulfur cycle. This was done by searching the literature for either empirical or genetic evidence of sulfur metabolic activity on the part of the taxa assigned to each OTU. Metabolic pathways of primary interest were those in which both the substrate and product are inorganic sulfur compounds (e.g., sulfate, elemental sulfur, thiosulfate, sulfide), and where the redox operations carried out on these compounds are used for energy

derivation (e.g., dissimilatory sulfate reduction) rather than metabolic reactions that acquire sulfur for use nutritionally (e.g., assimilatory sulfate reduction).

Research on each OTU typically began by searching the NCBI Taxonomy Browser for the lowest level taxon assigned for the OTU, which was most often at the genus level, to assess the known breadth of diversity within the taxon. To further refine this information, the taxon was then searched on the BacDive and KEGG databases. The advanced search tool on BacDive (<https://bacdive.dsmz.de/advsearch>) was used to find specific metabolite utilization within a taxon, and the publications that demonstrated the metabolite utilization. The sulfur pathway map on the KEGG website (https://www.genome.jp/kegg-bin/show_pathway?map00920) was also used to search across a list of all species in the KEGG database that possess genes that encode for enzymes involved in sulfur cycling. Taxa were then searched in reference books (e.g., “The Prokaryotes” series and “Bergey's Manual of Systematics of Archaea and Bacteria”) and then across the literature using Google. This process was also carried out for parent (higher) and child (lower) taxa in cases where the available evidence for sulfur metabolism in a specific taxon was ambiguous.

OTUs that were assigned to taxa with members known to metabolize sulfur were organized into seven functional categories: (1) green sulfur bacteria, (2) purple sulfur bacteria, (3) sulfate reducers, (4) sulfur disproportionators, (5) sulfur oxidizers, (6) sulfur reducers, and (7) those which can both reduce and oxidize sulfur facultatively. Many sulfur bacteria utilize multiple intermediate forms of sulfur (thiosulfate, sulfite, elemental sulfur, etc.). Because knowledge of the sulfur substrates used by many taxa is incomplete in the literature, and because substrate utilization is not always uniform within a given

taxon, “sulfur” in these functional names refers to any inorganic sulfur compound other than sulfate.

Green sulfur bacteria and purple sulfur bacteria were exceptions to these conventions and were given functional classifications designating their membership within the PSB or GSB, rather than being categorized as sulfur oxidizers. This was done because all members of these two groups share the same functional role (sulfide oxidation) and, as phototrophs with differing shade tolerances, their biomarkers been used to infer the depth of Proterozoic photic zone euxinia (Brocks et al., 2005), so they carry additional significance beyond their immediate role in the sulfur cycle.

If no evidence of sulfur metabolism was found in the literature for a particular taxon, then associated OTUs were classified as “Unknown”. If evidence to the contrary was found, then associated OTUs were classified as “Unlikely”. In cases where evidence was found of assimilatory sulfur pathways or where taxa degrade organic sulfur compounds and produce a mineralized sulfur product, the associated OTUs were classified as “adjacent” to the sulfur community. OTUs that fell into these three categories were not included as sulfur bacteria in the results or subsequent analyses.

When it was evident that some child taxa (a commonly used term synonymous to sub-taxa; for example, species are child taxa of a “parent” genus, which is in turn a child taxon of a family) of the lowest classified taxon for an OTU possess a particular sulfur pathway and some do not, the associated OTUs were evaluated as “potentially” possessing that pathway. For example, many sulfate reducing bacteria can disproportionate intermediate sulfur compounds in addition to reducing sulfate. In cases where all members of a taxon do sulfate reduction and only some members do

disproportionation, those associated OTUs were labeled “sulfate reducer/potential disproportionator”. Likewise, OTUs associated with taxa in which some members oxidize thiosulfate while the rest were not known to metabolize sulfur at all were labeled “Potential sulfur oxidizer”. OTUs were also classified as potential sulfur bacteria if a sulfur pathway was ubiquitous among the known members of its associated taxon but that taxon had few validly published members, especially if the taxon was at a high level (e.g., class *Kiritimatiellae*). This line of research was done for each OTU until there were none remaining with an abundance in a sample greater than 1% of the combined abundance of all classified sulfur OTUs (“potential” sulfur OTUs included) in that sample.

2.9. A note on abundances

When amplifying DNA samples during PCR, the affinity that amplification primers have for primer targets on sample sequences varies due to natural variation in primer target sequences. This results in sequences with higher affinity primer targets getting amplified more times over than sequences with lower affinity primer targets. Because of this PCR bias, sequences with higher affinity primer targets tend to be overrepresented in the resulting reads when the amplified samples are sequenced. Interpreting abundance counts in OTU tables was done with caution because there is not a reliable way to correct for PCR bias.

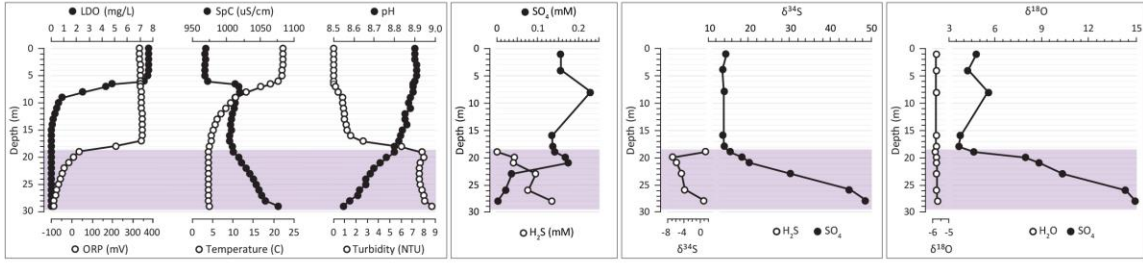
Because of PCR bias, abundances of individual OTUs do not always directly represent the abundances of their corresponding taxa in the original sample. Differences in the abundance of an individual OTU between samples, however, might represent a real

difference. This interpretation must be weighed against the fact that OTUs are clusters of sequences, each of which might be subject to a different degree of PCR bias. It is possible that a single OTU that appears in several different samples could be comprised of some sequences that are unique to individual samples, and these sequences might be subject to differing degrees of PCR bias.

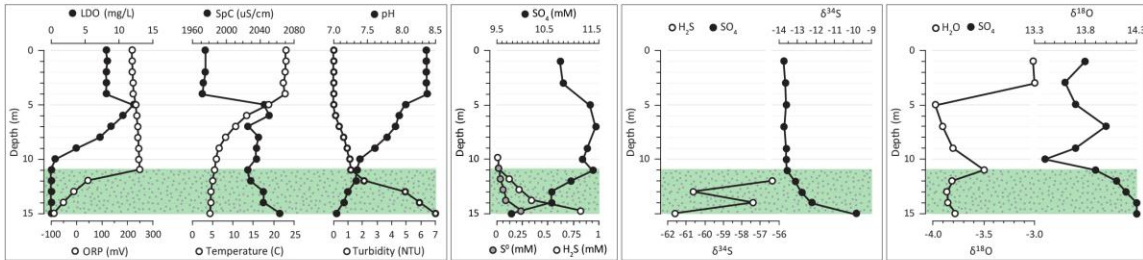
Grouping OTUs into functional groups and then summing their abundances, as done in this study, potentially mitigates the effect of PCR bias, as each additional OTU included in a functional group would have the effect of smoothing out the biases affecting the individual OTUs. In cases where an individual OTU represents the majority of a functional group in a sample, PCR bias will likely affect the abundance of that functional group in that sample. Regardless, OTUs and functional groups that comprise large percentages of the total sulfur bacteria in sample post-PCR still likely comprise large percentages of the community in their source environments and the abundances provided in the results below still bear interpretive power.

III. RESULTS

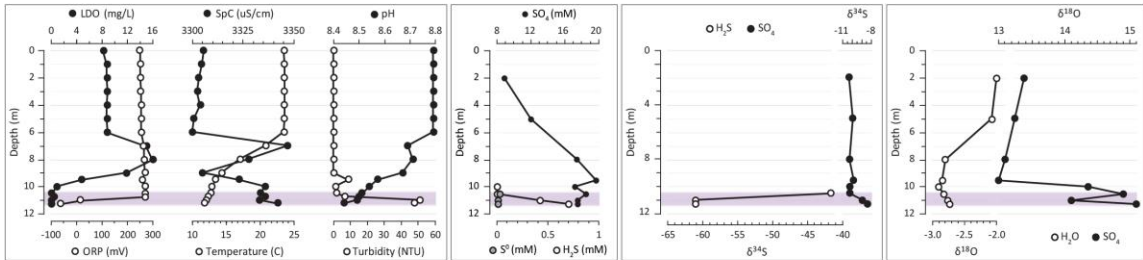
Cleland



Lime Blue



Castor



Scanlon

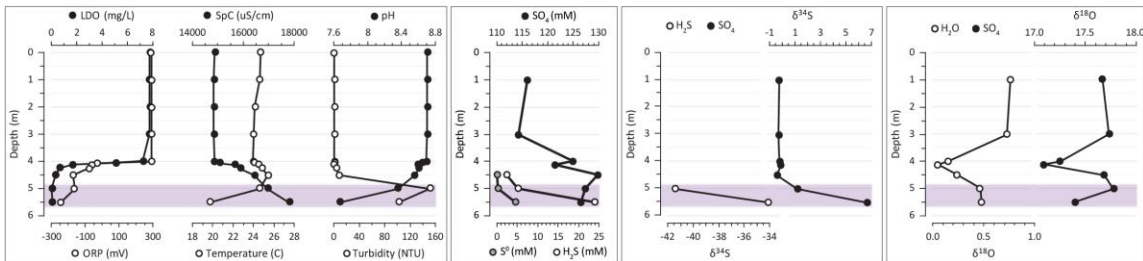


Figure 5: Water column profiles of dissolved oxygen (LDO), specific conductivity (SpC), pH, sulfate concentrations (SO₄), elemental sulfur concentrations (S⁰), sulfide concentrations (H₂S), the sulfur isotope compositions of sulfide and sulfate, and the oxygen isotope compositions of sulfate and water for all four study lakes. The shaded areas depict the depths where purple sulfur bacteria (in purple) or a mixture of green sulfur and purple sulfur bacteria (in green) were observed.

3.1. O₂, conductivity, pH, and temperature

Water column profiles of the study lakes varied markedly between one another in sulfate concentration and depth, as well as how abruptly redox state changed across the chemocline. Cleland Lake was the deepest study lake (29 m). Oxygen disappeared below 15 m water depth. Well above the redoxcline, there was a sharp 5% increase in conductivity (from ~970 to ~1015 $\mu\text{S}/\text{cm}$) between 6 and 6.5 m. This change in conductivity coincided with the onset of decreasing dissolved oxygen concentrations. Temperature also began to decrease at this depth, with a constant temperature of 21 °C above 6 m, decreasing monotonically to approximately 4 °C in the bottom waters. pH decreased from 8.90 at the surface to 8.55 in the bottom waters. The sharp increase in conductivity and the gradual decrease in temperature indicate that salinity, not temperature, was the driver of stratification in Cleland.

Lime Blue had a similar dissolved oxygen profile to Cleland but was much shallower, at 15 m. Oxygen and temperature begin to drop below the halocline between 4 and 5 m, which was about a meter above the halocline depth observed in Cleland Lake. Specific conductivity increased with depth from 1970 at the surface to 2063 $\mu\text{S}/\text{cm}$ at 15 m. Dissolved oxygen concentrations were 8.05 mg/L at the surface, increased to a maximum concentration of 12.15 mg/L at 5 m, and then decreased to zero below 11 m. Temperature decreased from 23 at the surface to ~4.5 °C in the bottom waters. The oxidative/reductive potential (ORP) dropped sharply from 248 mV at 11 m to 45 mV at 12 m, became negative before 13 m, and reached -89 mV at 15 m.

Castor Lake was slightly shallower than Lime Blue Lake, with a maximum depth of 11.25 m. The oxygen profile here was like that of Lime Blue, increasing immediately beneath the halocline between 6 and 7 m from 8.81 to 14.96 mg/L. Oxygen then decreased, reaching zero between 10 and 10.5 m. The rise in conductivity in Castor Lake was smaller than in Lime Blue and Cleland Lakes, increasing from 3300 to 3347 $\mu\text{S}/\text{cm}$ between 6 and 7 m. Like the previous lakes, here temperature dropped gradually below the sharp increase in conductivity, indicating a halocline rather than a thermocline. Surface temperatures were around 23.50 °C, decreasing to 11.81 °C at the deepest point. ORP decreased sharply between 10.75 and 11.25 m, dropping from 270 to -62 mV.

Scanlon Lake is the shallowest of the four study lakes, with its deepest point at 6 meters at the time of sampling. It is also the most saline of the study lakes, with conductivity at the surface measured at 14875 $\mu\text{S}/\text{cm}$, increasing sharply below 4 m to values of 17000 and 17810 $\mu\text{S}/\text{cm}$ at 5 and 6 m. This sharp increase in conductivity also marked the sharpest decrease in oxygen concentration among the study lakes. Here, between 4 and 5 m, oxygen decreased from 7.27 to 0 mg/L. Like in Cleland Lake, we did not detect an increase in oxygen immediately beneath the halocline, even with the relatively higher resolution sampling done across this gradient. The largest ORP change was seen in Scanlon Lake, with surface values of 294 dropping to -279 mV at the sediment water interface. Temperature, interestingly, increased immediately below the halocline from 23.96 to 25.41 °C between 4 and 4.5 m. It then decreased to 19.92 °C at the base of the water column.

3.2. Sulfur concentrations

In Cleland Lake, the concentration of sulfate in the surface waters is 0.156 mM. Beneath the halocline, the concentration increased to 0.228 mM at 8 m. Sulfate then decreased to near-surface values between 16 and 21 m. Below this depth, sulfate sharply decreased to 0.002 mM at 28 m. Sulfide was first detected at 19 m at a concentration of 0.002 mM and had increased to 0.135 mM by 28 m. The decrease in sulfate was concomitant to the increase in sulfide. This was a near complete conversion of reactant to product within the water column.

The concentration of sulfate in Lime Blue Lake was two orders of magnitude higher than in Cleland Lake. Sulfate was approximately 11 mM within the mixolimnion and decreased below the chemocline to 9.7 mM at 15 m. Sulfide was first detected at 10 m. Dissolved sulfide had a concave-up profile, with concentrations increasing from 0.001 mM at 10 m to 0.333 mM at 14 m. The concentration at 15 m then increased more sharply to 0.814 mM, coinciding with the relatively sharp drop in sulfate concentration between 14 and 15 m.

Elemental sulfur was first detected in Lime Blue Lake at 11 m and increased in a similar fashion to sulfide. The concentration rose slowly between 11 m and 14 m, from 0.00 mM to 0.079 mM. The concentration then increased more abruptly to 0.225 mM at 15 m, coinciding with the relatively abrupt increase in sulfide and decrease in sulfate that occurred at this depth.

Castor Lake had a markedly different sulfate concentration profile from that of Lime Blue and Cleland Lakes. In Castor Lake, steadily rose from 8.9 mM at the surface to 19.7 mM at 9.5 m. There was no clear increase in concentration coinciding with the

halocline in Castor Lake, unlike in Lime Blue and Cleland Lakes. Sulfate did not appreciably decrease below the first appearance of sulfide in the bottom waters. Sulfide was first detected in Castor Lake at 10 m at a concentration of 0.001 mM. As with Lime Blue, sulfide in Castor Lake increased in concentration with depth along a concave-up profile and reached a maximum concentration of 0.970 mM at 11.25 m. Elemental sulfur was first detected at 10.5 m at 0.0295 mM and decreased over the remaining 0.75 m of the water column to 0.0045 mM at 11.25 m.

The concentration of sulfate in Scanlon Lake was substantially higher than in the other study lakes, with a surface concentration of 116 mM. Coinciding with a pronounced increase in conductivity, sulfate increased to 125 mM at 4 m. Immediately below this depth, the concentration decreased to 121 mM at 4.125 m and then increased to 130 mM at 4.5 m. Below 4.5 m, sulfate decreased gradually by approximately 3 mM to 127 mM at 5.5 m. This decrease in sulfate below 4.5 m coincided with the first appearance of sulfide and elemental sulfur. Sulfide increased with depth along a concave-up profile from 2.3 mM at 4.5 m to a maximum of 24 mM at 5.5 m. Elemental sulfur was first measured at 5 m at a concentration of 0.17 mM and increased to 4.5 mM at 5.5 m.

3.3. Stable Isotopes

Cleland Lake had the highest epilimnion $\delta^{34}\text{S}_{\text{SO}_4}$ values among the study lakes, between 13.7 and 14.6‰. ^{34}S enrichment in sulfate began at 19 m, the same depth that sulfide was first measured. Below this point $\delta^{34}\text{S}_{\text{SO}_4}$ increased significantly, reaching 48.6‰ at the maximum depth of 28 m. At 19 m, sulfide was substantially ^{34}S -enriched relative to depths immediately below. $\delta^{34}\text{S}_{\text{H}_2\text{S}}$ was 1.3‰ at 19 m and decreased to -6.8‰

at 20 m. Below this, $\delta^{34}\text{S}_{\text{H}_2\text{S}}$ steadily increased to -3.8‰ at 26 m, followed by a larger increase to 0.9‰ at 28 m. This jump in $\delta^{34}\text{S}_{\text{H}_2\text{S}}$ coincided with $\delta^{34}\text{S}_{\text{SO}_4}$ enrichment becoming more gradual between 26 and 28 m relative to shallower depths. Where sulfide was first measured, at 19 m, $\Delta^{34}\text{S}_{\text{SO}_4\text{-H}_2\text{S}}$ was relatively small at 14.2‰, due to the high $\delta^{34}\text{S}_{\text{H}_2\text{S}}$ value at this depth. $\Delta^{34}\text{S}_{\text{SO}_4\text{-H}_2\text{S}}$ increased below 19 m, jumping to 25‰ at 20 m, steadily rising to a maximum value of 48.6‰ at 26 m, then decreasing slightly to 47.7‰ at 28 m.

Surface $\delta^{18}\text{O}_{\text{SO}_4}$ values in Cleland Lake were between 3.8 and 5.6‰. Like $\delta^{34}\text{S}_{\text{SO}_4}$, $\delta^{18}\text{O}_{\text{SO}_4}$ values began to steadily increase with depth below 19 m, reaching a maximum value of 15‰ at 28 m. Also like $\delta^{34}\text{S}_{\text{SO}_4}$, $\delta^{18}\text{O}_{\text{SO}_4}$ became gradual between 26 and 28 m relative to shallower depths. $\delta^{18}\text{O}_{\text{H}_2\text{O}}$ remained constant through the water column, fluctuating between -5.7 and -5.8‰.

In Lime Blue Lake, epilimnion $\delta^{34}\text{S}_{\text{SO}_4}$ values were lower than those in Cleland Lake, starting at -13.7‰ at 1 m and remaining within 0.1‰ of this value until the disappearance of dissolved oxygen 11 m. From here, $\delta^{34}\text{S}_{\text{SO}_4}$ values increased gradually to -12.2‰ at 14 m and then more abruptly to -9.8‰ at 15 m. Sulfide was more ^{34}S -depleted in Lime Blue Lake than at every depth in Cleland Lake, with $\delta^{34}\text{S}_{\text{H}_2\text{S}}$ beginning at -56.4‰ at 12 m. Below 12 m, there was not a clear trend in $\delta^{34}\text{S}_{\text{H}_2\text{S}}$ values, as there was in Cleland Lake – $\delta^{34}\text{S}_{\text{H}_2\text{S}}$ decreased to -60.6‰ at 13 m, increased to -57.4‰ at 14 m, and then decreased to -61.6‰ at 15 m. $\Delta^{34}\text{S}_{\text{SO}_4\text{-H}_2\text{S}}$ increased from 43.3‰ at 12 m to 51.8‰ at 15 m.

$\delta^{18}\text{O}_{\text{SO}_4}$ in Lime Blue Lake was higher than in Cleland Lake, with a surface value of 13.8‰. There was not a large change in $\delta^{18}\text{O}_{\text{SO}_4}$ in Lime Blue Lake, as there was in

Cleland Lake – $\delta^{18}\text{O}_{\text{SO}_4}$ was 13.4‰ at 10 m, where sulfide was first measured, and gradually increased to 14.3‰ by 15 m. $\delta^{18}\text{O}_{\text{H}_2\text{O}}$ values were slightly higher at the surface than at depth, starting at -3.01‰ at 1 m and decreasing to -3.97‰ at 5 m. Below 9 m, there was a positive $\delta^{18}\text{O}_{\text{H}_2\text{O}}$ excursion to -3.48‰ at 11 m. $\delta^{18}\text{O}_{\text{H}_2\text{O}}$ values then increased to -3.81 at 12 m and remained within 0.05‰ of this value through the remainder of the water column.

In Castor Lake, epilimnion $\delta^{34}\text{S}_{\text{SO}_4}$ values remained near -10‰ (within 0.3‰) and began to increase below 10.5 m, where sulfide was first measured. $\delta^{34}\text{S}_{\text{SO}_4}$ was -10.25‰ at 10.5 m and increased to -8.94 and -8.40‰ at 11 and 11.25 m. Similar to Cleland Lake, $\delta^{34}\text{S}_{\text{H}_2\text{S}}$ values began relatively low at -41.6‰ at 10.5 m and then increased substantially to -60.9‰ at both 11 and 11.25 m. Starting at 10.5 m, $\Delta^{34}\text{S}_{\text{SO}_4\text{-H}_2\text{S}}$ increased from 31.4‰ to 51.9 and 52.5‰ at 11 and 11.25 m.

$\delta^{18}\text{O}_{\text{SO}_4}$ was 13.4‰ at 2 m and decreased to 13.0‰ at 9.5 m. Below 9.5 m, $\delta^{18}\text{O}_{\text{SO}_4}$ increased to 14.4‰ at 10.5 m and further to 15.1‰ at 11.25 m.

In Scanlon Lake, $\delta^{34}\text{S}_{\text{SO}_4}$ was measured at -0.2‰ at 1 m and did not begin to increase until below 4.5 m, where $\delta^{34}\text{S}_{\text{SO}_4}$ was measured at -0.4‰. At 5 m, $\delta^{34}\text{S}_{\text{SO}_4}$ increased to 1.2 and then more sharply to 6.6‰ at 5.5 m. Where sulfide was first detected at 5 m, $\delta^{34}\text{S}_{\text{H}_2\text{S}}$ was measured at -41.4‰, increasing to -31.4‰ at 5.5 m. $\Delta^{34}\text{S}_{\text{SO}_4\text{-H}_2\text{S}}$ was 42.6‰ at 5 m, decreasing to 40.7‰ at 5.5 m.

$\delta^{18}\text{O}_{\text{SO}_4}$ values did not substantially change with depth, beginning at 17.7‰ at 1 m and decreasing to 17.1‰ at 4.125 m. From here, the value increased to 17.8‰ at 5 m, decreasing slightly to 17.4‰ at 5.5 m.

3.4. Community structure of sulfur bacteria

The structures of the sulfur bacterial communities in the samples were described in terms of relative abundances of OTUs after they were binned into functional categories based on the types of sulfur metabolisms they possessed. The confidence with which an OTU could be binned in this manner is subject to several complicating factors. (1) Some bacteria that carry genes for a given metabolic pathway will not phenotypically express those genes or will express them incompletely. (2) Some taxa are replete with members that are not well characterized in the literature, particularly those that are obligate to extreme or remote niches or are difficult to cultivate. (3) Some taxa are sparse, containing fewer validly published members than candidate members that are pending placement. (4) Sometimes, not all members of even low rank taxa will share the same metabolic pathway.

These all resulted in varying degrees of likelihood that a given OTU was representative of a given sulfur metabolism and necessitated representing the microbial abundance data using two different approaches – one in which false positives were minimized but may result in more false negatives (presented in section 3.4.1), and one in which false negatives were minimized but may result in more false positives (presented in section 3.4.2). The two approaches are visualized in Figure 6.

The first approach (section 3.4.1) assigned a functional category (e.g., sulfate reduction or disproportionation) to each OTU based on the most representative metabolism observed in members within a given taxon. The approach presents abundances of functional categories by binning tallies of only OTUs belonging to taxa with members that predominantly possessed a given type of sulfur metabolism. These

OTUs were associated with taxa which have been demonstrated in the literature to be homogenous, or nearly homogenous, with respect to the sulfur metabolism shared by the members of the taxon (e.g., if all members of a taxon are known to be sulfate reducers). If only a subset of the members of a taxon had a given metabolic capacity, (e.g., if some members were sulfate reducers and the remainder did not do any kind of sulfur redox), then no OTUs associated with this taxon were assigned to the sulfate reducer category. If all members performed one type of sulfur metabolism and a subset of members conducted a second type of sulfur metabolism in addition to the first (e.g., if all members carried out sulfate reduction and some members carried out both sulfate reduction *and* disproportionation), and if it was not possible to ensure that all members of the taxon that were present in a sample shared that second metabolism, then no OTUs belonging to that taxon were considered to possess the second metabolic capacity (disproportionation in this example) – only the metabolism that was likely shared by all members of the taxon. This kind of intra-taxon metabolic diversity was accounted for in the second approach. If an OTU belonged to a taxon in which every member identically possessed two sulfur metabolisms, for example if every member did both sulfate reduction and disproportionation, then that OTU would have been binned in a functional category specific to taxa that carry out both metabolisms, though no such taxa were present in this dataset.

The second approach (section 3.4.2) presents abundances of functional categories in the same manner as the first approach – by binning OTUs according to taxa – but differs in that OTUs were not excluded if they were associated with taxa which were not metabolically homogenous. These results represent the broadest possible description of

sulfur community structure. For example, if some members of a taxon were known to oxidize sulfur, then all OTUs associated with that taxon were considered to be sulfur oxidizers, regardless if Sox was prevalent among other known members of the taxon. If multiple sulfur metabolisms had been demonstrated by members of a taxon (e.g., sulfate reduction *and* disproportionation), then OTUs associated with that taxon were assigned to a functional category that encompassed both metabolisms (e.g., sulfate reduction + disproportionation). Taxa for which there was only genetic evidence of sulfur metabolism were also included in this approach – if a member of a taxon was discovered to have the full suite of Sox genes, then all OTUs associated with that taxon were counted as sulfur oxidizers.

The tandem use of these two binning methods addresses the irreducible uncertainty inherent in the varying degrees of metabolic heterogeneity present at the lowest taxonomic levels assigned to many of the OTUs in this dataset. It resulted in two sets of abundances that serve as approximate end members – upper and lower bounds of abundance range estimates that, between the two, likely capture the real abundances of each functional category in the samples. Characterizing the metabolic composition of natural samples in this way minimizes exposure to bias, and the methods are transparent and repeatable.

It is common practice in published literature to list all the abundant taxa present in a sample and then point out which are considered the key taxa relevant to the phenomena under study. Such an approach can be problematic because it can conflate representation in two ways. (1) Representation in literature – whether a taxon is considered notable is often based on whether there has been import placed on that taxon in prior literature, so

the attention given to these members is subject to the recognizability of their names. Metabolically classifying all taxa in this dataset, though much more time consuming, circumvented the risk of leaving less widely known and/or frequently discussed taxa out of consideration. (2) Representation in the sample data – more abundant taxa are not necessarily more metabolically active than less abundant taxa. This is exemplified by anoxygenic photosynthesis in Lake Cadagno, Switzerland, where GSB represented 95% of the microbial community within the water column yet a single species of PSB was at least 25% more photosynthetically active (Storelli et al., 2013). Binning taxa into functional categories and reporting the relative abundances of those functional groups of taxa, rather than of individual taxa, minimizes the risk of conflating abundance with activity by effectively averaging the activities of each of the taxa in a group. Abundances in the following two sections have been rounded to the nearest whole percentage.

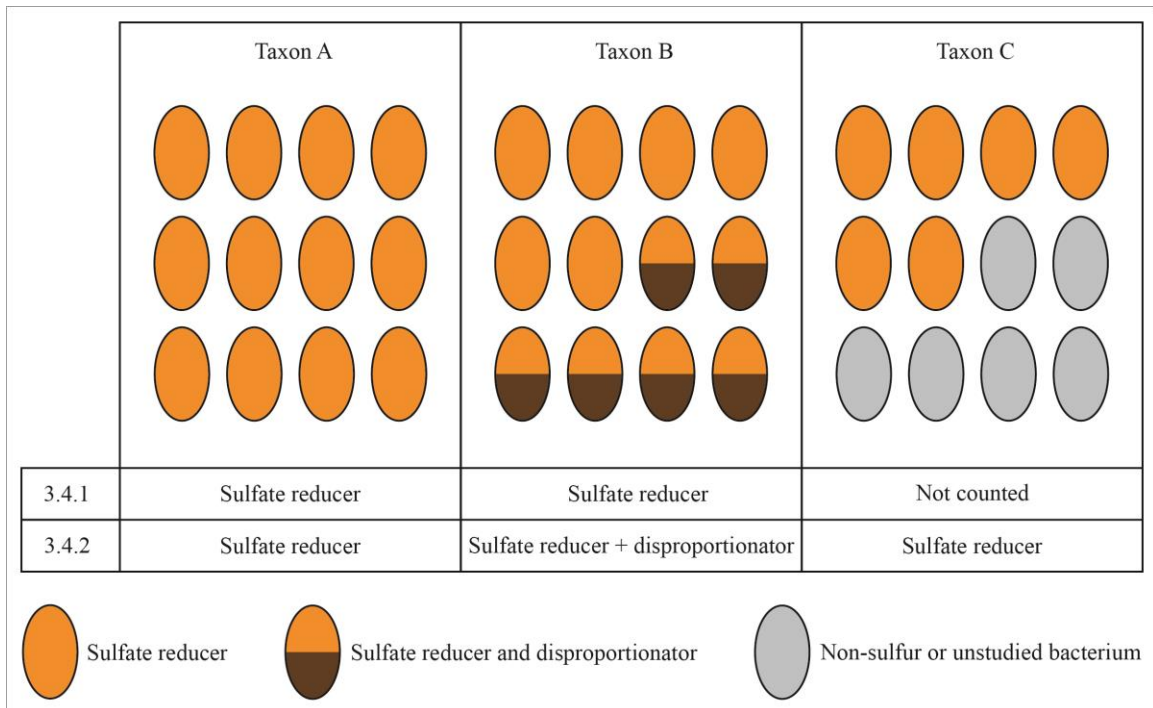


Figure 6: Visualization of how functional categories were assigned based on the metabolic composition of three hypothetical taxa.

Each oval represents a child taxon, and for the purpose of this example, all members of each child taxon share identical metabolisms. OTUs belonging to taxon A would be counted as sulfate reducers in both approaches. OTUs belonging to taxon B would be counted as sulfate reducers in section 3.4.1 and as “sulfate reducers that also disproportionate” in section 3.4.2. OTUs belonging to taxon C would not be counted as sulfur bacteria according to section 3.4.1 and would be counted as sulfate reducers in section 3.4.2.

3.4.1. Conservative representation of sulfur community structure

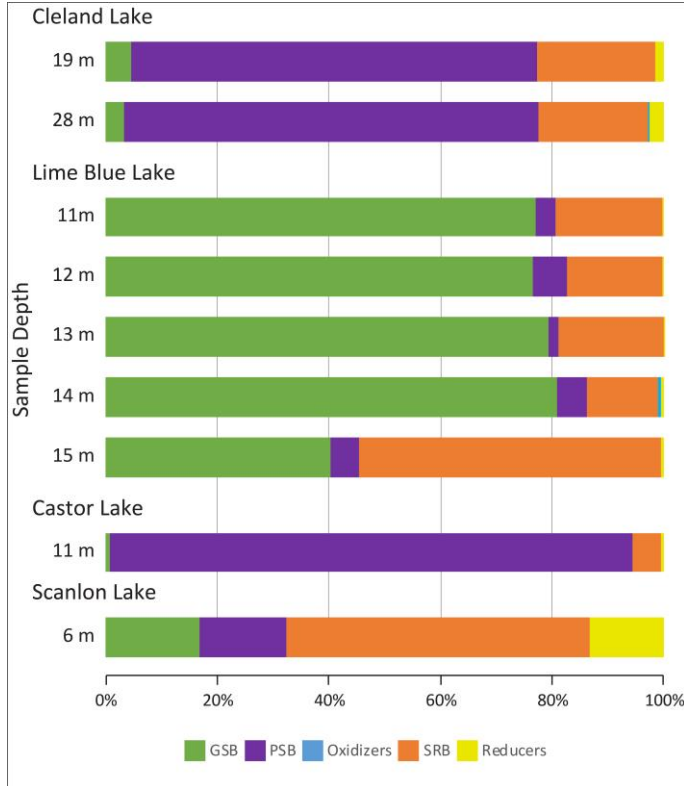


Figure 7: Relative (%) abundances of water column bacteria that were members of predominantly sulfur-metabolizing taxa. Percentages were calculated against the sum abundance of all OTUs that met these conditions.

In Cleland Lake, purple sulfur bacteria (73-74%) were the dominant anoxygenic phototrophs relative to green sulfur bacteria (3-5%) (Figure 7). Sulfate reducers comprised 20-21% of the sulfur community. Sulfur oxidizers were not detected at 19 m and were nearly absent at 28 m, at 0.1% of the community. The relative abundance of sulfur reducers was also low at 19 m (2%) and 28 m (3%). The community structure was almost identical at both 19 m and 28 m.

Depths 11-14 m in Lime Blue Lake were dominated by green sulfur bacteria (76-81%), with purple sulfur bacteria (1-6%) coexisting at the same depths (Figure 7). Sulfate reducers at these depths totaled between 12-19% of the community. At 15 m, just above the sediment-water interface, sulfate reducing bacteria became dominant members (51%). This shift was due to a larger number of sulfate reducers being present at 15 m, not a reduction in the number of other sulfur bacteria. Sulfur oxidizers were absent at 12-13 m and represented less than 1% of the community at 14 and 15 m. Sulfur reducers were present in similarly small numbers, below 1% at all depths.

Castor lake had the lowest percentage of green sulfur bacteria (<1%) (Figure 7). The majority (90%) of the sulfur-metabolizing community in the sample collected from Castor Lake was comprised of purple sulfur bacteria. Sulfate reducing bacteria represented 5% of the community. Sulfur oxidizers were not detected, and sulfur reducers constituted less than 1%.

The Scanlon Lake sample contained a comparatively small amount of sequenceable genetic material and, therefore, had a relatively even distribution of sulfur bacteria abundances that is likely not representative of the whole hypolimnion. This was probably in part due to the more limited volume of water that was filtered by virtue of this sample being a suspension of flocculant organic-rich material that quickly clogged the collection filter. Each of the seven metabolic categories were present in the 6 m sample (Figure 7), with the three reducer categories (SRB, SRB + DSP, and reducers) comprising 68% of the sulfur community that was represented in the sample. Due to the limited number of sequences recovered from this sample, OTU abundance data for Scanlon Lake have been excluded from the discussion section.

3.4.2. Broadest possible sulfur community structure

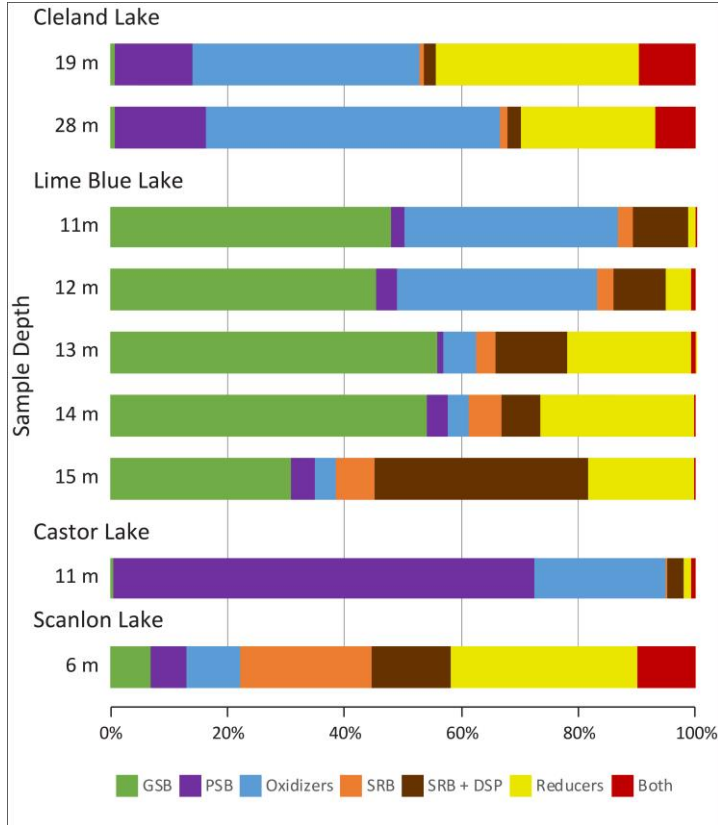


Figure 8: Abundances of all water column bacteria that share membership with any number of sulfur-metabolizers at their assigned taxonomic level or below. Percentages were calculated against the sum abundance of all OTUs that met these conditions.

With inclusion of the additional taxa (Figure 8), green sulfur bacteria constituted less than 1% of the Cleland Lake sulfur community. Purple sulfur bacteria were between 13% and 16% at both 19 m and 28 m, down from >70% in the previous section. Sulfate reducers were similarly a smaller percent in these broader Cleland assemblages. Non-disproportionating sulfate reducers were slightly below 2% at 19 and 28 m, and disproportionating sulfate reducers were slightly above 2% at both depths. Sulfur

oxidizers were nearly absent in the previous section, but here comprised 38% and 49% of the community at 19 m and 28 m. Sulfur reducers were also a much larger percentage in these assemblages, totaling 34% at 19 m and 23% at 28 m. Taxa with members that have a mixture of oxidative and reductive sulfur metabolisms were absent in 3.4.1 but comprised 10% and 7% of the community at 19 and 28 m here.

In Lime Blue Lake (Figure 8), green sulfur bacteria were still the most abundant group between 11 m and 14 m in these assemblages, comprising between 45-54% of the sulfur community before decreasing to 31% at 15 m. Purple sulfur bacteria comprised 1-4% across all depths. Approximately 2% of the assemblage at 11 m were non-disproportionating sulfate reducers, which steadily rose to 7% at 15 m.

Disproportionating sulfate reducers ranged from 7-12% between 11-14 m and increased to 37% at 15 m. Sulfur oxidizers (also virtually absent from Lime Blue in 3.4.1) were a large fraction of the population at 11 and 12 m (34-36%) and sharply decreased below this depth to 4-6% 13 m and below. Sulfur reducers followed an opposing trend, comprising 1-4% of the community at 11-12 m and immediately increasing to a range between 18% and 26% in the depths below. Metabolically heterogeneous taxa were less than 1% of the community at all depths.

The community at 11 m in Castor Lake (Figure 8) had almost no green sulfur bacteria (<1%) and was dominated by purple sulfur bacteria (71%). Non-disproportionating and disproportionating sulfate reducers respectively comprised 1% and 3%. Sulfur oxidizers were 22%, up from 0% in 3.4.1. Sulfur reducers and heterogeneous taxa were each approximately 1%.

In Scanlon Lake (Figure 8), green and purple sulfur bacteria were both between 6-7% of the community. Non-disproportionating sulfate reducing bacteria comprised 22%, and disproportionating sulfate reducers 14%. Sulfur oxidizers were 9%, and sulfur reducers were 32%. Heterogeneous taxa comprised 10%.

IV. DISCUSSION

4.1. Sulfate concentration and $\Delta^{34}\text{S}_{\text{SO}_4\text{-H}_2\text{S}}$

The isotopic fractionation between reactant and product tends to decrease when reactant concentrations are low (Mariotti et al., 1981). Sulfate concentrations lower than 0.2 mM have been associated with near-zero $\Delta^{34}\text{S}_{\text{SO}_4\text{-H}_2\text{S}}$ values (Harrison and Thode, 1958; Kaplan and Rittenberg, 1964; Canfield, 2001; Shen et al., 2001). Accordingly, small sulfur isotope fractionations in the rock record have been interpreted as an indication of paleo-seawater sulfate concentrations ranging below this threshold (Chambers and Trudinger, 1979; Cameron, 1982; Canfield and Teske, 1996; Habicht et al., 2002). Thus, an increase in $\Delta^{34}\text{S}_{\text{SO}_4\text{-H}_2\text{S}}$ values is expected when sulfate concentrations are greater than 0.2 mM.

The orders of magnitude difference in sulfate concentrations measured among the lakes in this study provided an opportunity to further evaluate the relationship between sulfate concentration and $\Delta^{34}\text{S}_{\text{SO}_4\text{-H}_2\text{S}}$. The average epilimnion concentration of sulfate in Scanlon Lake (118 mM), the highest among the lakes in this study, was tenfold higher than Lime Blue (11.1 mM) and Castor (12.8 mM) lakes, and nearly a thousandfold higher than in Cleland Lake (0.169 mM). Within Cleland Lake, the sulfate concentration differed by two orders of magnitude between the epilimnion and the sediment-water interface, where sulfate had decreased to 0.002 mM. At these micromolar sulfate concentrations, one would expect the isotopic offset between sulfate and sulfide to remain small throughout the water column and differ markedly from the $\Delta^{34}\text{S}_{\text{SO}_4\text{-H}_2\text{S}}$ measurements from Scanlon, Lime Blue, and Castor lakes. However, peak water column $\Delta^{34}\text{S}_{\text{SO}_4\text{-H}_2\text{S}}$ values ranged between 43‰ and 53‰ all four study lakes (Figure 9).

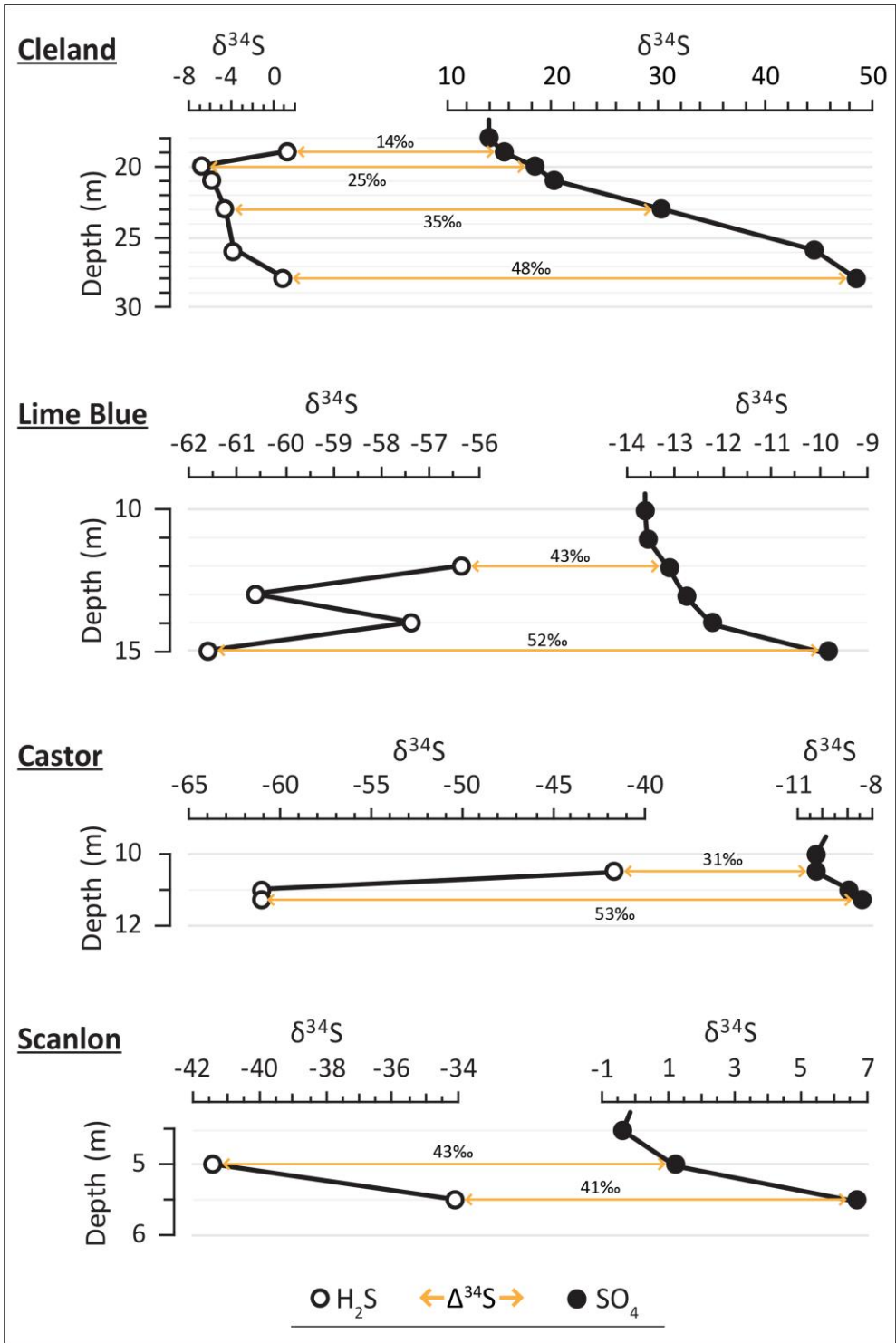


Figure 9: Water column sulfur isotope profiles. Arrows indicate the range of $\Delta^{34}\text{S}_{\text{SO}_4\text{-H}_2\text{S}}$ values.

The sulfur isotope composition of sulfate and sulfide in the Cleland Lake water column demonstrates that extremely low sulfate concentrations will not always constrain the magnitude of $\Delta^{34}\text{S}_{\text{SO}_4\text{-H}_2\text{S}}$ and represents a possibility that must be considered when using $\Delta^{34}\text{S}_{\text{SO}_4\text{-H}_2\text{S}}$ to estimate the concentration of sulfate in ancient waters. Accordingly, the sulfur isotope profiles of sulfate and sulfide in Cleland Lake provide important insights into the expression of isotope effects associated with sulfur cycling within sulfate limited systems. The sulfur isotope fractionation observed at the shallowest sulfidic depth in Cleland Lake ($\Delta^{34}\text{S}_{\text{SO}_4\text{-H}_2\text{S}} = 14.2\text{‰}$) was lower than those measured at the shallowest sulfidic depths in Lime Blue, Castor, and Scanlon lakes (31.4 to 43.3‰). Given that sulfate concentrations remained low below this depth and decreased by two orders of magnitude near the bottom (Figure 5), it would be reasonable to expect that $\Delta^{34}\text{S}_{\text{SO}_4\text{-H}_2\text{S}}$ values would remain low throughout the hypolimnion. However, $\Delta^{34}\text{S}_{\text{SO}_4\text{-H}_2\text{S}}$ increased substantially with depth to a maximum of 48.6‰ at 26 m, 2 m above the sediment-water interface. At this depth, sulfate had been consumed to a concentration of 0.021 mM, yet $\Delta^{34}\text{S}_{\text{SO}_4\text{-H}_2\text{S}}$ had approached a magnitude typical of a sulfate replete system. This suggests that micromolar sulfate concentrations will not necessarily limit $\Delta^{34}\text{S}_{\text{SO}_4\text{-H}_2\text{S}}$. Likewise, low $\Delta^{34}\text{S}_{\text{SO}_4\text{-H}_2\text{S}}$ values may not always be indicative of low sulfate concentrations. It is also possible that the 14.2‰ topmost $\Delta^{34}\text{S}_{\text{SO}_4\text{-H}_2\text{S}}$ value was due in part to comparatively rapid sulfate reduction at the top of the euxinic water column or to sulfide oxidation that was producing reverse fractionation, returning ^{34}S -depleted sulfide to the sulfate pool.

The sulfur isotope geochemistry in Cleland Lake is notable in that the large increase in $\Delta^{34}\text{S}_{\text{SO}_4\text{-H}_2\text{S}}$ was driven by a 34.6‰ increase in $\delta^{34}\text{S}_{\text{SO}_4}$ between 18 m (14.0‰) and 28 m (48.6‰), which outpaced the 8‰ increase in $\delta^{34}\text{S}_{\text{H}_2\text{S}}$ over the same depth

interval. This $\delta^{34}\text{S}_{\text{SO}_4}$ increase was exceedingly large compared to the other study lakes, where $\delta^{34}\text{S}_{\text{SO}_4}$ evolved by approximately 4‰ in Lime Blue, 2‰ in Castor, and 7‰ in Scanlon. Further, the large increase in $\delta^{34}\text{S}_{\text{SO}_4}$ occurred alongside a notably large increase in $\delta^{18}\text{O}_{\text{SO}_4}$. This rapid increase in $\delta^{18}\text{O}_{\text{SO}_4}$ is discussed further in section 4.3.

With so little sulfate remaining in the Cleland Lake bottom water relative to shallower depths, it is uncertain if the high $\Delta^{34}\text{S}_{\text{SO}_4\text{-H}_2\text{S}}$ value (48.6‰) at the bottom of the water column would be recorded in Cleland sediments. The isotope composition of mineralized sulfur species deposited in lake and marine sediment is a depth-integrated composite of the total precipitated throughout the entire water column. This composite signal is modulated by the reservoir effect (Gomes and Hurtgen, 2013), which stipulates that the bulk δ values of sedimentary sulfur minerals will be skewed toward the δ values carried by the source material at the depths where large fractions of the bulk precipitate formed. With most of the water column sulfate pool in Cleland residing further above the sediment-water interface, the majority of bulk sulfate mineral precipitation in the lake would have likely occurred at depths where $\Delta^{34}\text{S}_{\text{SO}_4\text{-H}_2\text{S}}$ was lower. Regardless, the fact that it is possible for $\Delta^{34}\text{S}_{\text{SO}_4\text{-H}_2\text{S}}$ values approaching 50‰ to be produced in an environment with trace sulfate concentrations is remarkable, and it represents the possibility that there are circumstances in which large $\Delta^{34}\text{S}_{\text{SO}_4\text{-H}_2\text{S}}$ values could be recorded in the sediments of extremely low sulfate environments.

4.2. Water column $\delta^{18}\text{O}_{\text{SO}_4}$ during cryptic sulfur cycling



Figure 10: Weathering pyritic shale and marble along the shoreline of Castor Lake.

Oxidation pathways that incorporate ambient water-bound (H_2O) and molecular (O_2) oxygen influence the isotope composition of sulfate-bound oxygen (Mayer, 2005; Kohl and Bao, 2011). The oxygen isotope composition of atmospheric oxygen ($\delta^{18}\text{O}_{\text{O}_2} = 23.5\text{‰}$) (Young et al., 2014) is distinct from surface water in eastern Washington, USA ($\delta^{18}\text{O}_{\text{H}_2\text{O}} = -22$ to -18‰) (Kendall and Coplen, 2001; Steinman et al., 2010; Steinman and Abbott, 2013). These widely differing compositions of sulfur-bound oxygen sources are useful for interpreting whether sulfide was oxidized in the presence or absence of molecular oxygen (Li et al., 2022). Based on sulfate and oxygen isotope chemistry,

sulfate in the study lakes is likely derived from weathering of pyritic shale and marble outcrops in Lime Blue, Castor, and Scanlon lakes (Figure 10). The low $\delta^{34}\text{S}_{\text{SO}_4}$ values (-0.2 to -13.7‰) of surface water in these three lakes is consistent with sulfide oxidation of pyrite. A two end-member mixing model of oxygen derived from the atmosphere (approximately 24‰) or meteoric water (approximately -24‰) during sulfide oxidation defines the boundaries for aerobic oxidation (100% O_2) and anaerobic oxidation (100% H_2O), or a 50:50 mixture of these sources (Figure 11). The $\delta^{18}\text{O}_{\text{SO}_4}$ of surface waters of the lakes in Washington are consistent with aerobic pyrite oxidation. In contrast, surface water $\delta^{18}\text{O}_{\text{SO}_4}$ in Cleland Lake likely formed during anaerobic oxidation.

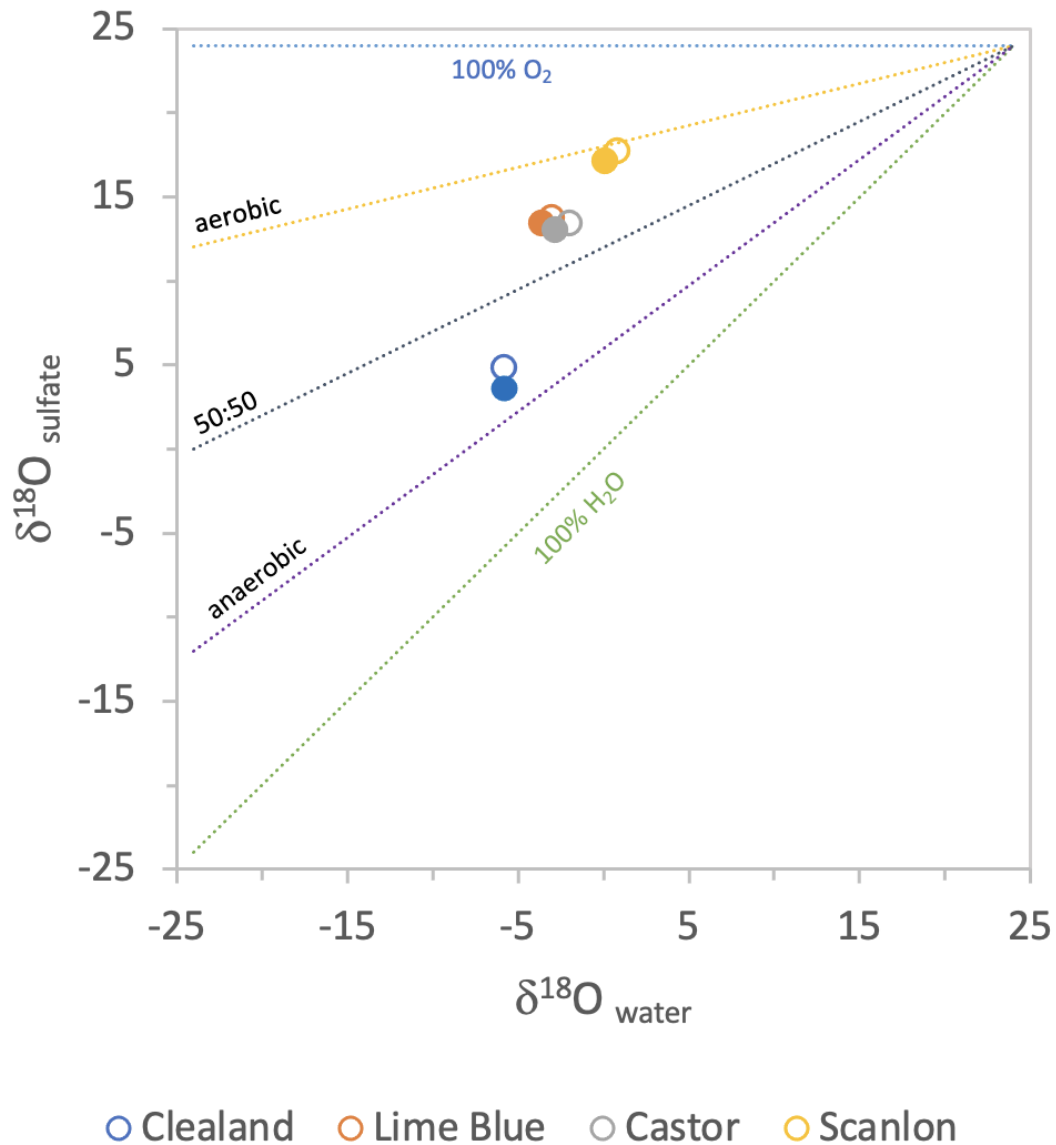


Figure 11: Comparison of $\delta^{18}\text{O}_{\text{SO}_4}$ and $\delta^{18}\text{O}_{\text{H}_2\text{O}}$ for surface waters (open symbols) and water column values at depth of oxygen isotope excursion (filled symbols) in each lake. Dashed lines represent mixing arrays for relative contributions of molecular oxygen ($\delta^{18}\text{O}_{\text{O}_2} = 24\text{‰}$) and meteoric water ($\delta^{18}\text{O}_{\text{H}_2\text{O}} = -24\text{‰}$).

The resulting $\delta^{18}\text{O}_{\text{SO}_4}$ value of sulfate produced from sulfide oxidation will reflect that of the oxygen source plus any fractionation effects associated with the oxidation

pathway, with in phototrophic sulfide oxidation resulting in ^{18}O enrichment in the product sulfate relative to the oxygen source ($\epsilon^{18}\text{O}_{\text{SO}_4\text{-H}_2\text{O}} = 5.3\text{‰}$ to 5.8‰) and chemolithotrophic oxidation resulting in ^{18}O depletion ($\epsilon^{18}\text{O}_{\text{H}_2\text{O-SO}_4} = -8.5\text{‰}$ to -1.3‰) (Gomes and Johnston, 2017).

In contrast, chemolithotrophic and abiotic sulfide oxidation produces sulfate with minimal to zero sulfur isotope fractionation, where the $\delta^{34}\text{S}_{\text{SO}_4}$ value of the product is usually slightly negative (e.g., $<1\text{‰}$) relative to the sulfide source when oxidized anaerobically and equivalent to the source (i.e., resultant $\delta^{34}\text{S}_{\text{SO}_4} \approx \delta^{34}\text{S}_{\text{H}_2\text{S}}$) if oxidized using O_2 (Balci et al., 2007; Zerkle et al., 2009). Phototrophic sulfide oxidation, however, predominantly produces sulfate that is slightly ^{34}S -enriched relative to the starting sulfide (Zerkle et al., 2009).

When sulfate is consumed in a closed system by sulfate reducing bacteria, the proportion of ^{34}S and ^{18}O in residual sulfate will increase relative to the initial isotope composition of the sulfate pool (Antler et al., 2017) This is due to (1) the kinetic oxygen and sulfur isotope effects associated with sulfate uptake into the dissimilatory sulfate reduction (DSR) pathway itself and (2) intracellular back reactions that reoxidize and return sulfur intermediates from along the DSR pathway to the sulfate pool (Brunner and Bernasconi, 2005; Brunner et al., 2012). Combined, the net isotope effects of microbial sulfate reduction can produce $\delta^{18}\text{O}_{\text{SO}_4}$ fractionations of up to 25‰ (Bertran et al., 2020).

The relatively larger sulfur isotope fractionations during microbial sulfate reduction tend to mask those of sulfide oxidation (Zerkle et al., 2009); however, when these microbial metabolisms occur at the same rate, repeated cycles of oxidation and reduction results in no observable change in sulfate concentration or net fractionation in

$\delta^{34}\text{S}_{\text{SO}_4}$. This phenomenon, known as cryptic sulfur cycling, occurs in environments where the relative availability of oxidants and reductants has resulted in a parity between the metabolic throughput of sulfur reducers and oxidizers (Canfield et al., 2010; Treude et al., 2021; Guibourdenche et al., 2022). Unlike the paired increase observed in oxygen and sulfur isotopes during sulfate reduction (Antler et al., 2013, 2017), $\delta^{18}\text{O}_{\text{SO}_4}$ can vary independently of $\delta^{34}\text{S}_{\text{SO}_4}$ during cryptic sulfur cycling and will be influenced by the oxygen isotope composition of the water and dissolved oxygen (Aller et al., 2010; Houghton et al., 2019). These systematics can make $\delta^{18}\text{O}_{\text{SO}_4}$ a diagnostic indicator of rapid recycling of sulfur within the upper hypolimnion. The evidence that follows suggests that (1) cryptic sulfur cycling can result in oxygen isotope excursions in sulfate that precede any net change in the sulfur isotope compositions of sulfate or sulfide, and (2) that conditions in which it is likely to occur can be identified with field measurements, explained below.

The chemical profiles of the four study lakes exhibit redox transitions where dissolved oxygen is either trace or absent and oxidants are present (measured as positive ORP; (Figure 12). In anoxic waters, positive ORP indicates that the concentration of oxidants remains high enough relative to reductants to maintain an oxidizing environment – one in which chemolithotrophic oxidation of sulfide is energetically expedient (Callbeck et al., 2021). It appears that cryptic sulfur cycling is likely to occur at depths where a decrease in ORP to near or below 0 mV lags the complete consumption of dissolved oxygen (Figure 12; Cleland, Lime Blue and Castor Lakes) or where ORP is negative but dissolved oxygen is still present (Figure 12; Scanlon Lake).

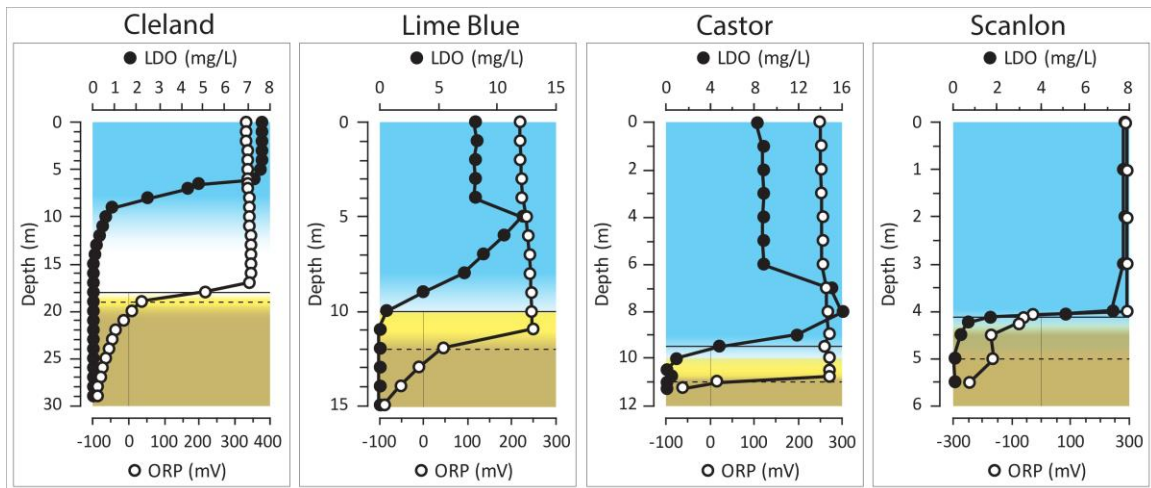


Figure 12: Water column profiles of dissolved oxygen (LDO) and oxidative redox potential (ORP) in Cleland, Lime Blue, Castor, and Scanlon Lakes. The solid horizontal line indicates the depth of the $\delta^{18}\text{O}_{\text{SO}_4}$ minimum, and the horizontal dashed line indicates the depth where $\delta^{34}\text{S}_{\text{SO}_4}$ increased and H_2S was first detected (i.e., the depth where net sulfate reduction was first observed). This also marks the depth where LDO and ORP had both respectively fallen to values near or below zero in each lake. The vertical solid line indicates the zero-point along the ORP axis. The color gradients represent relative oxygen and sulfide concentrations. Dark blue represents zones with abundant oxygen and grades to translucent where oxygen is depleted. Yellow-brown zones are where sulfide was present in trace amounts (<0.01 mM), and gradients to darker brown indicate where the concentration of sulfide increased beyond this threshold.

Coincident with the redoxcline (Figure 12), a negative excursion in $\delta^{18}\text{O}_{\text{SO}_4}$ was observed in all four lakes (Figure 14). In each lake, this excursion terminated at the lowest $\delta^{18}\text{O}_{\text{SO}_4}$ value measured in the water column, and at a depth above the first appearance of sulfide. Beneath this $\delta^{18}\text{O}_{\text{SO}_4}$ minimum, if there was a lag between the

ORP drop and LDO reaching 0 mg/L, then a subsequent, positive $\delta^{18}\text{O}_{\text{SO}_4}$ excursion would occur that preceded any sulfide accumulation or change in $\delta^{34}\text{S}_{\text{SO}_4}$. If there was no lag between LDO and ORP, then $\delta^{18}\text{O}_{\text{SO}_4}$ and $\delta^{34}\text{S}_{\text{SO}_4}$ enrichment would occur in tandem with accumulation of sulfide beneath the $\delta^{18}\text{O}_{\text{SO}_4}$ minimum.

This $\delta^{18}\text{O}_{\text{SO}_4}$ minimum had formed at 18 m water depth in Cleland Lake. $\delta^{34}\text{S}_{\text{SO}_4}$ and $\delta^{18}\text{O}_{\text{SO}_4}$ values began to increase with the first appearance of sulfide within a meter below. Dissolved oxygen was consumed (< 0.1 mg/L) 4 m above the $\delta^{18}\text{O}_{\text{SO}_4}$ minimum in the Cleland water column. Far separated from potential oxidant recharge from overlying oxic waters, chemolithotrophic sulfide oxidation likely became inhibited not far below the $\delta^{18}\text{O}_{\text{SO}_4}$ minimum. This is evidenced by the abrupt decline in ORP, from 344 mV a meter above the $\delta^{18}\text{O}_{\text{SO}_4}$ minimum, to 216 mV at the 18 m minimum, and to 35 mV a meter below. Chemolithotrophic sulfide oxidation had exhausted all available oxidants, giving way to net sulfide production by 19 m, where ORP converged with dissolved oxygen (dashed lines in Figure 12 and Figure 14) and $\delta^{34}\text{S}_{\text{SO}_4}$ values had already begun to increase.

In contrast, $\delta^{18}\text{O}_{\text{SO}_4}$ minima in the other three lakes occurred at depths where oxygen concentrations were low (0.58 to 4.3 mg/L), but not yet 0 mg/L. In Lime Blue Lake the $\delta^{18}\text{O}_{\text{SO}_4}$ minimum developed at 10 m (Figure 14) in water that contained low levels of dissolved oxygen (0.58 mg/L). At 11 m, oxygen had been completely consumed, while ORP remained unchanged and positive (248 mV). Here, where ORP lagged the drop in LDO to 0 mg/L, $\delta^{18}\text{O}_{\text{SO}_4}$ had begun to increase. This preceded any change in $\delta^{34}\text{S}_{\text{SO}_4}$, which did not begin to increase until sulfide had appeared and ORP had dropped to 45 mV a meter below at 12 m water depth (Figure 12).

The $\delta^{18}\text{O}_{\text{SO}_4}$ minimum in Castor Lake was in considerably more oxygenated water (4.3 mg/L) at 9.5 m water depth. Dissolved oxygen dropped rapidly and was consumed entirely by 10.5 m (Figure 12). As with Lime Blue Lake, complete oxygen consumption was accompanied by no drop in ORP. $\delta^{18}\text{O}_{\text{SO}_4}$ increased below the $\delta^{18}\text{O}_{\text{SO}_4}$ minimum with no accompanying change in $\delta^{34}\text{S}_{\text{SO}_4}$ and no appreciable accumulation of sulfide until 11 m, where a drop in ORP to 17 mV coincided with the first accumulation of sulfide and the onset of $\delta^{34}\text{S}_{\text{SO}_4}$ isotopic enrichment (Figure 14).

Redox gradients were much more abrupt in Scanlon Lake. Although ORP decreased rapidly (294 to -28 mV) a meter above (as opposed to below) complete oxygen consumption at 5 m (Figure 12), this interval still represents a lag between ORP and dissolved oxygen. The $\delta^{18}\text{O}_{\text{SO}_4}$ minimum occurred at 4.125 m (Figure 14), the first sample depth beneath the observed ORP drop. Below the $\delta^{18}\text{O}_{\text{SO}_4}$ minimum, $\delta^{18}\text{O}_{\text{SO}_4}$ increased and $\delta^{34}\text{S}_{\text{SO}_4}$ did not until dissolved oxygen was completely consumed at 5 m water depth.

In all four lakes, $\delta^{18}\text{O}_{\text{SO}_4}$ values were lowest at the chemocline (Figure 13), and in Lime Blue Lake, Castor Lake, and Scanlon Lake these values began to subsequently increase before any change in $\delta^{34}\text{S}_{\text{SO}_4}$ values or accumulation of dissolved sulfide. The chemocline isotope systematics suggest a complex interplay between microbial metabolisms acting in concert that produced the $\delta^{18}\text{O}_{\text{SO}_4}$ excursions.

All four oxygen atoms in sulfate are stripped from the sulfur atom during complete reduction to sulfide and replaced with water-bound oxygen when the sulfide is reoxidized. When subject to a cyclic process of reduction and reoxidation, the sulfate pool will invariably become comprised of sulfate bearing an increasingly large fraction of

ambiently-sourced oxygen that has been subject to fractionation during reoxidation (Mills et al., 2016).

Within the topmost zone of the anoxic portion of the water column, tandem chemotrophic and phototrophic sulfide oxidation can occur at rates sufficient to reoxidize all sulfide produced by sulfate reducers. Continuous quantitative sulfide oxidation within this band of water requires a constant supply of oxidants (e.g., Fe^{3+} , NO_3), which is made possible by the close proximity to the oxic portion of water column from which these oxidants steadily diffuse, and necessarily limits the spatial extent of this band to depths immediately beneath the oxic-anoxic interface. This band of cryptic sulfur cycling would result in a localized $\delta^{18}\text{O}_{\text{SO}_4}$ excursion that evolves sulfate towards the $\delta^{18}\text{O}_{\text{H}_2\text{O}}$ values at these depths. In natural waters, the apogee of this $\delta^{18}\text{O}_{\text{SO}_4}$ excursion will likely be found above the depth where free sulfide has first begun to accumulate.

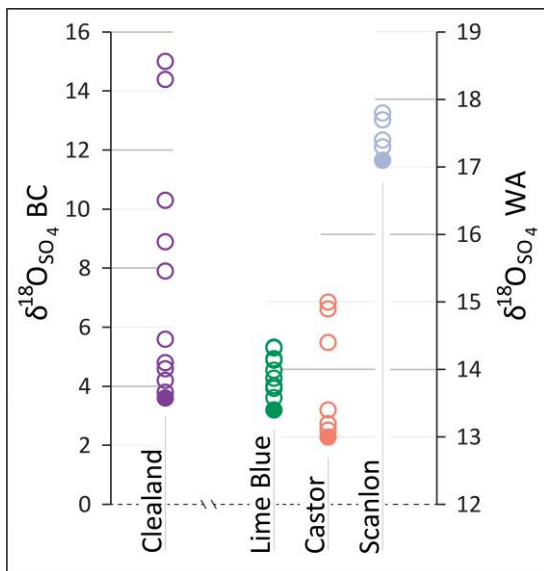


Figure 13: Distribution of $\delta^{18}\text{O}_{\text{SO}_4}$ in all four study lakes. The lowest $\delta^{18}\text{O}_{\text{SO}_4}$ values (filled symbols) for each lake are all at the chemocline where the oxygen isotope

excursions were observed. Cleland Lake data are on the “BC” axis and the three Washington State lakes are on the right “WA” axis.

Beneath this initial front of rapid sulfide reoxidation, the supply of oxidants will become increasingly constrained by the rate and distance of diffusion from the mixolimnion. Oxidant exhaustion will result in a shift to higher relative rates of sulfate reduction as chemolithotrophic oxidation subsides, eventually giving way to net sulfate reduction at a depth where phototrophic oxidation and waning chemotrophic oxidation cannot keep pace with sulfate reduction. Below the $\delta^{18}\text{O}_{\text{SO}_4}$ minimum, ^{18}O -enriched sulfate will accumulate with depth.

It is important to note that the transition from the negative $\delta^{18}\text{O}_{\text{SO}_4}$ excursion to the positive excursion below occurs before any change in $\delta^{34}\text{S}_{\text{SO}_4}$ is observed (Figure 14). $\delta^{18}\text{O}_{\text{SO}_4}$ will increase, $\delta^{34}\text{S}_{\text{SO}_4}$ will remain unaffected, and little to no free sulfide will accumulate where either ORP is positive or dissolved oxygen remains (Figure 12). The base of this zone will be marked by complete consumption of oxygen and ORP values becoming negative. Here, the delivery of oxidants from above will have become insufficient to maintain the quantitative reoxidation of sulfide to sulfate, so sulfide will begin to accumulate and $\delta^{34}\text{S}_{\text{SO}_4}$ will begin to increase. The relative vertical positions of the negative $\delta^{18}\text{O}_{\text{SO}_4}$ excursion and subsequent $\delta^{18}\text{O}_{\text{SO}_4}$ enrichment could be the result of diffusion, as it is not clear how quantitative reoxidation alone could cause both a negative $\delta^{18}\text{O}_{\text{SO}_4}$ excursion and then a positive one below it. This $\delta^{18}\text{O}_{\text{SO}_4}$ reversal is likely instead the result of isotope effects propagating upward via diffusion through a stack of redox conditions with functionally discrete boundaries. These can be visualized as three zones

vertically delineated by two horizons. In the bottommost zone, dominant (net) DSR imparts oxygen and sulfur isotope effects on sulfide ($-\delta^{34}\text{S}$) and sulfate ($+\delta^{34}\text{S}$, $+\delta^{18}\text{O}$). Some of this DSR-evolved sulfate and sulfide will diffuse up into the cryptic sulfur cycling zone above.

Here, the sulfide will be quantitatively oxidized back to sulfate, which will be markedly ^{34}S - and ^{18}O -depleted relative to the sulfate that accompanied it. This process will virtually neutralize the ^{34}S enrichment and offset the ^{18}O enrichment carried into the sulfate pool in this zone by diffusion of sulfate from below, which will retain an elevated ^{18}O content until it is reduced. Throughout this zone, sulfate reduction still occurs but it is balanced by an equal rate of sulfide oxidation. This balance sustains a cycle wherein all sulfate that is reduced will be rapidly and quantitatively reoxidized back to the sulfate pool. The passing of sulfur through this cycle continuously strips all oxygen from sulfate and replaces it with oxygen atoms from the ambient water. This has the effect of essentially scrubbing the ^{18}O enrichment from sulfate. The further up in this zone from the net-DSR horizon, the smaller the fraction of the sulfate pool that will retain enriched oxygen from below. This manifests as a negative $\delta^{18}\text{O}_{\text{SO}_4}$ excursion.

A second boundary, at the top of this zone, marks the termination of sulfate reduction in the water column. As with the depths below, some of the sulfide produced below this horizon will diffuse up across it. Likewise, the oxidation of this sulfide will further drive $\delta^{18}\text{O}_{\text{SO}_4}$ values toward $\delta^{18}\text{O}_{\text{H}_2\text{O}}$, though here it will happen independent of any ^{18}O -enriching effects of DSR. With oxidation being the only process imparting an isotope effect on sulfate above this horizon, the influence on $\delta^{18}\text{O}_{\text{SO}_4}$ here will be unimodal. If the LDO/ORP lag zone is small (i.e., if it occurs within a 1-2 m depth

interval), then it is near this horizon that the lowest $\delta^{18}\text{O}_{\text{SO}_4}$ value in the water column will likely be found. If this zone is larger, or if the concentration of sulfate is low, then it could be possible for the $\delta^{18}\text{O}_{\text{SO}_4}$ minimum to develop nearer to the base of the zone. This appears to have been the case in Cleland Lake, where the flux of sulfate through the zone of cryptic sulfur cycling was large enough relative to the small (<0.14 mM) sulfate pool to remove all $\delta^{18}\text{O}_{\text{SO}_4}$ enrichment from DSR-evolved sulfate diffusing from below within the span of 1 meter.

It is important to make clear that, although $\delta^{18}\text{O}_{\text{SO}_4}$ will increase with depth throughout the layer of water in which cryptic sulfur cycling occurs, this model stipulates that the effect of cryptic sulfur cycling on sulfate is not $\delta^{18}\text{O}_{\text{SO}_4}$ enrichment, rather enrichment *scrubbing*, with $\delta^{18}\text{O}_{\text{SO}_4}$ minima occurring just above or within water column layers or sediment strata where the cycle has developed. This trend was born out in each of the four study lakes (Figure 14). In each lake, there was a distinct negative $\delta^{18}\text{O}_{\text{SO}_4}$ excursion which terminated at a $\delta^{18}\text{O}_{\text{SO}_4}$ minimum that was either above or coincident with the first measurable presence of sulfate. The $\delta^{18}\text{O}_{\text{SO}_4}$ values were higher above and below the minima, throughout which $\delta^{34}\text{S}_{\text{SO}_4}$ remained unaltered unless or until ORP decisively dropped near or below 0 mV *and* LDO neared or reached 0 mg/L. (Figure 12).

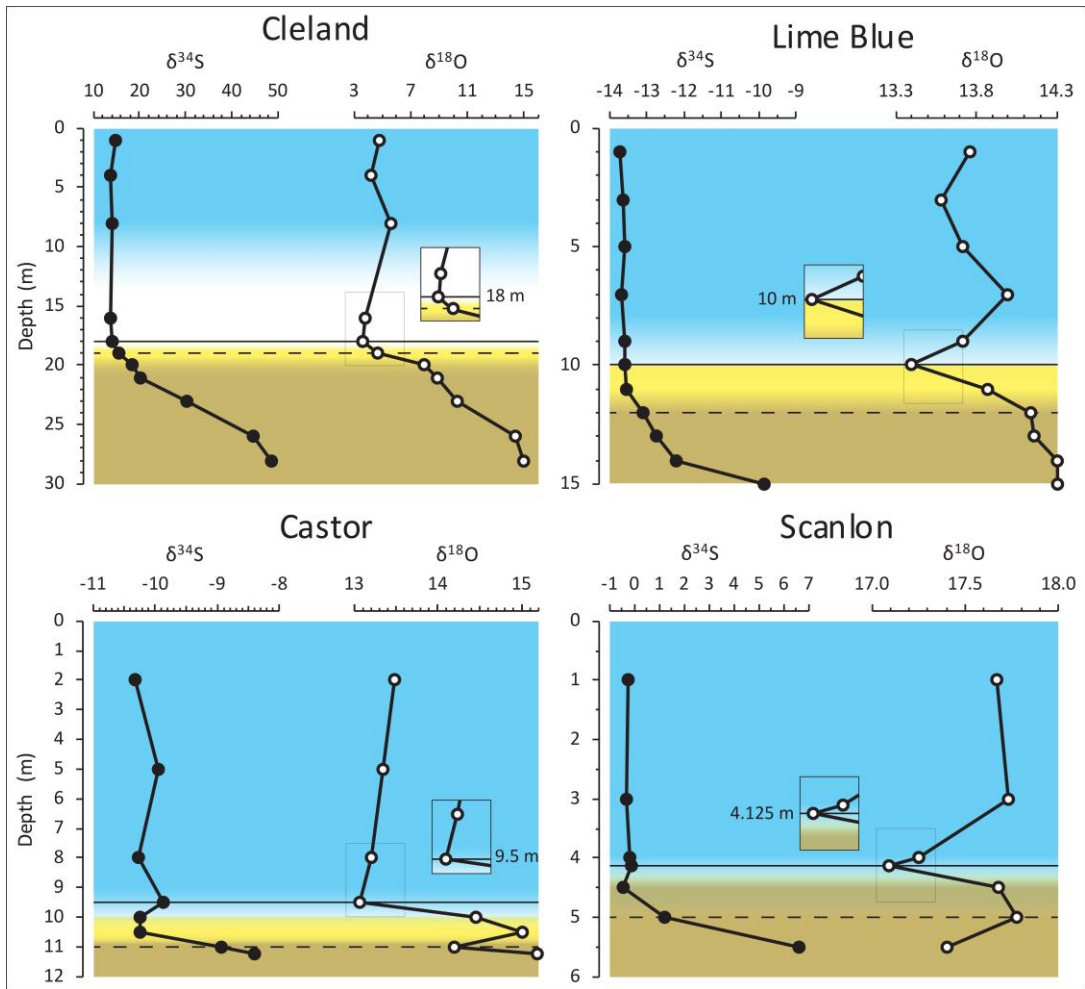


Figure 14: Water column $\delta^{34}\text{S}_{\text{SO}_4}$ and $\delta^{18}\text{O}_{\text{SO}_4}$ in each study lake. The solid horizontal line indicates the depth of the $\delta^{18}\text{O}_{\text{SO}_4}$ minimum, and the horizontal dashed line indicates the depth where $\delta^{34}\text{S}_{\text{SO}_4}$ increased and H_2S was first detected. The color gradients represent relative oxygen and sulfide concentrations. Dark blue represents zones with abundant oxygen and grades to translucent where oxygen is depleted. Yellow-brown zones are where sulfide is present in trace amounts (<0.01 mM), and the grade to darker brown indicates where the concentration of sulfide had increased beyond this threshold.

Whether the $\delta^{18}\text{O}_{\text{SO}_4}$ excursion at the chemocline is positive or negative relative to the overlying water column would depend on the ^{18}O content of the initial sulfate pool

relative to the ambient water ($\Delta^{18}\text{O}_{\text{SO}_4\text{-H}_2\text{O}}$). If initial $\Delta^{18}\text{O}_{\text{SO}_4\text{-H}_2\text{O}}$ values are positive (when sulfate is more ^{18}O -enriched than water), then the onset of cryptic sulfur cycling would almost certainly shift $\delta^{18}\text{O}_{\text{SO}_4}$ to more negative values. It is likely that negative initial $\delta^{18}\text{O}_{\text{SO}_4}$ excursions are exceedingly more common outcomes of cryptic sulfur cycling than positive excursions because a considerable fraction of the sulfate delivered to natural bodies of water is formed by subaerial oxidative weathering of sulfide minerals (Killingsworth et al., 2018) and thus carry an ^{18}O -enriched oxygen isotope composition closer to that of atmospheric O_2 (23.5‰; Young et al., 2014) than sulfate produced in the oxygen deficient environments typical for cryptic sulfur cycling.

4.3. Relative rates and magnitudes of $\delta^{18}\text{O}_{\text{SO}_4}$ evolution

The comparatively low initial $\Delta^{18}\text{O}_{\text{SO}_4\text{-H}_2\text{O}}$ value in Cleland Lake is likely what enabled the hypolimnion to exhibit a range of $\delta^{18}\text{O}_{\text{SO}_4}$ values that was considerably wider than those measured in the Washington lakes (Figure 15). In Cleland Lake, the change in $\delta^{18}\text{O}_{\text{SO}_4}$ parallels the increases with depth in $\delta^{34}\text{S}_{\text{SO}_4}$ (Figure 14). $\Delta^{18}\text{O}_{\text{SO}_4\text{-H}_2\text{O}}$ evolved substantially throughout the monimolimnion (Figure 15). $\Delta^{18}\text{O}_{\text{SO}_4\text{-H}_2\text{O}}$ at the top of the chemocline was 9.4‰, and by the bottom of the lake it increased to 20.7‰. This extensive evolution makes Cleland Lake distinctive for three reasons: (1) the 11.4‰ $\delta^{18}\text{O}_{\text{SO}_4}$ evolution that lead up to this final $\Delta^{18}\text{O}_{\text{SO}_4\text{-H}_2\text{O}}$ value exceed the $\delta^{18}\text{O}_{\text{SO}_4}$ evolution measured in the other study lakes by a large margin (Figure 16), (2) this evolution proceeded gradually over the course of the entire euxinic water column, and (3) the bottom water $\Delta^{18}\text{O}_{\text{SO}_4\text{-H}_2\text{O}}$ value in Cleland Lake was the largest that was measured among the four study lakes.

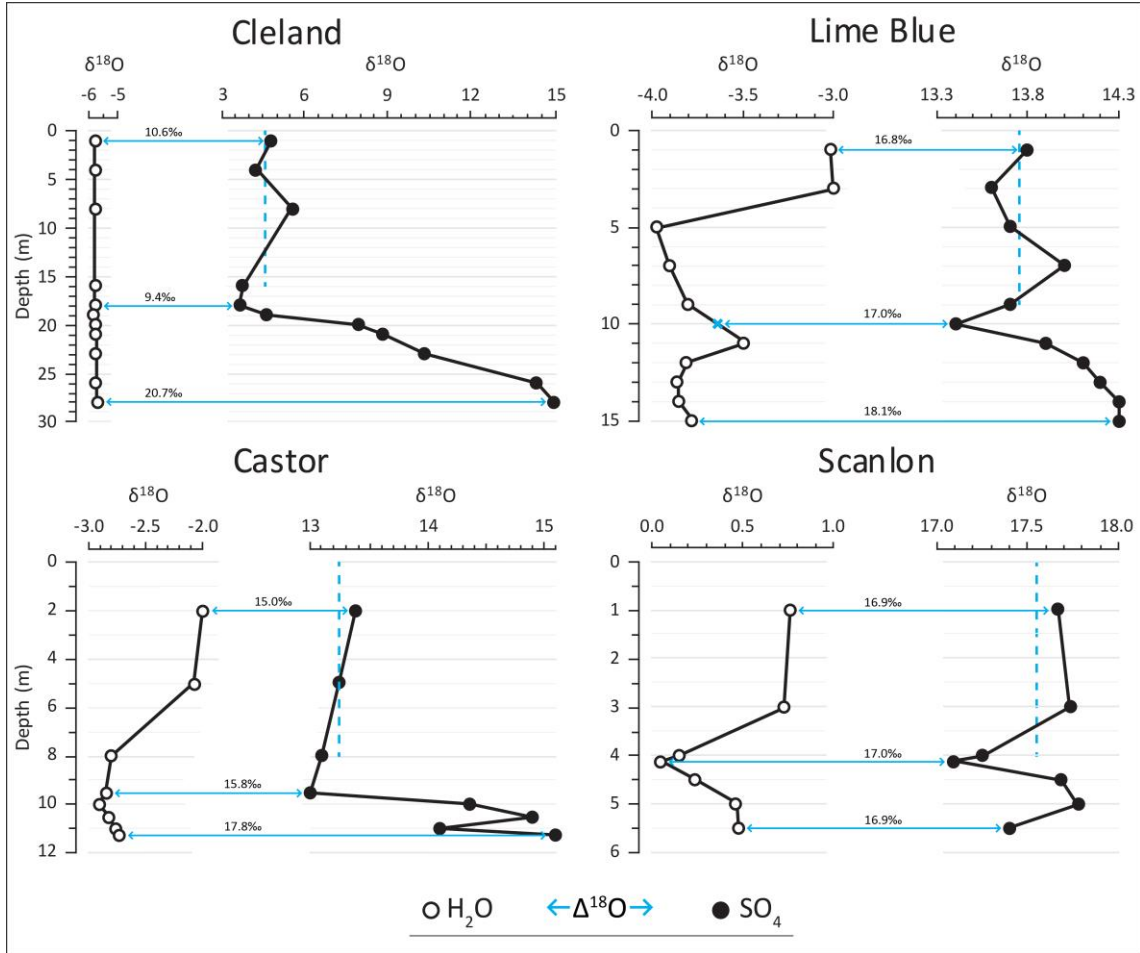


Figure 15: Oxygen isotope compositions of water ($\delta^{18}\text{O}_{\text{H}_2\text{O}}$) and sulfate ($\delta^{18}\text{O}_{\text{SO}_4}$). Blue arrows indicate $\Delta^{18}\text{O}_{\text{SO}_4\text{-H}_2\text{O}}$ values at the top of the water column, at the $\delta^{18}\text{O}_{\text{SO}_4}$ minimum, and at the deepest sample depth. Dotted blue lines indicate the average epilimnion $\delta^{18}\text{O}_{\text{H}_2\text{O}}$ values. The $\delta^{18}\text{O}_{\text{H}_2\text{O}}$ value used in calculating $\Delta^{18}\text{O}_{\text{SO}_4\text{-H}_2\text{O}}$ at 10 m in Lime Blue Lake was taken as the average of the $\delta^{18}\text{O}_{\text{H}_2\text{O}}$ values above and below, at 9 and 11 m.

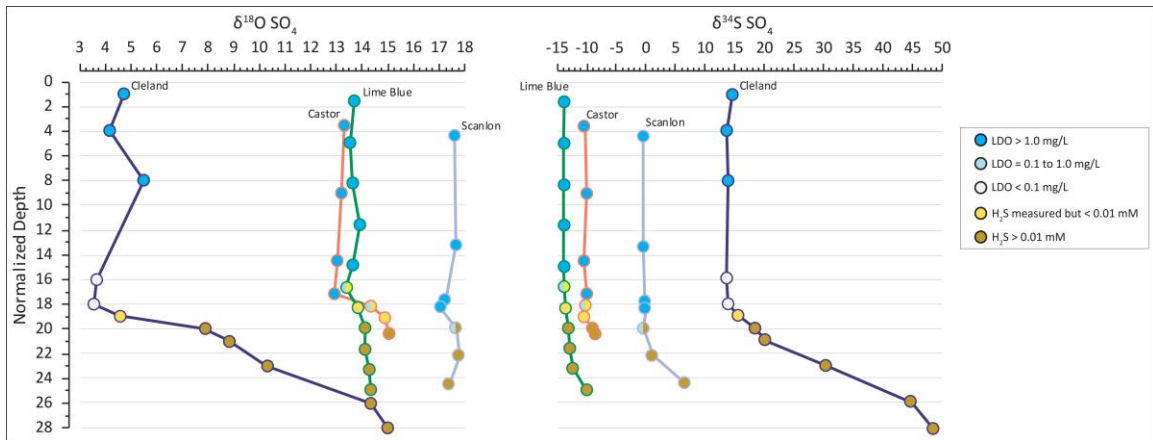


Figure 16: Depth-normalized $\delta^{18}\text{O SO}_4$ and $\delta^{34}\text{S SO}_4$ values from each lake. Sample depths in Lime Blue, Castor, and Scanlon were normalized to Cleland by assigning the first sample in each lake with a H_2S concentration above 0.01 mM a depth of 20 m (where this occurred in Cleland) and scaling the remaining sample depths accordingly. Data points are colorized according to both oxygen (dark/light blue) and sulfide (light/dark brown) concentrations.

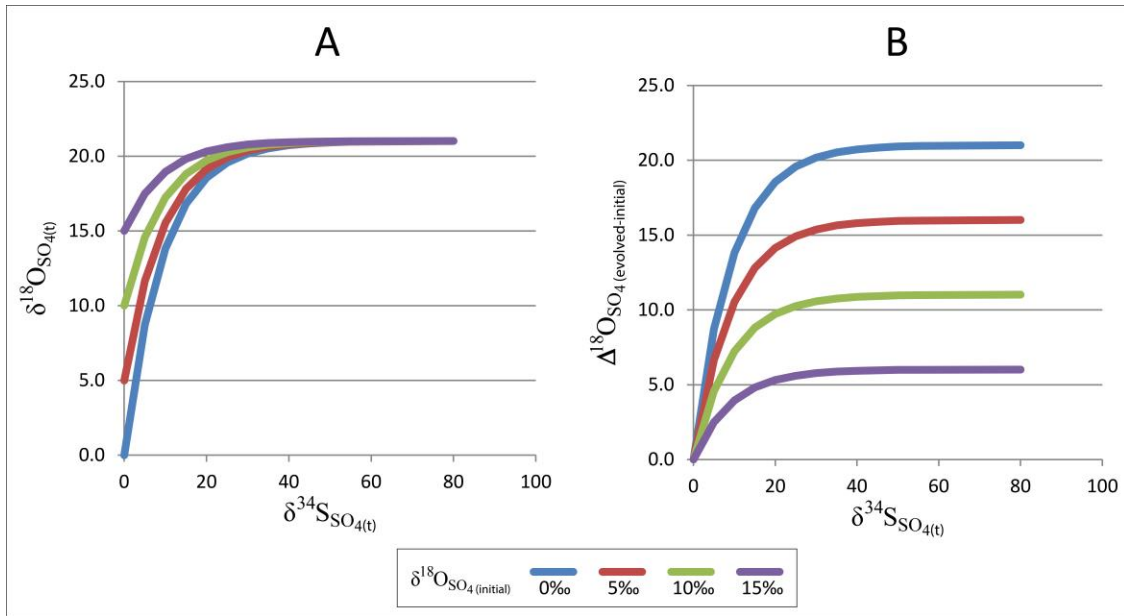


Figure 17: Model demonstration of how differences between $\delta^{18}\text{O}_{\text{H}_2\text{O}}$ and initial $\delta^{18}\text{O}_{\text{SO}_4}$ values influence the magnitude of $\delta^{18}\text{O}_{\text{SO}_4}$ evolution that can occur during sulfate reduction. Here, $\delta^{18}\text{O}_{\text{H}_2\text{O}}$ was held constant at -2‰ , and initial $\delta^{34}\text{S}_{\text{SO}_4}$ was 0‰ in four model scenarios. As the initial $\delta^{18}\text{O}_{\text{SO}_4}$ value is increased by increments of 0‰ , 5‰ , 10‰ , or 15‰ , the extent to which it can further increase becomes more limited (A), with $\Delta^{18}\text{O}_{\text{SO}_4\text{-H}_2\text{O}}$ (evolved-initial) approaching zero as the initial offset between $\delta^{18}\text{O}_{\text{SO}_4}$ and $\delta^{18}\text{O}_{\text{H}_2\text{O}}$ approaches the maximum theoretical $\epsilon^{18}\text{O}_{\text{SO}_4\text{-H}_2\text{O}}$ assumed by the model (B).

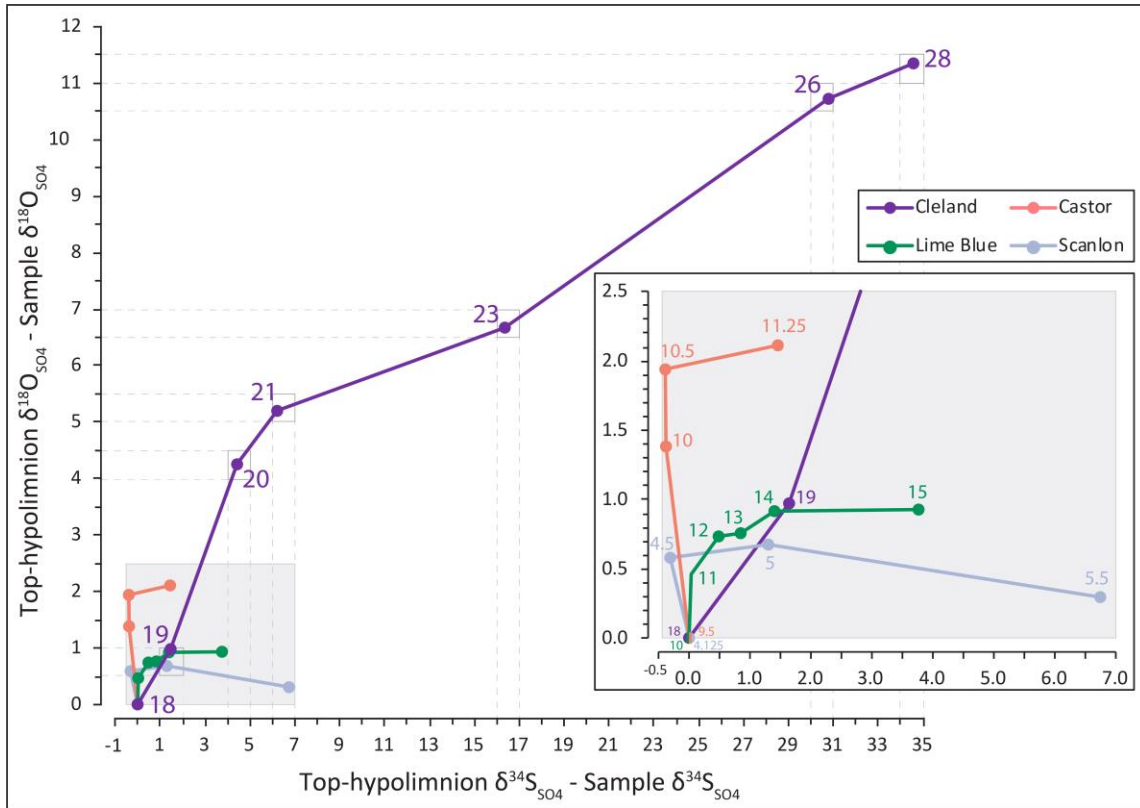


Figure 18: Plot showing hypolimnion $\delta^{34}\text{S}_{\text{SO}_4}$ and $\delta^{18}\text{O}_{\text{SO}_4}$ evolution with depth in each study lake. $\delta^{34}\text{S}_{\text{SO}_4}$ and $\delta^{18}\text{O}_{\text{SO}_4}$ values in this figure were normalized to the top-hypolimnion δ values measured at the $\delta^{18}\text{O}_{\text{SO}_4}$ -minima in each lake – presented in the same manner as the model in panel B on figure 17. The numbers next to each point are sample depths (m). The inset shows that sulfate at the top of the hypolimnion in all lakes is ^{18}O -depleted relative to the rest of the hypolimnion (zero on y-axis).

The relatively large $\delta^{18}\text{O}_{\text{SO}_4}$ increase observed in Cleland Lake was likely enabled by there being much more headroom for $\delta^{18}\text{O}_{\text{SO}_4}$ evolution in Cleland than in the other lakes. The 9.4‰ chemocline $\Delta^{18}\text{O}_{\text{SO}_4\text{-H}_2\text{O}}$ value at 18 m in Cleland was 6.4 to 7.6‰ lower than the chemocline $\Delta^{18}\text{O}_{\text{SO}_4\text{-H}_2\text{O}}$ values in the other study lakes. Because $\delta^{18}\text{O}_{\text{SO}_4}$ enrichment is largely driven by dissimilatory sulfate reduction (DSR), and because water

serves as the oxygen source in DSR back-reactions, the oxygen isotope compositions of ambient water and sulfate at the chemocline directly affect the extent to which DSR can enrich the bulk oxygen isotope composition of sulfate. All else held constant, the $\delta^{18}\text{O}$ value of back-reacted sulfate re-emerging from the DSR pathway will scale with the $\delta^{18}\text{O}$ value of ambient water. When $\delta^{18}\text{O}_{\text{H}_2\text{O}}$ is low relative to $\delta^{18}\text{O}_{\text{SO}_4}$ (i.e., when $\Delta^{18}\text{O}_{\text{SO}_4\text{-H}_2\text{O}}$ is large), reverse DSR will result in minimal $\delta^{18}\text{O}_{\text{SO}_4}$ enrichment beyond the initial value of the sulfate pool (Figure 17). This describes what was observed in Lime Blue, Castor, and Scanlon lakes. In all three, $\Delta^{18}\text{O}_{\text{SO}_4\text{-H}_2\text{O}}$ values were already high at the top of the euxinic zone, and the $\delta^{18}\text{O}_{\text{SO}_4}$ evolution that occurred in each was relatively limited (Figure 15, Figure 18). In Cleland Lake, however, initial $\Delta^{18}\text{O}_{\text{SO}_4\text{-H}_2\text{O}}$ values were markedly lower, affording headroom for $\delta^{18}\text{O}_{\text{SO}_4}$ enrichment that enabled the large $\delta^{18}\text{O}_{\text{SO}_4}$ evolution observed here.

The gradual and continuous increase in $\delta^{18}\text{O}_{\text{SO}_4}$ in Cleland Lake differs from the abrupt and truncated $\delta^{18}\text{O}_{\text{SO}_4}$ increases observed in the Washington State lakes, and this might indicate a difference in the relative rates of sulfate reduction between Cleland Lake and the others. The rate of $\delta^{18}\text{O}_{\text{SO}_4}$ enrichment is dependent on the cell-specific rate of sulfate reduction. As sulfate reduction rates decrease, DSR will more rapidly enrich the sulfate pool and cause $\delta^{18}\text{O}_{\text{SO}_4}$ to increase more rapidly relative to $\delta^{34}\text{S}_{\text{SO}_4}$ (Figure **2Error! Reference source not found.**). This is because, for every unit of sulfate that is reduced, DSR will reintroduce more ^{18}O -enriched sulfate back to the sulfate pool via back reaction when rates are slow. This leads to $\delta^{18}\text{O}_{\text{SO}_4}$ increasing rapidly and subsequently leveling off as the bulk oxygen composition of the sulfate pool reaches equilibrium with water (empirical $\Delta^{18}\text{O}_{\text{SO}_4\text{-H}_2\text{O}}$ values resulting from DSR range between

9.5 and 15.2‰) (Gomes and Johnston, 2017). These two factors – the amount headroom for $\delta^{18}\text{O}_{\text{SO}_4}$ evolution afforded by initial $\Delta^{18}\text{O}_{\text{SO}_4\text{-H}_2\text{O}}$ values and the relative rate of sulfate reduction – likely underpin much of the difference in oxygen isotope behavior between Cleland Lake and the others.

In Lime Blue Lake, $\delta^{18}\text{O}_{\text{SO}_4}$ rose by only 0.9‰ within the hypolimnion, with $\Delta^{18}\text{O}_{\text{SO}_4\text{-H}_2\text{O}}$ increasing from a high initial value of 17.0‰ at the $\delta^{18}\text{O}_{\text{SO}_4}$ -minimum depth to a maximum of 18.2‰ (2‰ lower than Cleland Lake). This $\Delta^{18}\text{O}_{\text{SO}_4\text{-H}_2\text{O}}$ value, recorded at 14 m, was nearly identical to the value recorded at the sediment-water interface at 15 m (18.1‰), as the $\delta^{18}\text{O}_{\text{H}_2\text{O}}$ and $\delta^{18}\text{O}_{\text{SO}_4}$ values used to make these calculations were near or within respective measurement precision ranges. Between 14 m and 15 m the largest water column consumption of sulfate was observed (10.6 mM to 9.8 mM), yet this was the depth interval with the smallest variation in $\Delta^{18}\text{O}_{\text{SO}_4\text{-H}_2\text{O}}$. This is likely the result of DSR quickly exhausting the limited $\Delta^{18}\text{O}_{\text{SO}_4\text{-H}_2\text{O}}$ headroom and reaching the maximum fractionation that was expressible under the conditions in the water column.

In Castor Lake, hypolimnion $\delta^{18}\text{O}_{\text{SO}_4}$ evolution was slightly more extensive, increasing by 2.1‰. This larger increase relative to Lime Blue Lake was likely afforded by the initial 15.8‰ $\Delta^{18}\text{O}_{\text{SO}_4\text{-H}_2\text{O}}$ value at 9.5 m being comparatively low relative to the maximum value of 17.8‰ near the sediment-water interface at 11.25 m. Though larger than in Lime Blue, this $\delta^{18}\text{O}_{\text{SO}_4}$ enrichment was still minor compared to what was observed Cleland Lake, where more $\Delta^{18}\text{O}_{\text{SO}_4\text{-H}_2\text{O}}$ headroom had been available.

Scanlon Lake also had a high initial hypolimnion $\Delta^{18}\text{O}_{\text{SO}_4\text{-H}_2\text{O}}$ value, at 17.0‰. This was the same top-hypolimnion value measured in Lime Blue Lake. Accordingly, the

0.7‰ $\delta^{18}\text{O}_{\text{SO}_4}$ evolution in Scanlon Lake was similarly limited. This suggests that, as in Lime Blue Lake, DSR had little $\Delta^{18}\text{O}_{\text{SO}_4\text{-H}_2\text{O}}$ headroom in which to express an effect on $\delta^{18}\text{O}_{\text{SO}_4}$ in Scanlon Lake.

The differences between $\Delta^{18}\text{O}_{\text{SO}_4\text{-H}_2\text{O}}$ values measured at the sediment-water interface in each lake are likely factors of lake depth and sulfate concentration, and consequentially, the extent of sulfate consumption that could occur within the confines of the water column. Cleland Lake was much deeper than the Washington lakes at the time of sampling and had a concentration of sulfate that was an order of magnitude lower. This allowed for nearly complete consumption of the sulfate pool to occur above the sediment-water interface. At 28 m, the concentration of sulfide (0.135 mM) had risen to the same level that sulfate had been before its precipitous drop between 21 and 23 m. This indicates that near quantitative conversion of sulfate to sulfide had taken place in the bottom waters.

There are kinetic oxygen isotope effects that occur during DSR in addition to the equilibrium effects associated with sulfite-water oxygen exchange that are presently still poorly characterized (Wankel et al., 2014), and these effects could have resulted in the relatively larger $\Delta^{18}\text{O}_{\text{SO}_4\text{-H}_2\text{O}}$ value measured at the sediment-water interface in Cleland Lake. These kinetic effects also appear to result in $\delta^{18}\text{O}_{\text{SO}_4}$ enrichment and, like the sulfur isotope effect of DSR, they would be additive as the fraction of consumed sulfate increases, occurring on top of the equilibrium effect. The $\Delta^{18}\text{O}_{\text{SO}_4\text{-H}_2\text{O}}$ value measured at 28 m in Cleland Lake is of a sulfate sample that represents the last remaining fraction of a nearly completely consumed pool. The bottom-water sulfates in Lime Blue, Castor, and Scanlon lakes had not been subject to anywhere near this degree of distillation. The

fraction of sulfate that had been converted to sulfide at the sediment-water interface in each was far from quantitative, and the $\Delta^{18}\text{O}_{\text{SO}_4\text{-H}_2\text{O}}$ values in each were lower than that measured in Cleland. Indeed, the $\Delta^{18}\text{O}_{\text{SO}_4\text{-H}_2\text{O}}$ values at the sediment-water interface of all four lakes scaled with the concentration of sulfate that was remaining there.

4.4 Microbial community structures

The question of how bacterial community structure can affect the isotopic composition of their environment is important to explore because we might be able to make inferences about the community composition and environmental conditions (e.g., sulfate concentration) in ancient environments by analyzing the sulfur isotope signatures the bacteria leave behind during those periods. Calibration of modern community assemblages and their isotope patterns can help refine and extend the range of inferences that can be made from isotopes about the microbes involved in sulfur cycling and the environments they lived in.

The difficulty in inferring the activity of multiple sulfur metabolisms using isotopes alone is largely because sulfate reducing- and sulfur disproportionating bacteria both produce relatively large $\delta^{34}\text{S}$ and $\delta^{18}\text{O}$ fractionations that tend to overprint those produced by sulfur oxidizing bacteria (Zerkle et al., 2009; Brabec et al., 2012; Gilhooly et al., 2016). Due to their dominant influence on the isotopic composition of sulfur compounds, sulfate reducers have come to be viewed as indicator species, and much attention in the last four decades has been focused on enumerating the environmental factors that influence the isotope effects associated with SRB activity. Environmental constraints on the range of sulfur and oxygen isotope fractionations produced by SRB

have been explored by experiments ranging from field-based in-situ analyses of functional gene expression and reduction rates to lab-based evaluations of pure culture growth in selective media (Canfield et al., 1998; Turchyn et al., 2010; Leavitt et al., 2013; Zhang et al., 2017). This research has informed a set of expectations regarding the manner and extent to which the isotopic compositions of water column sulfate and sulfide will fluctuate across a wide range of conditions. These models usually do not accommodate the influence of bacteria other than dissimilatory sulfate reducers – they often do not include the isotope effects of active cohabiting phototrophic and chemotrophic sulfur oxidizers, sulfur disproportionators, taxa with multiple/variable sulfur redox capacities, or myriad taxa which mineralize organic sulfur compounds.

In the natural environment, the isotopic compositions of sulfate and sulfide are, fundamentally, composite signatures that represent the sum of all individual members in a community of sulfur bacteria. Environmental genomic data can be a useful aid in investigating isotopic phenomena, as the taxonomical makeup of microbial communities simultaneously influences and is influenced *by* the very set of environmental conditions that isotopic analyses are often intended to investigate. In the case of lacustrine systems, fluctuations in prevailing redox chemistry (e.g., transitions from oxic to anoxic conditions) will invariably be attended by corresponding fluctuations in the composition of the microbial community (e.g., transitions from aerobic to anaerobic predominance). Once anoxia is established, the microbial consumption of available oxidants and eventual net accumulation of reduced products (e.g., free sulfide) will generate a progressively reducing environment which will, in turn, further select for a set of bacteria able to utilize electron acceptors with lower oxidation states or otherwise tolerate the presence of free

sulfide. Further, some sulfate-reducing species will actively maintain anoxia by transitioning from sulfate reduction to oxygen reduction in response to aeration, suspending their growth cycle until all oxygen has been removed (Sass and Cypionka, 2007).

These shifts in redox chemistry and community composition are reciprocal, and so are *both* inextricably linked to the isotopic evolutions of sulfate and sulfide that accompany them. This is evident in a cross-analysis of these data – the isotopic fractionations that are observed coincide with the presence of microbes that are known to induce those fractionations. Additionally, these analyses provide insight on the range of variability that can exist in the composition of microbial communities that produce broadly similar isotopic fractionations. The following discussion will draw on the broader, more taxonomically inclusive community structure profiles that were presented in section 3.4.2. These profiles (Figure 19) reveal more pronounced compositional differences between samples than do the profiles presented in section 3.4.1 (Figure 7), which encompass a decidedly smaller subset of taxa that met the more exacting inclusion criteria described in that section. For the remainder of this section, all discussion of abundance data will be made in reference to those presented in section 3.4.2 (Figure 8) and illustrated again in Figure 19.

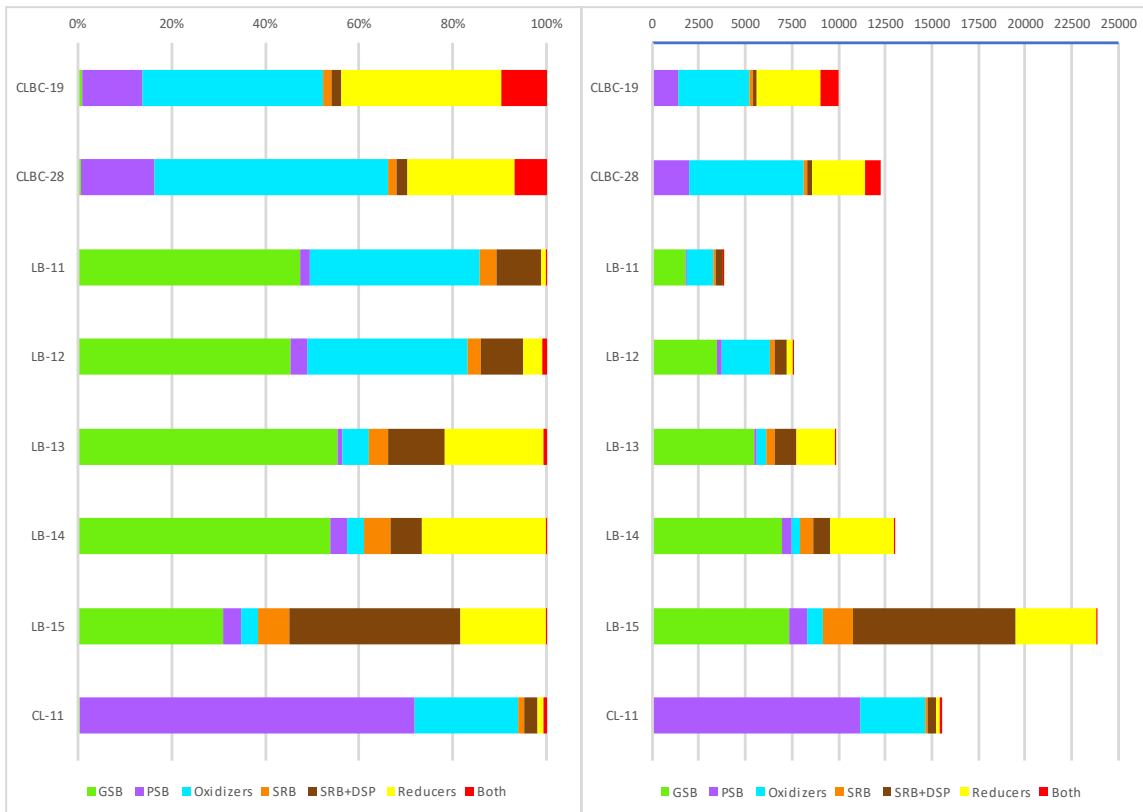


Figure 19: Taxonomically inclusive upper-bound estimations of sulfur bacterial abundances. Presented in section 3.4.2, these community structure estimations included all OTUs that shared taxonomic membership with known sulfur metabolizers.

The tight relationships between water redox chemistry, stable isotopes, and microbial community structure are exemplified in the Lime Blue Lake dissolved oxygen, ORP, isotope, and genetic profiles (Figure 19). The 16S abundance data, along with visual observations of bacterial mass in water samples, revealed that coincident fluctuations in redox (Figure 12) and sulfate isotopes (Figure 14) coincided, in turn, with marked fluctuations in community structure (Figure 19). Within the top two meters of the hypolimnion (11 and 12 m) there was a relatively large population of sulfur oxidizing bacteria compared to the remainder of the hypolimnion below. The positioning of this

sulfur oxidizer population in the top two meters of the hypolimnion is consistent with the expectation that anaerobic non-photosynthetic sulfur oxidation would be most viable just beneath the oxic/anoxic interface. Here, oxidants such as nitrate and ferrous iron would be continuously supplied by diffusion from above and support a community of sulfur oxidizing bacteria that do not require the presence of oxygen. Cryptic sulfur cycling can occur within this layer of water. If established, it will continue until the top of the euxinic zone, where flagging oxidant diffusion can no longer drive chemotrophic sulfide oxidation at a rate that, paired with phototrophic oxidation, outpaces sulfate reduction. As the diffusive oxidant supply tapers, there will be a marked decrease in the abundance of non-photosynthetic sulfur oxidizers, and ORP values will become negative as oxidants become replete and free sulfide begins to accumulate.

In Lime Blue Lake, this occurred between 12 and 13 m. There was a distinct redox transition between these two depths that was signaled by ORP values falling below 0 mV within this interval. This transition from an electropositive environment at 12 m to an electronegative one at 13 m also demarcated an ecological boundary in the water column. OTU counts for non-photosynthetic sulfur oxidizers, which had comprised 34% of the sulfur community at 12 m, sharply dropped across the ORP gradient, falling to just 6% of the community in the electronegative waters at 13 m and below. Counts of sulfur reducers (4% at 12 m, 21% at 13 m) concomitantly increased, favored by the reducing environment in the bottom waters of the lake.

The redox transition itself did not appear to have had a strong effect on the abundances of GSB or PSB, but the sharp disappearance of Sox bacteria might have bolstered GSB growth to some degree across the 12 – 13 m interval. Though Sox counts

dropped by ~80%, the total abundance of all oxidizer OTUs remained the same over the interval because Sox bacteria were effectively replaced in number by GSB, for which OTU counts increased by ~60%. This could suggest that the disappearance of Sox bacteria across the ORP gradient had left a vacancy in a niche that was shared by both phototrophic and chemotrophic oxidizers, wherein competition over reduced sulfur compounds could have been occurring above 13 m. While niche vacancy may have been a factor promoting some of the increase in GSB abundance observed over this interval, a comparison of Sox and GSB population changes over adjacent depth intervals suggests that any competition that was occurring between the two at 12 m would have likely been minimal. The increase in GSB counts over the 12-13 m interval (+2017) was indeed larger than the GSB increases measured over the adjacent 11-12 m (+1642) and 13-14 m (+1521) intervals by a margin of $+450 \pm 50$ counts. However, Sox counts between 12-13 m decreased by 2050, a value four times larger. If the sharp decline in Sox numbers did enable some of this +450 count margin by removing competition for available sulfur or some other shared resource, the effect was relatively small compared to the accumulation of GSB with depth that was already otherwise occurring through most of the hypolimnion. This trend in rising GSB counts halted over the bottommost meter of the lake, between 14 and 15 m, where GSB OTU counts increased only marginally (+390).

Conversely, SRB+DSP counts increased tenfold over the same interval, from ~1,000 at 14 m to ~10,000 at 15 m. This was the largest change observed in the study between any two samples in terms of both absolute OTU counts and percent abundance (+~30%). This large shift coincided with the abrupt increase in both sulfide concentration

and $\delta^{34}\text{S}_{\text{SO}_4}$ values measured between 14 m (0.33 mM; -12.2‰) and 15 m (0.81 mM; -9.8‰), which indicates that the high SRB+DSP OTU counts at 15 m represent an increase that materially impacted the sulfur cycle. It is notable that, unlike GSB, there was not a steady increase in SRB+DSP abundance with depth. The only substantial change in SRB+DSP abundance was highly localized between 14 and 15 m.

The steady accumulation of GSB with depth between 11 and 14 m was surprising, as GSB are light dependent. If OTU abundance measurements truly do scale with the respective quantities of active bacteria present at the time of sampling, then these data show (1) that anoxygenic phototrophy in Lime Blue Lake increased with depth throughout the hypolimnion and (2) that the highest density of anoxygenic phototrophs in the water column could be found immediately above the sediment-water interface, where sunlight was most attenuated. The abrupt 80% reduction in Sox OTUs between 12 and 13 m demonstrates that sequenceable genetic material from bacteria that are prolific within a restricted depth interval did not diffuse far on the scale of meters. Whether this holds true in other settings would depend on the diffusivity of the water column (e.g., if temperature, salinity, or turbidity gradients are present) and with how rapidly heterotrophic degradation of the genetic material takes place. There was also no appreciable increase in OTU counts in any category of sulfur bacteria between 14 and 15 m other than SRB+DSP. These observations suggest the utility of OTU counts to characterize large changes in abundance at this sampling resolution. The increase in measured GSB abundances was thus not the result of sinking dead or senescent cellular material accumulating with depth – it is highly likely that some of the GSB species sampled in Lime Blue Lake were benthic and that these taxa were in fact most abundant

in the bottom water, as were the considerably large number of SRB+DSP bacteria present there.

It is notable that the increase in sulfate reducer abundance at 15 m was solely attributable to the proliferation of a single *Desulfomonile* OTU in the SRB+DSP category, and that there was no equivalent appreciable increase in any strictly SRB OTUs. Many members of sulfate reducer taxa have the capacity to do sulfur disproportionation in addition to sulfate reduction. This capacity often varies at the species level, and though no sulfate reducer in this dataset was identified at a low enough taxonomic level to definitively ascertain if it can disproportionate, many sulfate reducers were identified to a level low enough to be nearly certain that they cannot (most of these sulfate reducers were identified to the genus or candidate genus level). The environment at the 15 m sediment-water interface was strongly selecting for an OTU that belonged to a genus with members that are known to disproportionate, and the selection excluded the plurality of other SRB taxa present throughout the entire hypolimnion.

That the conditions at 15 m had been uniquely well suited to the growth of a taxonomically narrow population of SRB+DSP bacteria suggests that this SRB+DSP group possessed metabolic capacities that differed from the other sulfate reducing taxa. Outside of dense plates of anoxygenic phototrophs, the sediment-water interface is where the highest concentration of insoluble elemental sulfur is likely to be found in the water column, provided it is produced at a rate in the waters above that outpaces its consumption or alteration as the particles settle. This was the case in Lime Blue Lake – the concentration of elemental sulfur increased through the hypolimnion to 0.23 mM at 15 m. The accumulation of elemental sulfur and insoluble polysulfides in the bottom

waters would necessarily promote the growth of microbial taxa that can utilize them and, thus, favor the growth of sulfate reducer species that have the capacity to disproportionate over sulfate reducer species that do not. It is telling that it was a population of sulfate reducing bacteria belonging to a genus with members known to be capable of sulfur disproportionation that was an order of magnitude larger than the populations of the strictly-SRB taxa under these conditions and not the other way around.

It is also worth noting that this OTU was a 100% match to a *Desulfomonile* bacterium discovered in a 25 m water column sample collected from Fayetteville Green Lake, New York. Like Lime Blue Lake, Green Lake becomes permanently stratified during the summer months and develops a euxinic hypolimnion that hosts a well-studied community of sulfur bacteria (Deevey et al., 1963; Zerkle et al., 2010; Meyer et al., 2011). The large increase in the abundance of this *Desulfomonile* bacterium coincides with the comparatively large increases in both sulfide concentration (0.33 to 0.81 mM) and $\Delta^{34}\text{S}_{\text{SO}_4\text{-H}_2\text{S}}$ (45.2 to 51.8‰) that occurred between 14 and 15 m. Expression of potentially large isotope effects, strong niche specificity, and potential ubiquity in North American lacustrine waters, makes this bacterium a compelling candidate for further research.

The community structure in Lime Blue Lake differed considerably from those in Cleland Lake and Castor Lake. While GSB were the predominant anoxygenic phototrophs in Lime Blue Lake, the opposite was found in Cleland and Castor. In each, GSB counts were respectively 1 to 2 orders of magnitude lower than those of PSB. Cleland Lake also had relatively little change in community structure between 19 and 28 m. There was no increase in reducer abundances in the bottom waters, and both PSB

and Sox taxa appeared to have slightly increased in number in the deeper sample. There was not a transition to a more reducing community at the base of the hypolimnion.

The 11 m Castor Lake sample consisted almost entirely of oxidizers, which comprised over 90% of the counted OTUs. The majority of these (71% of the community) were PSB, which is consistent with the physiochemical conditions at this depth at the time of sampling. The sample was collected from the relatively thin layer of anoxic water at 11 m, just above the bed of the lake. Constrained by the presence of oxygen above and the sediments below, this layer would have been the only position in the water column in which PSB could have grown at the time of sampling. With the layer of anoxia having formed immediately above the sediment/water interface, diffusion of sulfide from the sediments into the open water here would have facilitated conditions principally favorable for the development of a dense plate of sulfide-oxidizing anoxygenic phototrophs.

Despite harboring structurally dissimilar communities of bacteria, $\Delta^{34}\text{S}_{\text{SO}_4\text{-H}_2\text{S}}$ and $\Delta^{18}\text{O}_{\text{SO}_4\text{-H}_2\text{O}}$ values in the bottom waters of each lake broadly converged, approaching a similar set of values as hypolimnion isotopic evolution proceeded (Figure 9, Figure 15). The large differences in magnitude between the isotope effects of the dissimilatory sulfate reduction pathway and sulfur oxidation pathways would make this an eventuality in most natural environments in which sulfate reducers are present. However, the Lime Blue Lake data show that the vertical positions in the water column where these isotopic evolutions occur and the rapidity with which they proceed *do* appear to relate strongly to the composition of the sulfur bacterial communities that are present at these key points in the water column. It will be important to understand the extent to which the contours of

these ecologically-driven spatial (and almost certainly temporal) variabilities in isotope composition have a measurable impact on the $\delta^{34}\text{S}$ and $\delta^{18}\text{O}$ values that are ultimately recorded in sediments. This greatly depends on whether the isotopic evolutions of a compound of interest occur at depths where it is also being precipitated, also known as the reservoir effect (e.g., Gomes and Hurtgen, 2013). For example, in carbonate-rich lakes, temperature spikes in warmer months can lead to whiting events, where rapid elevation in water column temperature causes carbonate solubility to acutely decrease, driving it out of solution near the surface and clouding the water. CAS that is precipitated during one of these events will record the sulfate isotope composition at the depths where carbonate precipitation is occurring. In a lake like Scanlon, where the shallow (~ 4.125 m) chemocline had formed above the thermal stratification boundary (5 - 5.5 m), it could be possible for CAS precipitation to extend to the $\delta^{18}\text{O}_{\text{SO}_4}$ minimum or into the subsequent enrichment further below and capture the isotope compositions of sulfate at these locations in some portion of the bulk precipitate. These events would result in depositions of CAS with depth-integrated compositions that vary by some degree relative to CAS that was strictly precipitated well above the chemocline within the epilimnion.

V. CONCLUSIONS

This project resulted in six key findings – (1) the measurement of large $\Delta^{34}\text{S}_{\text{SO}_4\text{-H}_2\text{S}}$ values at micromolar sulfate concentrations in Cleland Lake, (2) the consistent occurrence of $\delta^{18}\text{O}_{\text{SO}_4}$ minima at the chemocline, (3) that subsequent $\delta^{18}\text{O}_{\text{SO}_4}$ enrichments consistently preceded sulfide accumulation and $\delta^{34}\text{S}_{\text{SO}_4}$ enrichment in layers of water in which there was a delay between complete consumption of dissolved oxygen and ORP values becoming negative, (4) that initial epilimnion $\Delta^{18}\text{O}_{\text{SO}_4\text{-H}_2\text{O}}$ values placed constraints on the maximum extent of $\delta^{18}\text{O}_{\text{SO}_4}$ evolution that occurred beneath the chemocline, (5) that observable changes in the metabolic composition of sulfur bacterial communities accompanied key inflections in the sulfur and oxygen isotope profiles of sulfate and sulfide within the water column, and (6) that, despite large overall differences in community structure, $\Delta^{34}\text{S}_{\text{SO}_4\text{-H}_2\text{S}}$ and $\Delta^{18}\text{O}_{\text{SO}_4\text{-H}_2\text{O}}$ values ultimately reached similar magnitudes in each lake.

5.1 Recommendations for future work

Extending high resolution sampling into the suboxic depths above the chemocline would reveal the behavior of $\delta^{18}\text{O}_{\text{SO}_4}$ and any corresponding transitions in community structure that might occur across the onset of the negative $\delta^{18}\text{O}_{\text{SO}_4}$ excursion. It was the inclusion of some anoxic depths above the euxinic zone in the focused sampling of the hypolimnion that facilitated the discovery of the $\delta^{18}\text{O}_{\text{SO}_4}$ minima. It is likely that the full spatial extent, shape, and magnitude of the negative excursions that lead to these minima were not captured.

Similarly, extending isotope sampling into the sediments in Lime Blue, Castor, and Scanlon lakes could reveal the full complement of coincident compositional changes that occur in sulfate and sulfide in each of the lakes as sulfate is more completely consumed. Capturing the remainder of distillation within sediment pore water would permit a more direct comparison between the $\delta^{18}\text{O}$ and $\delta^{34}\text{S}$ behavior in these lakes and the entire Cleland Lake water column dataset.

The inclusion of water column iron and nitrate concentrations would complement ORP and dissolved oxygen measurements in delineating the layers of water in which cryptic sulfur cycling is likely occurring. Correlating these data with variability in relative OTU abundances would serve to indicate which OTUs are utilizing these oxidants and, therefore, which of them are likely Sox candidates. It might also shed light on the high abundance of potentially sulfur oxidizing bacteria in the bottom water of Cleland Lake – if the concentration of sulfate was low enough relative to nitrate or iron for sulfate reduction and subsequent sulfide reoxidation by nitrate-utilizing Sox bacteria to not have fully exhausted the nitrate or iron pools, then this community could have been supported throughout the water column, even down to 28 m. General metabolic categorization of OTUs and abundance calibration would also be improved by sequencing samples from both the epilimnion and sediment pore waters in addition to the hypolimnion, and by the inclusion of functional gene sequencing.

APPENDICES

Appendix A $\delta^{34}\text{S}$ vs $\delta^{18}\text{O}$ distillation models

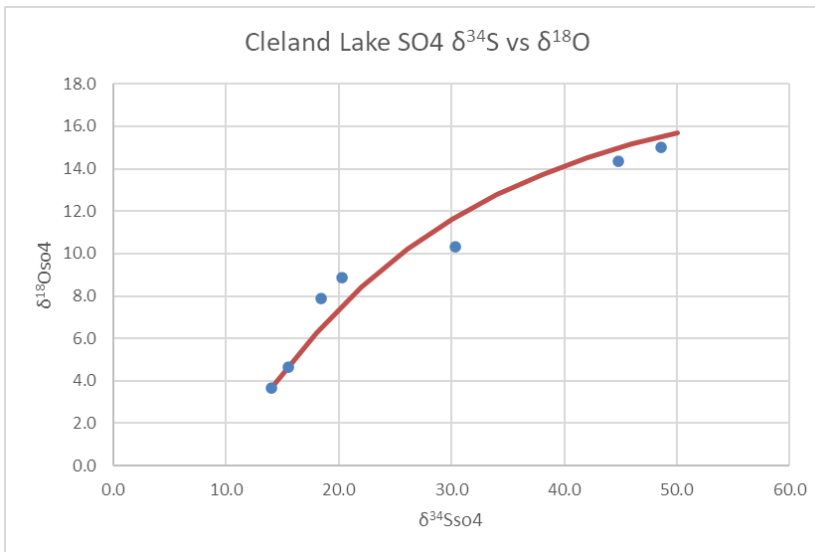
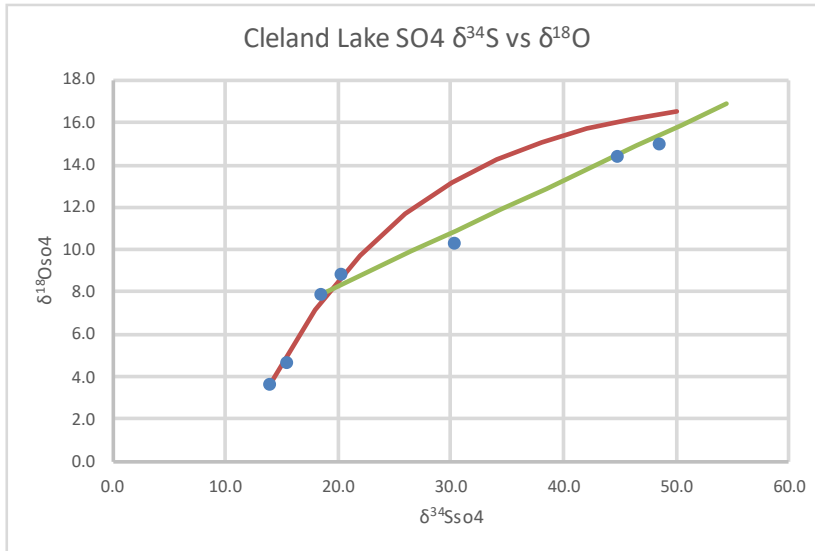


Figure 20: Cleland Lake $\delta^{34}\text{S}_{\text{SO}_4}$ and $\delta^{18}\text{O}_{\text{SO}_4}$ data plotted over distillation model results.

The Cleland Lake hypolimnion $\delta^{34}\text{S}_{\text{SO}_4}$ and $\delta^{18}\text{O}_{\text{SO}_4}$ data are the only two profiles to which the model could be fit, though achieving this required X1 and X2 values to be set close to 1 (Figure 20). The first plot above demonstrates that the composition of sulfate at 18, 19, 20, and 21 m could have been the result of exceedingly slow sulfate

reduction, where $X1=X3=0.85$, followed by a transition to rapid reduction below 21 m with zero back reaction. The second plot above shows an attempt to track the composition of sulfate using a uniform rate of sulfate reduction throughout the entire water column, where $X1=X3=0.788$. Both cases demonstrate that sulfate in Cleland Lake evolved through a range of $\delta^{34}\text{S}$ and $\delta^{18}\text{O}$ values that remained within the bounds allowed by the model.

The model cannot, however, be adjusted in any way to adhere to the Lime Blue Lake, Castor Lake, and Scanlon Lake hypolimnion data (Figure 21). In each case, the data follow a trajectory in which they flatten along the $\delta^{18}\text{O}_{\text{SO}_4}$ axis too abruptly for the model to accommodate. This indicates that there was an external factor limiting $\delta^{18}\text{O}_{\text{SO}_4}$ evolution in each of the three lakes that cannot be accounted for by the model. These failures are likely the result of the high (16‰ to 18‰) epilimnion/top-hypolimnion $\Delta^{18}\text{O}_{\text{SO}_4\text{-H}_2\text{O}}$ values in each of the three lakes. These high values appear to have left little headroom for further $\delta^{18}\text{O}_{\text{SO}_4}$ enrichment via sulfite-water equilibrium oxygen exchange during sulfate reduction, causing $\delta^{18}\text{O}_{\text{SO}_4}$ values to increase only marginally in each lake before hitting a $\Delta^{18}\text{O}_{\text{SO}_4\text{-H}_2\text{O}}$ ceiling. The plots below are examples of failure cases in Lime Blue Lake ($X1 = X3 = 0.95$), Castor Lake ($X1 = X3 = 0.95$), and Scanlon Lake ($X1 = 0.85, X3 = 0.9$).

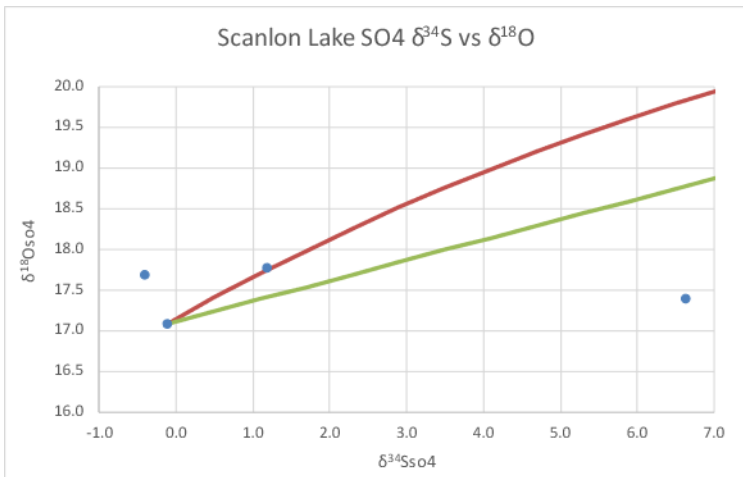
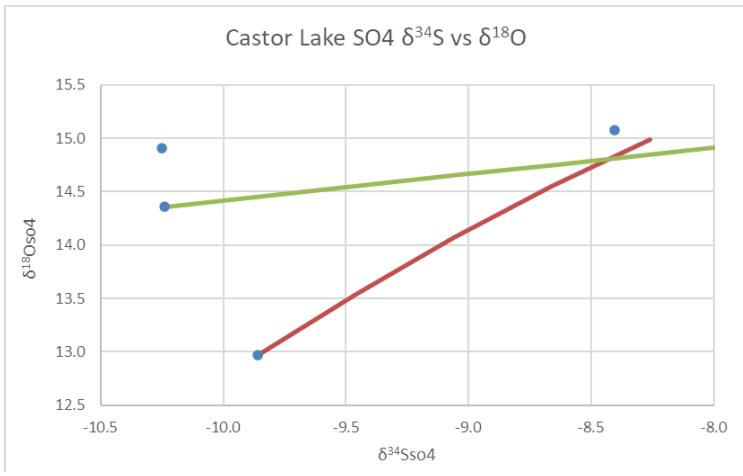
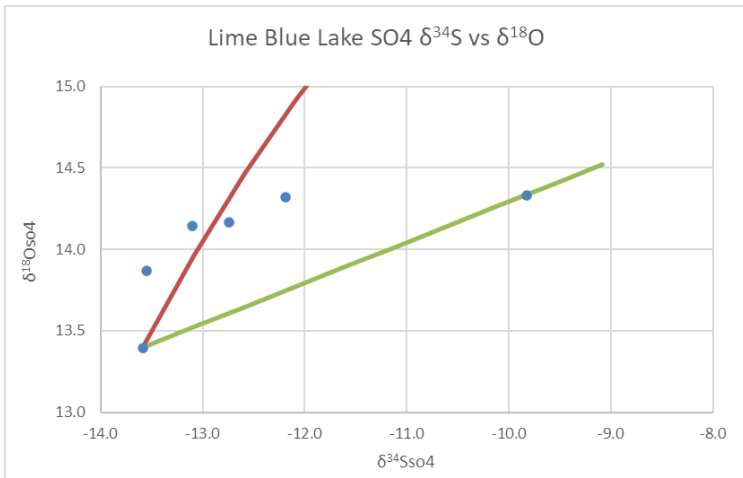


Figure 21: Lime Blue Lake, Castor Lake, and Scanlon Lake $\delta^{34}\text{S}_{\text{SO}_4}$ and $\delta^{18}\text{O}_{\text{SO}_4}$ data plotted over distillation model results.

Appendix B: Categorized operational taxonomic unit abundances

Below are abundance counts for each individual OTU included in the results and discussion sections. Taxonomies are reported here to the lowest levels assigned during the CLC Workbench OTU table creation workflow. Those OTUs listed with identical taxonomies in these tables diverge at lower taxonomic levels than were assigned during the workflow. Sample names are given as [abbreviated lake name]-[sample depth (m)], where Cleland Lake is denoted CLBC, Lime Blue Lake is LB, Castor Lake is CL, and Scanlon Lake is SL. OTU counts for the Lime Blue Lake 11 m sample are presented in a standalone table at the end of this appendix section.

Table 1: Green sulfur bacteria

Taxonomy	CLBC-19	CLBC-28	LB-12	LB-13	LB-14	LB-15	CL-11	SL-6
Bacteria, Bacteroidetes, Chlorobia, Chlorobiales, Chlorobiaceae, Chlorobium,	40	45	3294	4399	5178	3616	43	28
Bacteria, Bacteroidetes, Chlorobia, Chlorobiales, Chlorobiaceae, Chlorobium,	40	36	157	1043	1806	3722	28	31
Bacteria, Bacteroidetes, Chlorobia, Chlorobiales, Chlorobiaceae, Chlorobium, Ambiguous_taxa	1	2	3	29	8	44	5	2

Table 2: Purple sulfur bacteria

Taxonomy	CLBC-19	CLBC-28	LB-12	LB-13	LB-14	LB-15	CL-11	SL-6
Bacteria, Proteobacteria, Gammaproteobacteria, Chromatiales, Chromatiaceae, Thiocapsa, Ambiguous_taxa	1112	1590	5	5	15	8	147	4
Bacteria, Proteobacteria, Gammaproteobacteria, Chromatiales, Chromatiaceae, Thiocapsa, Ambiguous_taxa	131	241	1	0	1	3	57	1
Bacteria, Proteobacteria, Gammaproteobacteria, Chromatiales, Chromatiaceae, Thiocapsa, Thiocapsa roseopersicina	55	55	15	15	33	52	9954	14
Bacteria, Proteobacteria, Gammaproteobacteria, Chromatiales, Chromatiaceae, Thiocapsa, Thiocapsa roseopersicina	9	17	1	0	6	6	914	1
Bacteria, Proteobacteria, Gammaproteobacteria, Chromatiales, Chromatiaceae, Thiocystis, Ambiguous_taxa	2	3	150	27	166	546	9	2
Bacteria, Proteobacteria, Gammaproteobacteria, Chromatiales, Chromatiaceae, Thiohalocapsa, uncultured Chromatiaceae bacterium ML_Gamma	0	0	0	0	0	0	0	30
Bacteria, Proteobacteria, Gammaproteobacteria, Chromatiales, Chromatiaceae, Chromatium, uncultured Chromatiaceae bacterium	1	1	23	10	94	185	3	0
Bacteria, Proteobacteria, Gammaproteobacteria, Chromatiales, Chromatiaceae, Lamprocystis, Ambiguous_taxa	2	1	24	4	97	32	3	3

Bacteria, Proteobacteria, Gammaproteobacteria, Chromatiales, Chromatiaceae, Thiocystis, Ambiguous_taxa	0	0	7	0	13	67	7	1
Bacteria, Proteobacteria, Gammaproteobacteria, Chromatiales, Chromatiaceae, Thiodictyon, Ambiguous_taxa	1	2	52	55	44	28	0	0

Table 3: Sulfate reducers

Taxonomy	CLBC-19	CLBC-28	LB-12	LB-13	LB-14	LB-15	CL-11	SL-6
Bacteria, Proteobacteria, Deltaproteobacteria, Desulfobacterales, Desulfobacteraceae, Desulfatirhabdium, Ambiguous_taxa	1	0	2	4	100	562	0	1
Bacteria, Proteobacteria, Deltaproteobacteria, Desulfobacterales, Desulfobacteraceae, Desulfatirhabdium, Ambiguous_taxa	0	0	0	0	53	23	0	0
Bacteria, Proteobacteria, Deltaproteobacteria, Desulfobacterales, Desulfobacteraceae, Desulfatirhabdium, Ambiguous_taxa	0	0	0	1	0	37	2	0
Bacteria, Proteobacteria, Deltaproteobacteria, Desulfobacterales, Desulfobacteraceae, Desulfatirhabdium, Ambiguous_taxa	0	0	0	0	0	21	0	1
Bacteria, Firmicutes, Clostridia, Clostridiales, Peptococcaceae, Desulfotomaculum, Desulfotomaculum defluvii	2	1	1	0	6	9	0	0
Bacteria, Proteobacteria, Deltaproteobacteria, Desulfovibrionales, Desulfomicrobiaceae, Desulfomicrobium, uncultured bacterium	39	129	0	0	1	0	8	1

Bacteria, Proteobacteria, Deltaproteobacteria, Desulfuromonadales, Geobacteraceae, Geobacter,	0	0	26	1	0	24	1	0
Bacteria, Proteobacteria, Deltaproteobacteria, Desulfuromonadales, Geobacteraceae, Geobacter, Ambiguous_taxa	0	0	9	0	0	4	0	0
Bacteria, Proteobacteria, Deltaproteobacteria, Desulfuromonadales, Geobacteraceae, Geobacter, uncultured bacterium	3	2	44	33	54	44	0	0
Bacteria, Proteobacteria, Deltaproteobacteria, Desulfuromonadales, Geobacteraceae, Geobacter, uncultured bacterium	4	19	0	0	0	0	0	0
Bacteria, Proteobacteria, Deltaproteobacteria, Syntrophobacteriales, Syntrophaceae, Desulfobacca, Ambiguous_taxa	2	0	1	0	20	462	2	1
Bacteria, Proteobacteria, Deltaproteobacteria, Desulfobacteriales, Desulfobacteraceae, SEEP-SRB1, Ambiguous_taxa	0	0	0	0	0	0	0	45
Bacteria, Proteobacteria, Deltaproteobacteria, Desulfobacteriales, Desulfobacteraceae, SEEP-SRB1, Ambiguous_taxa	0	0	0	0	0	0	0	25
Bacteria, Proteobacteria, Deltaproteobacteria, Desulfobacteriales, Desulfobulbaceae, [Desulfobacterium] catecholicum group, uncultured bacterium	120	73	1	2	4	7	138	1
Bacteria, Proteobacteria, Deltaproteobacteria, Desulfobacteriales, Desulfobulbaceae, [Desulfobacterium] catecholicum group, Ambiguous_taxa	0	0	7	74	0	3	0	0
Bacteria, Proteobacteria, Deltaproteobacteria, Desulfobacteriales, Desulfobulbaceae, [Desulfobacterium] catecholicum group, uncultured bacterium	1	0	1	10	0	2	0	0

Bacteria, Proteobacteria, Deltaproteobacteria, Desulfobacterales, Desulfobulbaceae, [Desulfobacterium] catecholicum group, uncultured Desulfobulbaceae bacterium	1	1	4	0	8	5	6	0
--	---	---	---	---	---	---	---	---

Table 4: Potential sulfate reducers

Taxonomy	CLBC-19	CLBC-28	LB-12	LB-13	LB-14	LB-15	CL-11	SL-6
Bacteria, Bacteroidetes, Bacteroidia, Bacteroidales, Marinilabiliaceae, uncultured, Ambiguous_taxa	12	6	129	287	449	389	7	5
Bacteria, Bacteroidetes, Bacteroidia, Bacteroidales, Marinilabiliaceae, uncultured, Ambiguous_taxa	0	0	0	0	0	0	0	105
Bacteria, Bacteroidetes, Bacteroidia, Bacteroidales, Marinilabiliaceae, uncultured, Ambiguous_taxa	0	0	0	0	0	0	0	16

86

Table 5: Sulfate reducers that can potentially disproportionate

Taxonomy	CLBC-19	CLBC-28	LB-12	LB-13	LB-14	LB-15	CL-11	SL-6
Bacteria, Proteobacteria, Deltaproteobacteria, Desulfarculales, Desulfarculaceae, Desulfatiglans, uncultured bacterium	0	0	0	0	0	0	0	46
Bacteria, Proteobacteria, Deltaproteobacteria, Desulfobacterales, Desulfobulbaceae, Desulfobulbus, Ambiguous_taxa	140	82	0	1	0	0	29	0

Bacteria, Proteobacteria, Deltaproteobacteria, Desulfobacterales, Desulfobulbaceae, Desulfocapsa, Ambiguous_taxa	1	7	413	605	214	361	2	5
Bacteria, Proteobacteria, Deltaproteobacteria, Desulfobacterales, Desulfobulbaceae, Desulfocapsa, uncultured delta proteobacterium	4	5	84	54	153	260	4	0
Bacteria, Proteobacteria, Deltaproteobacteria, Desulfobacterales, Desulfobulbaceae, Desulforhopalus, Ambiguous_taxa	2	5	2	1	4	9	385	0
Bacteria, Proteobacteria, Deltaproteobacteria, Desulfobacterales, Desulfobulbaceae, uncultured, Ambiguous_taxa	5	1	16	210	72	338	2	2
Bacteria, Proteobacteria, Deltaproteobacteria, Desulfovibrionales, Desulfonatronaceae, Desulfonatronum, Ambiguous_taxa	0	0	0	0	0	0	0	40
Bacteria, Proteobacteria, Deltaproteobacteria, Desulfovibrionales, Desulfonatronaceae, Desulfonatronum, uncultured bacterium	0	0	0	0	0	0	0	16
Bacteria, Proteobacteria, Deltaproteobacteria, Syntrophobacterales, Syntrophaceae, Desulfomonile, Ambiguous_taxa	26	17	31	267	299	7643	24	12
Bacteria, Proteobacteria, Deltaproteobacteria, Desulfarculales, Desulfarculaceae, Desulfatiglans, uncultured bacterium	0	1	1	0	59	18	0	0
Bacteria, Proteobacteria, Deltaproteobacteria, Desulfobacterales, Desulfobulbaceae, Desulfocapsa, Ambiguous_taxa	0	0	60	0	30	28	0	0
Bacteria, Proteobacteria, Deltaproteobacteria, Desulfobacterales, Desulfobulbaceae, Desulforhopalus, uncultured bacterium	0	0	50	0	4	16	0	0

Bacteria, Proteobacteria, Deltaproteobacteria, Desulfobacterales, Desulfobulbaceae, uncultured, uncultured bacterium	1	1	9	9	23	37	0	0
Bacteria, Proteobacteria, Deltaproteobacteria, Desulfovibrionales, Desulfovibrionaceae, Desulfovibrio, Ambiguous_taxa	13	62	0	0	0	0	0	0
Bacteria, Proteobacteria, Deltaproteobacteria, Desulfobacterales, Desulfobacteraceae, Desulfobacterium, Ambiguous_taxa	0	0	0	11	0	0	0	0
Bacteria, Proteobacteria, Deltaproteobacteria, Desulfobacterales, Desulfobacteraceae, Desulfobacterium, Ambiguous_taxa	0	0	0	0	0	9	1	0
Bacteria, Proteobacteria, Deltaproteobacteria, Desulfobacterales, Desulfobacteraceae, uncultured, uncultured bacterium	0	0	7	26	0	7	1	0
Bacteria, Proteobacteria, Deltaproteobacteria, Desulfobacterales, Desulfobacteraceae, uncultured, uncultured Desulfatibacillum sp.	10	63	0	0	0	0	1	0
Bacteria, Proteobacteria, Deltaproteobacteria, Desulfobacterales, Desulfobacteraceae, uncultured, uncultured Desulfatibacillum sp.	5	39	1	0	0	0	1	0

Table 6: Sulfur oxidizers

Taxonomy	CLBC-19	CLBC-28	LB-12	LB-13	LB-14	LB-15	CL-11	SL-6
Bacteria, Epsilonbacteraeota, Campylobacteria, Campylobacterales, Sulfurovaceae, Sulfurovum, uncultured bacterium	0	3	0	0	0	8	0	0
Bacteria, Epsilonbacteraeota, Campylobacteria, Campylobacterales, Thiovulaceae, Sulfuricurvum, uncultured bacterium	0	0	0	0	32	0	0	0

Table 7: Potential sulfur oxidizers

Taxonomy	CLBC-19	CLBC-28	LB-12	LB-13	LB-14	LB-15	CL-11	SL-6
Bacteria, Proteobacteria, Gammaproteobacteria, Betaproteobacteriales, Burkholderiaceae, Limnohabitans, Ambiguous_taxa	2	0	218	70	33	51	0	2
Bacteria, Proteobacteria, Gammaproteobacteria, Betaproteobacteriales, Burkholderiaceae, Limnohabitans, Ambiguous_taxa	49	153	1	0	1	0	9	0
Bacteria, Proteobacteria, Gammaproteobacteria, Betaproteobacteriales, Burkholderiaceae, Limnohabitans, uncultured bacterium	1080	3771	23	7	62	31	556	1
Bacteria, Proteobacteria, Gammaproteobacteria, Betaproteobacteriales, Burkholderiaceae, Polynucleobacter, uncultured bacterium	521	325	258	198	22	55	235	4

Bacteria, Proteobacteria, Gammaproteobacteria, Betaproteobacteriales, Burkholderiaceae, Polynucleobacter, uncultured Polynucleobacter sp.	1521	688	419	130	74	55	254	4
Bacteria, Proteobacteria, Gammaproteobacteria, Betaproteobacteriales, Burkholderiaceae, Limnohabitans, uncultured bacterium	15	32	3	0	0	4	130	0
Bacteria, Proteobacteria, Alphaproteobacteria, Rhizobiales, Hyphomicrobiaceae, Filomicrobium, Ambiguous_taxa	0	0	0	0	0	0	0	13
Bacteria, Proteobacteria, Alphaproteobacteria, Rhizobiales, Xanthobacteraceae, Bradyrhizobium, Ambiguous_taxa	1	0	245	0	0	0	0	1
Bacteria, Proteobacteria, Gammaproteobacteria, Betaproteobacteriales, Burkholderiaceae, Hydrogenophaga, Ambiguous_taxa	11	42	0	0	3	1	178	1
Bacteria, Proteobacteria, Gammaproteobacteria, Betaproteobacteriales, Burkholderiaceae, Hydrogenophaga, Hydrogenophaga taeniospiralis	44	215	16	0	0	2	26	0
Bacteria, Proteobacteria, Gammaproteobacteria, Betaproteobacteriales, Burkholderiaceae, Hydrogenophaga, uncultured Alicyclophilus sp.	61	143	2	0	2	2	101	0
Bacteria, Proteobacteria, Gammaproteobacteria, Betaproteobacteriales, Burkholderiaceae, Hydrogenophaga, uncultured bacterium	387	396	56	5	2	11	257	2
Bacteria, Proteobacteria, Gammaproteobacteria, Betaproteobacteriales, Burkholderiaceae, Hydrogenophaga, uncultured bacterium	111	287	0	1	0	0	29	1
Bacteria, Proteobacteria, Gammaproteobacteria, Betaproteobacteriales, Burkholderiaceae, Hydrogenophaga, uncultured bacterium	10	28	0	0	0	0	0	0

Bacteria, Bacteroidetes, Bacteroidia, Flavobacteriales, Flavobacteriaceae, Flavobacterium, Ambiguous_taxa	13	9	767	6	56	265	1571	4
Bacteria, Bacteroidetes, Bacteroidia, Flavobacteriales, Flavobacteriaceae, Flavobacterium, uncultured bacterium	0	3	135	2	22	70	3	0
Bacteria, Bacteroidetes, Bacteroidia, Flavobacteriales, Flavobacteriaceae, Flavobacterium, uncultured bacterium	0	0	147	0	13	38	2	0
Bacteria, Bacteroidetes, Bacteroidia, Flavobacteriales, Flavobacteriaceae, Flavobacterium, Ambiguous_taxa	0	0	15	80	0	11	1	0
Bacteria, Bacteroidetes, Bacteroidia, Flavobacteriales, Flavobacteriaceae, Flavobacterium, Ambiguous_taxa	0	1	51	0	0	47	1	0
Bacteria, Bacteroidetes, Bacteroidia, Flavobacteriales, Flavobacteriaceae, Flavobacterium, Ambiguous_taxa	0	0	3	0	62	12	0	0
Bacteria, Bacteroidetes, Bacteroidia, Flavobacteriales, Flavobacteriaceae, Flavobacterium, Ambiguous_taxa	0	1	2	0	50	7	0	0
Bacteria, Bacteroidetes, Bacteroidia, Flavobacteriales, Flavobacteriaceae, Flavobacterium, Ambiguous_taxa	0	1	18	0	0	2	4	0
Bacteria, Bacteroidetes, Bacteroidia, Flavobacteriales, Flavobacteriaceae, Flavobacterium, Ambiguous_taxa	0	0	17	0	0	7	0	0
Bacteria, Bacteroidetes, Bacteroidia, Flavobacteriales, Flavobacteriaceae, Flavobacterium, Ambiguous_taxa	0	0	20	0	0	0	0	0

Bacteria, Bacteroidetes, Bacteroidia, Flavobacteriales, Flavobacteriaceae, Flavobacterium, uncultured bacterium	0	0	12	0	0	12	0	0
Bacteria, Bacteroidetes, Bacteroidia, Flavobacteriales, Flavobacteriaceae, Flavobacterium, uncultured bacterium	0	0	8	0	0	4	0	0
Bacteria, Proteobacteria, Alphaproteobacteria, Rhodobacterales, Rhodobacteraceae, Ambiguous_taxa, Ambiguous_taxa	5	1	64	0	2	38	17	48
Bacteria, Proteobacteria, Alphaproteobacteria, Rhodobacterales, Rhodobacteraceae, Ambiguous_taxa, Ambiguous_taxa	3	3	31	1	0	27	16	0
Bacteria, Proteobacteria, Alphaproteobacteria, Rhodobacterales, Rhodobacteraceae, Ambiguous_taxa, Ambiguous_taxa	0	0	0	0	0	1	14	0
Bacteria, Proteobacteria, Alphaproteobacteria, Rhodobacterales, Rhodobacteraceae, Rhodobacter, Ambiguous_taxa	0	2	69	49	23	84	1	1
Bacteria, Proteobacteria, Alphaproteobacteria, Rhodobacterales, Rhodobacteraceae, Rhodobacter, Ambiguous_taxa	3	0	6	0	1	2	33	0
Bacteria, Proteobacteria, Alphaproteobacteria, Rhodobacterales, Rhodobacteraceae, Rhodobacter, uncultured bacterium	0	0	2	0	0	1	13	0
Bacteria, Proteobacteria, Gammaproteobacteria, Chromatiales, Chromatiaceae, Thiocapsa, Ambiguous_taxa	1112	1590	5	5	15	8	147	4
Bacteria, Proteobacteria, Gammaproteobacteria, Chromatiales, Chromatiaceae, Thiocapsa, Ambiguous_taxa	131	241	1	0	1	3	57	1

Bacteria, Proteobacteria, Gammaproteobacteria, Chromatiales, Chromatiaceae, Thiocapsa, Thiocapsa roseopersicina	55	55	15	15	33	52	9954	14
Bacteria, Proteobacteria, Gammaproteobacteria, Chromatiales, Chromatiaceae, Thiocapsa, Thiocapsa roseopersicina	9	17	1	0	6	6	914	1
Bacteria, Proteobacteria, Gammaproteobacteria, Chromatiales, Chromatiaceae, Thiocystis, Ambiguous_taxa	2	3	150	27	166	546	9	2
Bacteria, Proteobacteria, Gammaproteobacteria, Chromatiales, Chromatiaceae, Thiohalocapsa, uncultured Chromatiaceae bacterium ML_Gamma	0	0	0	0	0	0	0	30
Bacteria, Proteobacteria, Gammaproteobacteria, Chromatiales, Chromatiaceae, Chromatium, uncultured Chromatiaceae bacterium	1	1	23	10	94	185	3	0
Bacteria, Proteobacteria, Gammaproteobacteria, Chromatiales, Chromatiaceae, Lamprocystis, Ambiguous_taxa	2	1	24	4	97	32	3	3
Bacteria, Proteobacteria, Gammaproteobacteria, Chromatiales, Chromatiaceae, Thiocystis, Ambiguous_taxa	0	0	7	0	13	67	7	1
Bacteria, Proteobacteria, Gammaproteobacteria, Chromatiales, Chromatiaceae, Thiodictyon, Ambiguous_taxa	1	2	52	55	44	28	0	0

Table 8: Potential sulfur reducers

Taxonomy	CLBC-19	CLBC-28	LB-12	LB-13	LB-14	LB-15	CL-11	SL-6
Bacteria, Chloroflexi, Dehalococcoidia, GIF9, uncultured bacterium, uncultured bacterium, uncultured bacterium	27	67	6	2	382	168 2	2	7
Bacteria, Kiritimatiellaeota, Kiritimatiellae, Kiritimatiellales, Kiritimatiellaceae, MSBL3, Ambiguous_taxa	2562	1390	14	10	62	257	26	6
Bacteria, Kiritimatiellaeota, Kiritimatiellae, WCHB1-41, uncultured bacterium, uncultured bacterium, uncultured bacterium	136	137	47	0	802	381	14	2
Bacteria, Kiritimatiellaeota, Kiritimatiellae, WCHB1-41, uncultured bacterium, uncultured bacterium, uncultured bacterium	3	3	5	330	215	341	3	0
Bacteria, Kiritimatiellaeota, Kiritimatiellae, WCHB1-41, uncultured bacterium, uncultured bacterium, uncultured bacterium	49	167	9	235	155	88	0	2
Bacteria, Kiritimatiellaeota, Kiritimatiellae, WCHB1-41, uncultured bacterium, uncultured bacterium, uncultured bacterium	13	35	13	299	114	62	0	0
Bacteria, Kiritimatiellaeota, Kiritimatiellae, WCHB1-41, uncultured bacterium, uncultured bacterium, uncultured bacterium	1	1	7	294	129	31	0	1
Bacteria, Kiritimatiellaeota, Kiritimatiellae, WCHB1-41, uncultured bacterium, uncultured bacterium, uncultured bacterium	133	314	1	3	0	3	2	1

Bacteria, Kiritimatiellaeota, Kiritimatiellae, WCHB1-41, uncultured bacterium, uncultured bacterium, uncultured bacterium	28	36	4	14	238	90	1	1
Bacteria, Kiritimatiellaeota, Kiritimatiellae, WCHB1-41, uncultured bacterium, uncultured bacterium, uncultured bacterium	0	1	13	244	64	26	0	1
Bacteria, Kiritimatiellaeota, Kiritimatiellae, WCHB1-41, uncultured bacterium, uncultured bacterium, uncultured bacterium	0	2	0	0	129	12	0	0
Bacteria, Kiritimatiellaeota, Kiritimatiellae, WCHB1-41, uncultured Verrucomicrobia bacterium, uncultured Verrucomicrobia bacterium, uncultured Verrucomicrobia bacterium	103	12	2	0	5	10	22	0
Bacteria, Kiritimatiellaeota, Kiritimatiellae, Kiritimatiellales, Kiritimatiellaceae, MSBL3, Ambiguous_taxa	78	100	3	1	0	30	5	1
Bacteria, Kiritimatiellaeota, Kiritimatiellae, Kiritimatiellales, Kiritimatiellaceae, MSBL3, Ambiguous_taxa	24	10	2	5	38	76	24	0
Bacteria, Kiritimatiellaeota, Kiritimatiellae, Kiritimatiellales, Kiritimatiellaceae, MSBL3, Ambiguous_taxa	1	2	0	9	5	97	0	0
Bacteria, Kiritimatiellaeota, Kiritimatiellae, Kiritimatiellales, Kiritimatiellaceae, MSBL3, Ambiguous_taxa	0	1	0	0	0	20	0	0
Bacteria, Kiritimatiellaeota, Kiritimatiellae, Kiritimatiellales, Kiritimatiellaceae, MSBL3, uncultured bacterium	1	1	3	41	2	164	0	2
Bacteria, Kiritimatiellaeota, Kiritimatiellae, Kiritimatiellales, Kiritimatiellaceae, R76-B128, uncultured bacterium	0	4	5	0	0	3	1	0

Bacteria, Kiritimatiellaeota, Kiritimatiellae, WCHB1-41, Ambiguous_taxa, Ambiguous_taxa, Ambiguous_taxa	0	1	0	96	0	123	0	0
Bacteria, Kiritimatiellaeota, Kiritimatiellae, WCHB1-41, Ambiguous_taxa, Ambiguous_taxa, Ambiguous_taxa	87	102	1	0	1	1	1	1
Bacteria, Kiritimatiellaeota, Kiritimatiellae, WCHB1-41, Ambiguous_taxa, Ambiguous_taxa, Ambiguous_taxa	0	0	1	64	27	8	0	0
Bacteria, Kiritimatiellaeota, Kiritimatiellae, WCHB1-41, Ambiguous_taxa, Ambiguous_taxa, Ambiguous_taxa	3	80	0	0	0	0	0	0
Bacteria, Kiritimatiellaeota, Kiritimatiellae, WCHB1-41, Ambiguous_taxa, Ambiguous_taxa, Ambiguous_taxa	17	14	0	0	0	1	16	0
Bacteria, Kiritimatiellaeota, Kiritimatiellae, WCHB1-41, Ambiguous_taxa, Ambiguous_taxa, Ambiguous_taxa	0	3	0	0	35	5	0	0
Bacteria, Kiritimatiellaeota, Kiritimatiellae, WCHB1-41, Ambiguous_taxa, Ambiguous_taxa, Ambiguous_taxa	0	4	0	0	24	0	0	0
Bacteria, Kiritimatiellaeota, Kiritimatiellae, WCHB1-41, Ambiguous_taxa, Ambiguous_taxa, Ambiguous_taxa	1	24	0	0	0	1	0	0
Bacteria, Kiritimatiellaeota, Kiritimatiellae, WCHB1-41, Ambiguous_taxa, Ambiguous_taxa, Ambiguous_taxa	2	3	2	0	8	3	0	0
Bacteria, Kiritimatiellaeota, Kiritimatiellae, WCHB1-41, metagenome, metagenome, metagenome	0	0	0	0	32	0	0	0

Bacteria, Kiritimatiellaeota, Kiritimatiellae, WCHB1-41, uncultured bacterium, uncultured bacterium, uncultured bacterium	1	4	9	58	50	17	0	0
Bacteria, Kiritimatiellaeota, Kiritimatiellae, WCHB1-41, uncultured bacterium, uncultured bacterium, uncultured bacterium	2	1	0	1	62	31	0	0
Bacteria, Kiritimatiellaeota, Kiritimatiellae, WCHB1-41, uncultured bacterium, uncultured bacterium, uncultured bacterium	1	1	0	0	86	6	0	0
Bacteria, Kiritimatiellaeota, Kiritimatiellae, WCHB1-41, uncultured bacterium, uncultured bacterium, uncultured bacterium	3	2	2	0	72	3	0	0
Bacteria, Kiritimatiellaeota, Kiritimatiellae, WCHB1-41, uncultured bacterium, uncultured bacterium, uncultured bacterium	2	6	8	29	22	12	0	0
Bacteria, Kiritimatiellaeota, Kiritimatiellae, WCHB1-41, uncultured bacterium, uncultured bacterium, uncultured bacterium	5	34	3	0	0	34	0	1
Bacteria, Kiritimatiellaeota, Kiritimatiellae, WCHB1-41, uncultured bacterium, uncultured bacterium, uncultured bacterium	0	0	1	64	0	1	0	0
Bacteria, Kiritimatiellaeota, Kiritimatiellae, WCHB1-41, uncultured bacterium, uncultured bacterium, uncultured bacterium	0	0	2	1	47	15	0	0
Bacteria, Kiritimatiellaeota, Kiritimatiellae, WCHB1-41, uncultured bacterium, uncultured bacterium, uncultured bacterium	9	12	0	0	33	1	0	0
Bacteria, Kiritimatiellaeota, Kiritimatiellae, WCHB1-41, uncultured bacterium, uncultured bacterium, uncultured bacterium	2	0	4	0	32	11	0	0

Bacteria, Kiritimatiellaeota, Kiritimatiellae, WCHB1-41, uncultured bacterium, uncultured bacterium, uncultured bacterium	15	31	0	0	0	0	0	0
Bacteria, Kiritimatiellaeota, Kiritimatiellae, WCHB1-41, uncultured bacterium, uncultured bacterium, uncultured bacterium	4	21	0	0	0	0	0	0
Bacteria, Kiritimatiellaeota, Kiritimatiellae, WCHB1-41, uncultured bacterium, uncultured bacterium, uncultured bacterium	8	4	0	0	0	0	7	1
Bacteria, Kiritimatiellaeota, Kiritimatiellae, WCHB1-41, uncultured bacterium, uncultured bacterium, uncultured bacterium	0	10	0	0	0	0	0	0
Bacteria, Kiritimatiellaeota, Kiritimatiellae, WCHB1-41, uncultured organism, uncultured organism, uncultured organism	71	82	0	0	1	0	0	0
Bacteria, Kiritimatiellaeota, Kiritimatiellae, WCHB1-41, uncultured organism, uncultured organism, uncultured organism	0	0	1	0	11	69	0	0
Bacteria, Kiritimatiellaeota, Kiritimatiellae, WCHB1-41, uncultured organism, uncultured organism, uncultured organism	0	1	9	0	0	19	1	0
Bacteria, Kiritimatiellaeota, Kiritimatiellae, WCHB1-41, uncultured organism, uncultured organism, uncultured organism	0	0	0	0	0	16	0	0
Bacteria, Kiritimatiellaeota, Kiritimatiellae, WCHB1-41, uncultured Verrucomicrobia bacterium, uncultured Verrucomicrobia bacterium, uncultured Verrucomicrobia bacterium	0	0	0	0	0	48	0	0
Bacteria, Spirochaetes, Spirochaetia, Spirochaetales, Spirochaetaceae, Sediminispirochaeta, uncultured bacterium	0	0	0	0	1	0	1	84

Table 9: Potential oxidizers and/or reducers

Taxonomy	CLBC-19	CLBC-28	LB-12	LB-13	LB-14	LB-15	CL-11	SL-6
Bacteria, Spirochaetes, Spirochaetia, Spirochaetales, Spirochaetaceae, Spirochaeta 2, uncultured organism	0	0	0	1	0	0	0	82
Bacteria, Spirochaetes, Spirochaetia, Spirochaetales, Spirochaetaceae, uncultured, Ambiguous_taxa	57	39	7	1	4	16	4	1
Bacteria, Spirochaetes, Spirochaetia, Spirochaetales, Spirochaetaceae, uncultured, Ambiguous_taxa	3	0	0	0	7	5	1	0
Bacteria, Spirochaetes, Spirochaetia, Spirochaetales, Spirochaetaceae, uncultured, uncultured bacterium	769	590	2	1	4	36	99	5
Bacteria, Proteobacteria, Gammaproteobacteria, Pseudomonadales, Pseudomonadaceae, Pseudomonas, Ambiguous_taxa	122	197	0	0	3	1	13	1
Bacteria, Proteobacteria, Gammaproteobacteria, Pseudomonadales, Pseudomonadaceae, Pseudomonas, Ambiguous_taxa	5	0	56	52	0	0	2	0
Bacteria, Proteobacteria, Gammaproteobacteria, Pseudomonadales, Pseudomonadaceae, Pseudomonas, uncultured Pseudomonas sp.	12	14	1	0	0	0	0	0
Bacteria, Proteobacteria, Gammaproteobacteria, Pseudomonadales, Pseudomonadaceae, Pseudomonas, uncultured Pseudomonas sp.	0	1	0	13	0	0	0	0

The total sequence count in sample LB-11 was <50% of the sample batch size median for all samples, which caused the sample to be excluded from the OTU table by CLC Workbench. This is a locked threshold value set in the workflow, so the separate OTU table below was created for this sample. Because the pool of sequences in this sample was an order of magnitude smaller than the combined pool comprised of all other samples, the resulting OTUs in this table were proportionally less abundant. For this reason, OTUs with abundance counts lower than 2 were discarded from this table, as opposed to the abundance cutoff of 10 counts that was used for the tables above to avoid disproportionate culling from this sample.

Table 10: Lime Blue Lake 11 m OTU counts for all sulfur-metabolizing taxa

Classification	Taxonomy	Count
Green sulfur bacteria	Bacteria, Bacteroidetes, Chlorobia, Chlorobiales, Chlorobiaceae, Chlorobium,	1721
Green sulfur bacteria	Bacteria, Bacteroidetes, Chlorobia, Chlorobiales, Chlorobiaceae, Chlorobium,	91
Purple sulfur bacteria	Bacteria, Proteobacteria, Gammaproteobacteria, Chromatiales, Chromatiaceae, Thiocystis, Ambiguous_taxa	71
Purple sulfur bacteria	Bacteria, Proteobacteria, Gammaproteobacteria, Chromatiales, Chromatiaceae, Thiocystis, Ambiguous_taxa	6
Purple sulfur bacteria	Bacteria, Proteobacteria, Gammaproteobacteria, Chromatiales, Chromatiaceae, Thiodictyon, Ambiguous_taxa	4
Purple sulfur bacteria	Bacteria, Proteobacteria, Gammaproteobacteria, Chromatiales, Chromatiaceae, Lamprocystis, Ambiguous_taxa	2
Purple sulfur bacteria	Bacteria, Proteobacteria, Gammaproteobacteria, Chromatiales, Chromatiaceae, Thiocapsa, Thiocapsa roseopersicina	2

Sulfate reducer	Bacteria, Proteobacteria, Deltaproteobacteria, Desulfuromonadales, Geobacteraceae, Geobacter, uncultured bacterium	22
Sulfate reducer	Bacteria, Proteobacteria, Deltaproteobacteria, Desulfuromonadales, Geobacteraceae, Geobacter, Ambiguous_taxa	10
Sulfate reducer	Bacteria, Proteobacteria, Deltaproteobacteria, Desulfuromonadales, Geobacteraceae, Geobacter, Ambiguous_taxa	2
Sulfate reducer	Bacteria, Proteobacteria, Deltaproteobacteria, Desulfuromonadales, Geobacteraceae, Geobacter, Ambiguous_taxa	2
Sulfate reducer	Bacteria, Proteobacteria, Deltaproteobacteria, Desulfuromonadales, Geobacteraceae, Geobacter, uncultured bacterium	2
Sulfate reducer	Bacteria, Proteobacteria, Deltaproteobacteria, Desulfobacterales, Desulfobulbaceae, [Desulfobacterium] catecholicum group, uncultured bacterium	48
Sulfate reducer	Bacteria, Proteobacteria, Deltaproteobacteria, Desulfobacterales, Desulfobulbaceae, [Desulfobacterium] catecholicum group, uncultured Desulfobulbaceae bacterium	4
Potential sulfate reducer	Bacteria, Bacteroidetes, Bacteroidia, Bacteroidales, Marinilabiliaceae, uncultured, Ambiguous_taxa	55
Sulfate reducer that can potentially disproportionate	Bacteria, Proteobacteria, Deltaproteobacteria, Desulfobacterales, Desulfobulbaceae, Desulfocapsa, Ambiguous_taxa	220
Sulfate reducer that can potentially disproportionate	Bacteria, Proteobacteria, Deltaproteobacteria, Desulfobacterales, Desulfobulbaceae, Desulfocapsa, uncultured delta proteobacterium	43

Sulfate reducer that can potentially disproportionate	Bacteria, Proteobacteria, Deltaproteobacteria, Desulfobacterales, Desulfobulbaceae, Desulforhopalus, uncultured bacterium	39
Sulfate reducer that can potentially disproportionate	Bacteria, Proteobacteria, Deltaproteobacteria, Desulfobacterales, Desulfobulbaceae, Desulfocapsa, Ambiguous_taxa	37
Sulfate reducer that can potentially disproportionate	Bacteria, Proteobacteria, Deltaproteobacteria, Desulfobacterales, Desulfobulbaceae, uncultured, Ambiguous_taxa	9
Sulfate reducer that can potentially disproportionate	Bacteria, Proteobacteria, Deltaproteobacteria, Syntrophobacterales, Syntrophaceae, Desulfomonile, Ambiguous_taxa	8
Sulfate reducer that can potentially disproportionate	Bacteria, Proteobacteria, Deltaproteobacteria, Desulfovibrionales, Desulfovibrionaceae, Desulfovibrio, Ambiguous_taxa	2
Sulfate reducer that can potentially disproportionate	Bacteria, Proteobacteria, Deltaproteobacteria, Syntrophobacterales, Syntrophaceae, Desulfomonile, uncultured bacterium	2
Potential sulfur oxidizer	Bacteria, Proteobacteria, Gammaproteobacteria, Betaproteobacteriales, Burkholderiaceae, Polynucleobacter, uncultured Polynucleobacter sp.	241
Potential sulfur oxidizer	Bacteria, Proteobacteria, Gammaproteobacteria, Betaproteobacteriales, Burkholderiaceae, Polynucleobacter, uncultured bacterium	148
Potential sulfur oxidizer	Bacteria, Proteobacteria, Gammaproteobacteria, Betaproteobacteriales, Burkholderiaceae, Limnohabitans, Ambiguous_taxa	128
Potential sulfur oxidizer	Bacteria, Proteobacteria, Gammaproteobacteria, Betaproteobacteriales, Burkholderiaceae, Limnohabitans, uncultured bacterium	11

Potential sulfur oxidizer	Bacteria, Proteobacteria, Gammaproteobacteria, Betaproteobacteriales, Burkholderiaceae, uncultured, uncultured bacterium	9
Potential sulfur oxidizer	Bacteria, Proteobacteria, Gammaproteobacteria, Betaproteobacteriales, Burkholderiaceae, Hydrogenophaga, uncultured bacterium	28
Potential sulfur oxidizer	Bacteria, Proteobacteria, Gammaproteobacteria, Betaproteobacteriales, Burkholderiaceae, Hydrogenophaga, Hydrogenophaga taeniospiralis	4
Potential sulfur oxidizer	Bacteria, Proteobacteria, Gammaproteobacteria, Betaproteobacteriales, Burkholderiaceae, Hydrogenophaga, Ambiguous_taxa	3
Potential sulfur oxidizer	Bacteria, Bacteroidetes, Bacteroidia, Flavobacteriales, Flavobacteriaceae, Flavobacterium, Ambiguous_taxa	418
Potential sulfur oxidizer	Bacteria, Bacteroidetes, Bacteroidia, Flavobacteriales, Flavobacteriaceae, Flavobacterium, uncultured bacterium	95
Potential sulfur oxidizer	Bacteria, Bacteroidetes, Bacteroidia, Flavobacteriales, Flavobacteriaceae, Flavobacterium, uncultured bacterium	87
Potential sulfur oxidizer	Bacteria, Bacteroidetes, Bacteroidia, Flavobacteriales, Flavobacteriaceae, Flavobacterium, Ambiguous_taxa	24
Potential sulfur oxidizer	Bacteria, Bacteroidetes, Bacteroidia, Flavobacteriales, Flavobacteriaceae, Flavobacterium, Ambiguous_taxa	10
Potential sulfur oxidizer	Bacteria, Bacteroidetes, Bacteroidia, Flavobacteriales, Flavobacteriaceae, Flavobacterium, Ambiguous_taxa	4

Potential sulfur oxidizer	Bacteria, Bacteroidetes, Bacteroidia, Flavobacteriales, Flavobacteriaceae, Flavobacterium, Ambiguous_taxa	4
Potential sulfur oxidizer	Bacteria, Bacteroidetes, Bacteroidia, Flavobacteriales, Flavobacteriaceae, Flavobacterium, Ambiguous_taxa	4
Potential sulfur oxidizer	Bacteria, Bacteroidetes, Bacteroidia, Flavobacteriales, Flavobacteriaceae, Flavobacterium, Ambiguous_taxa	2
Potential sulfur oxidizer	Bacteria, Bacteroidetes, Bacteroidia, Flavobacteriales, Flavobacteriaceae, Flavobacterium, uncultured bacterium	2
Potential sulfur oxidizer	Bacteria, Proteobacteria, Alphaproteobacteria, Rhodobacterales, Rhodobacteraceae, Ambiguous_taxa, Ambiguous_taxa	75
Potential sulfur oxidizer	Bacteria, Proteobacteria, Alphaproteobacteria, Rhodobacterales, Rhodobacteraceae, Rhodobacter, Ambiguous_taxa	53
Potential sulfur oxidizers	Bacteria, Proteobacteria, Alphaproteobacteria, Rhodobacterales, Rhodobacteraceae, Ambiguous_taxa, Ambiguous_taxa	30
Sulfur reducer	Bacteria, Epsilonbacteraeota, Campylobacteria, Campylobacterales, Sulfurospirillaceae, Sulfurospirillum, uncultured bacterium	6
Potential sulfur reducer	Bacteria, Chloroflexi, Dehalococcoidia, GIF9, uncultured bacterium, uncultured bacterium, uncultured bacterium	2
Potential sulfur reducer	Bacteria, Kiritimatiellaeota, Kiritimatiellae, Kiritimatiellales, Kiritimatiellaceae, MSBL3, Ambiguous_taxa	17

Potential sulfur reducer	Bacteria, Kiritimatiellaeota, Kiritimatiellae, WCHB1-41, uncultured bacterium, uncultured bacterium, uncultured bacterium	8
Potential sulfur reducer	Bacteria, Kiritimatiellaeota, Kiritimatiellae, WCHB1-41, Ambiguous_taxa, Ambiguous_taxa, Ambiguous_taxa	2
Potential sulfur reducer	Bacteria, Kiritimatiellaeota, Kiritimatiellae, WCHB1-41, uncultured bacterium, uncultured bacterium, uncultured bacterium	2
Potential sulfur reducer	Bacteria, Kiritimatiellaeota, Kiritimatiellae, WCHB1-41, uncultured bacterium, uncultured bacterium, uncultured bacterium	2
Potential sulfur reducer	Bacteria, Kiritimatiellaeota, Kiritimatiellae, WCHB1-41, uncultured bacterium, uncultured bacterium, uncultured bacterium	2
Potential sulfur reducer	Bacteria, Kiritimatiellaeota, Kiritimatiellae, WCHB1-41, uncultured bacterium, uncultured bacterium, uncultured bacterium	2
Potential oxidizers and/or reducer	Bacteria, Spirochaetes, Spirochaetia, Spirochaetales, Spirochaetaceae, uncultured, Ambiguous_taxa	2

REFERENCES

- Aller R. C., Madrid V., Chistoserdov A., Aller J. Y. and Heilbrun C. (2010) Unsteady diagenetic processes and sulfur biogeochemistry in tropical deltaic muds: Implications for oceanic isotope cycles and the sedimentary record. *Geochim Cosmochim Acta* **74**, 4671–4692.
- Antler G., Turchyn A. V., Ono S., Sivan O. and Bosak T. (2017) Combined 34S, 33S and 18O isotope fractionations record different intracellular steps of microbial sulfate reduction. *Geochim Cosmochim Acta* **203**, 364–380.
- Antler G., Turchyn A. V., Rennie V., Herut B. and Sivan O. (2013) Coupled sulfur and oxygen isotope insight into bacterial sulfate reduction in the natural environment. *Geochim Cosmochim Acta* **118**, 98–117.
- Balci N., Shanks W. C., Mayer B. and Mandernack K. W. (2007) Oxygen and sulfur isotope systematics of sulfate produced by bacterial and abiotic oxidation of pyrite. *Geochim Cosmochim Acta* **71**, 3796–3811.
- Bertran E., Waldeck A., Wing B. A., Halevy I., Leavitt W. D., Bradley A. S. and Johnston D. T. (2020) Oxygen isotope effects during microbial sulfate reduction: applications to sediment cell abundances. *ISME Journal* **14**, 1508–1519.
- Betts R. H. and Voss R. H. (1970) The kinetics of oxygen exchange between the sulfite ion and water. *Can J Chem* **48**, 2035–2041.
- Booth I. R. (1985) Regulation of cytoplasmic pH in bacteria. *Microbiol Rev* **49**, 359–378.

- Böttcher M. E., Oelschläger B., Höpner T., Brumsack H. J. and Rullkötter J. (1998) Sulfate reduction related to the early diagenetic degradation of organic matter and “black spot” formation in tidal sandflats of the German Wadden Sea (southern North Sea): Stable isotope (^{13}C , ^{34}S , ^{18}O) and other geochemical results. *Org Geochem* **29**, 1517–1530.
- Böttcher M. E., Thamdrup B., Gehre M. and Theune A. (2005) $^{34}\text{S}/^{32}\text{S}$ and $^{18}\text{O}/^{16}\text{O}$ Fractionation During Sulfur Disproportionation by *Desulfobulbus propionicus*. *Geomicrobiol J* **22**, 219–226.
- Böttcher M. E., Thamdrup B. and Vennemann T. W. (2001) Anaerobic sulfide oxidation and stable isotope fractionation associated with bacterial sulfur disproportionation in the presence of MnO_2 . *Geochim Cosmochim Acta* **65**, 1573–1581.
- Böttcher, M. E., Thamdrup B. and Vennemann T. W. (2001) Oxygen and sulfur isotope fractionation during anaerobic bacterial disproportionation of elemental sulfur. *Geochim Cosmochim Acta* **65**, 1601–1609.
- Brabec M. Y., Lyons T. W. and Mandernack K. W. (2012) Oxygen and sulfur isotope fractionation during sulfide oxidation by anoxygenic phototrophic bacteria. *Geochim Cosmochim Acta* **83**, 234–251.
- Bradley A. S., Leavitt W. D. and Johnston D. T. (2011) Revisiting the dissimilatory sulfate reduction pathway. *Geobiology* **9**, 446–457.
- Brocks J. J., Love G. D., Summons R. E., Knoll A. H., Logan G. A. and Bowden S. A. (2005) Biomarker evidence for green and purple sulphur bacteria in a stratified Palaeoproterozoic sea. *Nature* **437**, 866–870.

- Brunner B. and Bernasconi S. M. (2005) A revised isotope fractionation model for dissimilatory sulfate reduction in sulfate reducing bacteria. *Geochim Cosmochim Acta* **69**, 4759–4771.
- Brunner B., Bernasconi S. M., Kleikemper J. and Schroth M. H. (2005a) A model for oxygen and sulfur isotope fractionation in sulfate during bacterial sulfate reduction processes. *Geochim Cosmochim Acta* **69**, 4773–4785.
- Brunner B., Bernasconi S. M., Kleikemper J. and Schroth M. H. (2005b) A model for oxygen and sulfur isotope fractionation in sulfate during bacterial sulfate reduction processes. *Geochim Cosmochim Acta* **69**, 4773–4785.
- Brunner B., Einsiedl F., Arnold G. L., Müller I., Templer S. and Bernasconi S. M. (2012) The reversibility of dissimilatory sulphate reduction and the cell-internal multi-step reduction of sulphite to sulphide: insights from the oxygen isotope composition of sulphate. *Isotopes Environ Health Stud* **48**, 33–54.
- Burke A., Present T. M., Paris G., Rae E. C. M., Sandilands B. H., Gaillardet J., Peucker-Ehrenbrink B., Fischer W. W., McClelland J. W., Spencer R. G. M., Voss B. M. and Adkins J. F. (2018) Sulfur isotopes in rivers: Insights into global weathering budgets, pyrite oxidation, and the modern sulfur cycle. *Earth Planet Sci Lett* **496**, 168–177.
- Callbeck C. M., Canfield D. E., Kuypers M. M. M., Yilmaz P., Lavik G., Thamdrup B., Schubert C. J. and Bristow L. A. (2021) Sulfur cycling in oceanic oxygen minimum zones. *Limnol Oceanogr* **66**, 2360–2392.
- Cameron E. M. (1982) Sulphate and sulphate reduction in early Precambrian oceans. *Nature* **296**, 145–148.

- Canfield D. E. (1998) A new model for Proterozoic ocean chemistry. *Nature* **396**, 450–453.
- Canfield D. E. (2001) Biogeochemistry of Sulfur Isotopes. *Rev Mineral Geochem* **43**, 607–636.
- Canfield D. E. (2005) The early history of atmospheric oxygen: homage to Robert A Garrels. *Annu Rev Earth Planet Sci* **33**, 1–36.
- Canfield Donald E., Farquhar J. and Zerkle A. L. (2010) High isotope fractionations during sulfate reduction in a low-sulfate euxinic ocean analog. *Geology* **38**, 415–418.
- Canfield D. E., Poulton S. W. and Narbonne G. M. (2007) Late-Neoproterozoic deep-ocean oxygenation and the rise of animal life. *Science (1979)* **315**, 92–95.
- Canfield D. E. and Raiswell R. (1999) The evolution of the sulfur cycle. *Am J Sci* **299**, 697–723.
- Canfield Don E., Stewart F. J., Thamdrup B., De Brabandere L., Dalsgaard T., Delong E. F., Revsbech N. P. and Ulloa O. (2010) A cryptic sulfur cycle in oxygen-minimum-zone waters off the Chilean coast. *Science (1979)* **330**, 1375–1378.
- Canfield D. E. and Teske A. (1996) Late proterozoic rise in atmospheric oxygen concentration inferred from phylogenetic and sulphur-isotope studies. *Nature* **382**, 127–132.
- Canfield D. E. and Thamdrup B. (1994) The production of ³⁴S-depleted sulfide during bacterial disproportionation of elemental sulfur. *Science (1979)* **266**, 1973–1975.

- Canfield D. E., Thamdrup B. and Fleischer S. (1998) Isotope fractionation and sulfur metabolism by pure and enrichment cultures of elemental sulfur-disproportionating bacteria. *Limnol Oceanogr* **43**, 253–264.
- Chambers L. A. and Trudinger P. A. (1979) Microbiological fractionation of stable sulfur isotopes: A review and critique. *Geomicrobiol J* **1**, 249–293.
- CLINE J. D. (1969) Spectrophotometric determination of hydrogen sulfide in natural waters. *Limnol Oceanogr* **14**, 454–458.
- Coplen T. B., Böhlke J. K., De Bièvre P., Ding T., Holden N. E., Hopple J. A., Krouse H. R., Lamberty A., Peiser H. S., Revesz K., Rieder S. E., Rosman K. J. R., Roth E., Taylor P. D. P., Vocke R. D. and Xiao Y. K. (2002) Isotope-abundance variations of selected elements (IUPAC Technical Report). *Pure and Applied Chemistry* **74**, 1987–2017.
- Crowe S. A., Paris G., Katsev S., Jones C. A., Kim S. T., Zerkle A. L., Nomosatryo S., Fowle D. A., Adkins J. F., Sessions A. L., Farquhar J. and Canfield D. E. (2014) Sulfate was a trace constituent of Archean seawater. *Science (1979)* **346**, 735–739.
- Cui Y., Miller D., Schiarizza P. and Diakow L. J. (2017) *British Columbia Geological Survey Open File 2017-8.*
- Deevey E. S., Nakai N. and Stuiver M. (1963) Fractionation of Sulfur and Carbon Isotopes in a Meromictic Lake. *Science (1979)* **139**, 407–408.
- Farquhar J., Bao H. and Thiemens M. (2000) Atmospheric Influence of Earth's Earliest Sulfur Cycle. *Science (1979)* **289**, 756–758.
- Fike D. A., Bradley A. S. and Rose C. V. (2015) Rethinking the ancient sulfur cycle. *Annu Rev Earth Planet Sci* **43**, 593–622.

- Findlay A. J., Boyko V., Pellerin A., Avetisyan K., Guo Q., Yang X. and Kamyshny A. (2019) Sulfide oxidation affects the preservation of sulfur isotope signals. *Geology* **47**, 739–743.
- Van Geldern R. and Barth J. A. C. (2012) Optimization of instrument setup and post-run corrections for oxygen and hydrogen stable isotope measurements of water by isotope ratio infrared spectroscopy (IRIS). *Limnol Oceanogr Methods* **10**, 1024–1036.
- Ghosh W. and Dam B. (2009) Biochemistry and molecular biology of lithotrophic sulfur oxidation by taxonomically and ecologically diverse bacteria and archaea. *FEMS Microbiol Rev* **33**, 999–1043.
- Gilhooly W. P., Reinhard C. T. and Lyons T. W. (2016) A comprehensive sulfur and oxygen isotope study of sulfur cycling in a shallow, hyper-euxinic meromictic lake. *Geochim Cosmochim Acta* **189**, 1–23.
- Gomes M. L. and Hurtgen M. T. (2013) Sulfur isotope systematics of a euxinic, low-sulfate lake: Evaluating the importance of the reservoir effect in modern and ancient oceans. *Geology* **41**, 663–666.
- Gomes M. L. and Johnston D. T. (2017) Oxygen and sulfur isotopes in sulfate in modern euxinic systems with implications for evaluating the extent of euxinia in ancient oceans. *Geochim Cosmochim Acta* **205**, 331–359.
- Guibourdenche L., Cartigny P., Dela Pierre F., Natalicchio M. and Aloisi G. (2022) Cryptic sulfur cycling during the formation of giant gypsum deposits. *Earth Planet Sci Lett* **593**, 117676.

- Guo W., Cecchetti A. R., Wen Y., Zhou Q. and Sedlak D. L. (2020) Sulfur Cycle in a Wetland Microcosm: Extended ^{34}S -Stable Isotope Analysis and Mass Balance. *Environ Sci Technol* **54**, 5498–5508.
- Habicht K. S., Canfield D. E. and Rethmeier J. (1998) Sulfur isotope fractionation during bacterial reduction and disproportionation of thiosulfate and sulfite. *Geochim Cosmochim Acta* **62**, 2585–2595.
- Habicht K. S., Gade M., Thamdrup B., Berg P. and Canfield D. E. (2002) Calibration of sulfate levels in the Archean ocean. *Science (1979)* **298**, 2372–2374.
- Hamilton T. L., Bovee R. J., Thiel V., Sattin S. R., Mohr W., Schaperdoth I., Vogl K., Gilhooly W. P., Lyons T. W., Tomsho L. P., Schuster S. C., Overmann J., Bryant D. A., Pearson A. and Macalady J. L. (2014) Coupled reductive and oxidative sulfur cycling in the phototrophic plate of a meromictic lake. *Geobiology* **12**, 451–468.
- Harrison A. G. and Thode H. G. (1958) Mechanism of the bacterial reduction of sulphate from isotope fractionation studies. *Transactions of the Faraday Society* **54**, 84.
- Havig J. R., Hamilton T. L., Bachan A. and Kump L. R. (2017) Sulfur and carbon isotopic evidence for metabolic pathway evolution and a four-stepped Earth system progression across the Archean and Paleoproterozoic. *Earth Sci Rev* **174**, 1–21.
- Houghton J. L., Gilhooly W. P., Kafantaris F. C. A., Druschel G. K., Lu G. S., Amend J. P., Godelitsas A. and Fike D. A. (2019) Spatially and temporally variable sulfur cycling in shallow-sea hydrothermal vents, Milos, Greece. *Mar Chem* **208**, 83–94.
- Johnson J. E., Gerpheide A., Lamb M. P. and Fischer W. W. (2014) O₂ constraints from Paleoproterozoic detrital pyrite and uraninite. *Bulletin of the Geological Society of America* **126**, 813–830.

- Johnston D. T. (2011) Multiple sulfur isotopes and the evolution of Earth's surface sulfur cycle. *Earth Sci Rev* **106**, 161–183.
- Johnston D. T., Farquhar J. and Canfield D. E. (2007) Sulfur isotope insights into microbial sulfate reduction: When microbes meet models. *Geochim Cosmochim Acta* **71**, 3929–3947.
- Johnston D. T., Wolfe-Simon F., Pearson A. and Knoll A. H. (2009) Anoxygenic photosynthesis modulated Proterozoic oxygen and sustained Earth's middle age. *Proceedings of the National Academy of Sciences* **106**, 16925–16929.
- Jørgensen B. B. (1990) A thiosulfate shunt in the sulfur cycle of marine sediments. *Science (1979)* **249**, 152–154.
- Jørgensen B. B. (1977) The sulfur cycle of a coastal marine sediment (Limfjorden, Denmark). *Limnol Oceanogr* **22**, 814–832.
- Jørgensen B. B., Findlay A. J. and Pellerin A. (2019) The biogeochemical sulfur cycle of marine sediments. *Front Microbiol* **10**, 1–27.
- Kaplan I. R. and Rafter T. A. (1958) Fractionation of Stable Isotopes of Sulfur by Thiobacilli. *Science (1979)* **127**, 517–518.
- Kaplan I. R. and Rittenberg S. C. (1964) Microbiological Fractionation of Sulphur Isotopes. *J Gen Microbiol* **34**, 195–212.
- Kendall C. and Coplen T. B. (2001) Distribution of oxygen-18 and deuterium in river waters across the United States. *Hydrol Process* **15**, 1363–1393.
- Killingsworth B. A., Bao H. and Kohl I. E. (2018) Assessing Pyrite-Derived Sulfate in the Mississippi River with Four Years of Sulfur and Triple-Oxygen Isotope Data. *Environ Sci Technol* **52**, 6126–6136.

- Kohl I. and Bao H. (2011) Triple-oxygen-isotope determination of molecular oxygen incorporation in sulfate produced during abiotic pyrite oxidation (pH=2-11). *Geochim Cosmochim Acta* **75**, 1785–1798.
- Kurek M. R., Gilhooly W. P., Druschel G. K., O’Beirne M. D. and Werne J. P. (2018) The use of dithiothreitol for the quantitative analysis of elemental sulfur concentrations and isotopes in environmental samples. *Chem Geol* **481**, 18–26.
- Leavitt W. D., Halevy I., Bradley A. S. and Johnston D. T. (2013) Influence of sulfate reduction rates on the Phanerozoic sulfur isotope record. *Proc Natl Acad Sci U S A* **110**, 11244–11249.
- Li L., Wei S., Sherwood Lollar B., Wing B., Bui T. H., Ono S., Lau Vetter M. C. Y., Onstott T. C., Kieft T. L., Borgonie G., Linage-Alvarez B., Kuloyo O. and van Heerden E. (2022) In situ oxidation of sulfide minerals supports widespread sulfate reducing bacteria in the deep subsurface of the Witwatersrand Basin (South Africa): Insights from multiple sulfur and oxygen isotopes. *Earth Planet Sci Lett* **577**, 117247.
- Luther G. W., Findlay A. J., MacDonald D. J., Owings S. M., Hanson T. E., Beinart R. A. and Girguis P. R. (2011) Thermodynamics and kinetics of sulfide oxidation by oxygen: A look at inorganically controlled reactions and biologically mediated processes in the environment. *Front Microbiol* **2**, 1–9.
- Lyons T. W., Reinhard C. T. and Planavsky N. J. (2014) The rise of oxygen in Earth’s early ocean and atmosphere. *Nature* **506**, 307–315.

- Mariotti A., Germon J. C., Hubert P., Kaiser P., Letolle R., Tardieux A. and Tardieux P. (1981) Experimental determination of nitrogen kinetic isotope fractionation: Some principles; illustration for the denitrification and nitrification processes. *Plant Soil* **62**, 413–430.
- Markovic S., Paytan A., Li H. and Wortmann U. G. (2016) A revised seawater sulfate oxygen isotope record for the last 4Myr. *Geochim Cosmochim Acta* **175**, 239–251.
- Mayer B. (2005) Assessing Sources and Transformations of Sulphate and Nitrate in the Hydrosphere Using Isotope Techniques. In *Isotopes in the Water Cycle* Springer-Verlag, Berlin/Heidelberg. pp. 67–89.
- Meyer K. M. and Kump L. R. (2008) Oceanic euxinia in earth history: Causes and consequences. *Annu Rev Earth Planet Sci* **36**, 251–288.
- Meyer K. M., Macalady J. L., Fulton J. M., Kump L. R., Schaperdoth I. and Freeman K. H. (2011) Carotenoid biomarkers as an imperfect reflection of the anoxygenic phototrophic community in meromictic Fayetteville Green Lake. *Geobiology* **9**, 321–329.
- Mills J. V., Antler G. and Turchyn A. V. (2016) Geochemical evidence for cryptic sulfur cycling in salt marsh sediments. *Earth Planet Sci Lett* **453**, 23–32.
- Mizutani Y. and Rafter T. A. (1969) Oxygen isotopic composition of sulphates - Part 4. *NZ J. Sci* **12**, 60–68.
- Mullineaux D. R. (1996) Pre-1980 tephra-fall deposits erupted from Mount St. Helens, Washington. *US Geological Survey Professional Paper* **1563**.
- Och L. M. and Shields-Zhou G. A. (2012) The Neoproterozoic oxygenation event: Environmental perturbations and biogeochemical cycling. *Earth Sci Rev* **110**, 26–57.

- Overmann J., Beatty J. T., Krause H. R. and Hall K. J. (1996) The sulfur cycle in the chemocline of a meromictic salt lake. *Limnol Oceanogr* **41**, 147–156.
- Ozaki K., Thompson K. J., Simister R. L., Crowe S. A. and Reinhard C. T. (2019) Anoxygenic photosynthesis and the delayed oxygenation of Earth's atmosphere. *Nat Commun* **10**, 1–10.
- Pasquier V., Sansjofre P., Rabineau M., Revillon S., Houghton J. and Fike D. A. (2017) Pyrite sulfur isotopes reveal glacial-interglacial environmental changes. *Proc Natl Acad Sci U S A* **114**, 5941–5945.
- Pavlov A. A. and Kasting J. F. (2002) Mass-independent fractionation of sulfur isotopes in Archean sediments: strong evidence for an anoxic Archean atmosphere. *Astrobiology* **2**, 27–41.
- Paytan A. and Griffith E. M. (2007) Marine barite: Recorder of variations in ocean export productivity. *Deep Sea Res 2 Top Stud Oceanogr* **54**, 687–705.
- Paytan A., Kastner M. and Chavez F. P. (1996) Glacial to interglacial fluctuations in productivity in the equatorial Pacific as indicated by marine barite. *Science (1979)* **274**, 1355–1357.
- Paytan A., Mearon S., Cobb K. and Kastner M. (2002) Origin of marine barite deposits: Sr and S isotope characterization. *Geology* **30**, 747–750.
- Pellerin A., Antler G., Holm S. A., Findlay A. J., Crockford P. W., Turchyn A. V., Jørgensen B. B. and Finster K. (2019) Large sulfur isotope fractionation by bacterial sulfide oxidation. *Sci Adv* **5**, 1–6.

- Pellerin A., Bui T. H., Rough M., Mucci A., Canfield D. E. and Wing B. A. (2015) Mass-dependent sulfur isotope fractionation during reoxidative sulfur cycling: A case study from Mangrove Lake, Bermuda. *Geochim Cosmochim Acta* **149**, 152–164.
- Poser A., Vogt C., Knöller K., Ahlheim J., Weiss H., Kleinstüber S. and Richnow H. H. (2014) Stable sulfur and oxygen isotope fractionation of anoxic sulfide oxidation by two different enzymatic pathways. *Environ Sci Technol* **48**, 9094–9102.
- Poser A., Vogt C., Knöller K., Sorokin D. Y., Finster K. W. and Richnow H.-H. H. (2016) Sulfur and Oxygen Isotope Fractionation During Bacterial Sulfur Disproportionation Under Anaerobic Haloalkaline Conditions. *Geomicrobiol J* **33**, 934–941.
- Sass H. and Cypionka H. (2007) *Response of sulphate-reducing bacteria to oxygen.*, Sessions A. L., Doughty D. M., Welander P. V., Summons R. E. and Newman D. K. (2009) The Continuing Puzzle of the Great Oxidation Event. *Current Biology* **19**, R567–R574.
- Shen Y. and Buick R. (2004) The antiquity of microbial sulfate reduction. *Earth Sci Rev* **64**, 243–272.
- Shen Y., Buick R. and Canfield D. E. (2001) Isotopic evidence for microbial sulphate reduction in the early Archaean era. *Nature* **410**, 77–81.
- Sim M. S. (2019) Effect of sulfate limitation on sulfur isotope fractionation in batch cultures of sulfate reducing bacteria. *Geosciences Journal* **23**, 687–694.
- Sim M. S., Bosak T. and Ono S. (2011) Large sulfur isotope fractionation does not require disproportionation. *Science (1979)* **333**, 74–77.

- Steinman B. A. and Abbott M. B. (2013) Isotopic and hydrologic responses of small, closed lakes to climate variability: Hydroclimate reconstructions from lake sediment oxygen isotope records and mass balance models. *Geochim Cosmochim Acta* **105**, 342–359.
- Steinman B. A., Rosenmeier M. F., Abbott M. B. and Bain D. J. (2010) The isotopic and hydrologic response of small, closed-basin lakes to climate forcing from predictive models: Application to paleoclimate studies in the upper Columbia River basin. *Limnol Oceanogr* **55**, 2231–2245.
- Storelli N., Peduzzi S., Saad M. M., Frigaard N. U., Perret X. and Tonolla M. (2013) CO₂ assimilation in the chemocline of Lake Cadagno is dominated by a few types of phototrophic purple sulfur bacteria. *FEMS Microbiol Ecol* **84**, 421–432.
- Thamdrup B., Finster K., Hansen J. W. and Bak F. (1993) Bacterial disproportionation of elemental sulfur coupled to chemical reduction of iron or manganese. *Appl Environ Microbiol* **59**, 101–108.
- Treude T., Hamdan L. J., Lemieux S., Dale A. W. and Sommer S. (2021) Rapid sulfur cycling in sediments from the Peruvian oxygen minimum zone featuring simultaneous sulfate reduction and sulfide oxidation. *Limnol Oceanogr* **66**, 2661–2671.
- Turchyn A. V., Brüchert V., Lyons T. W., Engel G. S., Balci N., Schrag D. P. and Brunner B. (2010) Kinetic oxygen isotope effects during dissimilatory sulfate reduction: A combined theoretical and experimental approach. *Geochim Cosmochim Acta* **74**, 2011–2024.

- Wankel S. D., Bradley A. S., Eldridge D. L. and Johnston D. T. (2014) Determination and application of the equilibrium oxygen isotope effect between water and sulfite. *Geochim Cosmochim Acta* **125**, 694–711.
- Washington State Department of Natural Resources Division of Geology and Earth Resources (2016) 1:100,000-scale geologic mapping database of Washington State Digital Data Series 18 (DS-18), Version 3.1.
- Wilbanks E. G., Jaekel U., Salman V., Humphrey P. T., Eisen J. A., Facciotti M. T., Buckley D. H., Zinder S. H., Druschel G. K., Fike D. A. and Orphan V. J. (2014) Microscale sulfur cycling in the phototrophic pink berry consortia of the Sippewissett Salt Marsh. *Environ Microbiol* **16**, 3398–3415.
- Wing B. A. and Halevy I. (2014) Intracellular metabolite levels shape sulfur isotope fractionation during microbial sulfate respiration. *Proceedings of the National Academy of Sciences* **111**, 18116–18125.
- Yoon S. H., Ha S. M., Kwon S., Lim J., Kim Y., Seo H. and Chun J. (2017) Introducing EzBioCloud: A taxonomically united database of 16S rRNA gene sequences and whole-genome assemblies. *Int J Syst Evol Microbiol* **67**, 1613–1617.
- Young E. D., Yeung L. Y. and Kohl I. E. (2014) On the $\delta^{17}\text{O}$ budget of atmospheric O_2 . *Geochim Cosmochim Acta* **135**, 102–125.
- Zerkle A. L., Farquhar J., Johnston D. T., Cox R. P. and Canfield D. E. (2009) Fractionation of multiple sulfur isotopes during phototrophic oxidation of sulfide and elemental sulfur by a green sulfur bacterium. *Geochim Cosmochim Acta* **73**, 291–306.

- Zerkle A. L., Kamyshny A., Kump L. R., Farquhar J., Oduro H. and Arthur M. A. (2010) Sulfur cycling in a stratified euxinic lake with moderately high sulfate: Constraints from quadruple S isotopes. *Geochim Cosmochim Acta* **74**, 4953–4970.
- Zhang Y., Wang X., Zhen Y., Mi T., He H. and Yu Z. (2017) Microbial diversity and community structure of sulfate-reducing and sulfur-oxidizing bacteria in sediment cores from the East China Sea. *Front Microbiol* **8**, 1–17.
- Zopfi J., Ferdelman T. G. and Fossing H. (2004) Distribution and fate of sulfur intermediates—sulfite, tetrathionate, thiosulfate, and elemental sulfur—in marine sediments. In *Special Paper 379: Sulfur Biogeochemistry - Past and Present* Geological Society of America. pp. 97–116.
- Zopfi J., Ferdelman T. G., Jorgensen B. B., Teske A. and Thamdrup B. (2001) Influence of water column dynamics on sulfide oxidation and other major biogeochemical processes in the chemocline of Mariager Fjord (Denmark). *Mar Chem* **74**, 29–51.

CURRICULUM VITAE

James Howard Harris IV

Education

- Master of Science
Major in Geology
Indiana University-Purdue University Indianapolis, December 2023
- Bachelor of Science, Cum Laude
Major in Biogeosciences
University of Tulsa, August 2013
- Undergraduate student (Transferred to University of Tulsa)
Major in Geology
Oklahoma State University, January 2009 – December 2010
- Undergraduate student (Transferred to Oklahoma State University)
Major in Environmental Science
Tulsa Community College, August 2007 – December 2008

Professional Experience

- IT Engineer
IT Voice
December 2015 – Present
- Graduate Teaching Assistant
Department of Earth Science
Indiana University-Purdue University Indianapolis
August 2013 – May 2015

Honors and Awards

- Geological Society of America Research Grant, April 2015
- Society for Sedimentary Geology Student Research Grant, April 2015
- IUPUI University Fellowship, August 2013 – May 2015
- Susan M. Pfiffner Award for Outstanding Academic Achievement in
Biogeosciences, March 2013